

University of Massachusetts Medical School
eScholarship@UMMS

GSBS Dissertations and Theses

Graduate School of Biomedical Sciences


2016-04-07

The Mechanistic Role and Therapeutic Potential of microRNA-122 in Alcoholic Liver Disease: A Dissertation

Abhishek Satishchandran
University of Massachusetts Medical School

Let us know how access to this document benefits you.

Follow this and additional works at: https://escholarship.umassmed.edu/gsbs_diss

 Part of the [Cellular and Molecular Physiology Commons](#), [Digestive System Diseases Commons](#), and the [Nucleic Acids, Nucleotides, and Nucleosides Commons](#)

Repository Citation

Satishchandran A. (2016). The Mechanistic Role and Therapeutic Potential of microRNA-122 in Alcoholic Liver Disease: A Dissertation. GSBS Dissertations and Theses. <https://doi.org/10.13028/M2GP4W>. Retrieved from https://escholarship.umassmed.edu/gsbs_diss/838

This material is brought to you by eScholarship@UMMS. It has been accepted for inclusion in GSBS Dissertations and Theses by an authorized administrator of eScholarship@UMMS. For more information, please contact Lisa.Palmer@umassmed.edu.

**The Mechanistic Role and Therapeutic Potential of microRNA-122 in Alcoholic
Liver Disease**

By

Abhishek Satishchandran

Submitted to the Faculty of the

University of Massachusetts Graduate School of Biomedical Sciences, Worcester

in partial fulfillment of the requirements for the degree of

DOCTOR OF PHILOSOPHY

April 7, 2016

MD/PhD Program in Biomedical Sciences

*“The heights by great men reached and kept
Were not attained by sudden flight,
But they, while their companions slept,
Were toiling upward in the night.”*

- Henry Wordsworth Longfellow (and my Father),
The Ladder of St. Augustine

**THE MECHANISTIC ROLE AND THERAPEUTIC POTENTIAL OF
MICRORNA-122 IN ALCOHOLIC LIVER DISEASE**

A Dissertation Presented
By
Abhishek Satishchandran

This work was undertaken in the Graduate School of Biomedical Sciences
MD/PhD Program in Biomedical Sciences

The signature of the Thesis Advisor signifies validation of Dissertation content

Gyongyi Szabo MD PhD, Thesis Advisor

The Signatures of the Dissertation Defense Committee signify completion and
approval as to style and content of the Dissertation

Guangping Gao PhD, Member of Committee

Pranoti Mandrekar PhD, Member of Committee

Terence Flotte MD, Member of Committee

Jack Wands MD, External Member of Committee

The signature of the Chair of the Committee signifies that the written dissertation
meets the requirements of the Dissertation Committee

Brian Lewis PhD, Chair of Committee

The signature of the Dean of the Graduate School of Biomedical Sciences
signifies that the student has met all the graduation requirements of the school.

Anthony Carruthers PhD, Dean of the Graduate School of Biomedical Sciences

April 7, 2016

DEDICATION

To my wife, parents, family, and friends;

you are the giants whose shoulders I stand upon.

ACKNOWLEDGEMENTS

If it takes a village to raise a child, the many needed to raise an MD/PhD are innumerable. Truth be told, the list of people who deserve acknowledgements is longer than this dissertation, but I shall keep it brief.

I am very thankful to Dr. Gyongyi Szabo for her mentorship throughout my years at UMass. Always leading by example, I have been in awe of her relentless dedication and drive to create an environment which champions physician scientists. Throughout my time in lab, she has fostered an atmosphere where I was encouraged to pursue my own ideas. I will be forever grateful, not only for her guidance and commitment to my growth as a professional, but for her friendship as well.

I am immensely grateful to Dr. Guangping Gao for his mentorship and collaboration. Dr. Gao has served as the chair of my committee and collaborator on my work and despite his busy schedule, he has always maintained an open door policy for which I am very grateful. I would also like to thank members of the Gao Lab who played an integral part in the development and use of the AAV vector systems used here. This work could not have been accomplished without the contributions of Dr. Li Zhong, Dr. Jun Xie, and Jia Li.

I thank the rest of my committee, Dr. Brian Lewis, Dr. Terry Flotte, and Dr. Pranoti Mandrekar, for their wisdom and guidance throughout these past several years. I am undoubtedly fortunate to have such a great group of mentors.

I would like to thank Dr. Jack Wands, my external advisor, for taking the time to review my dissertation and provide feedback during my defense.

I wish to thank many members of the Szabo lab, including many administrators and project coordinators: Merin Macdonald, Michelle Morrison, Candice Dufour, and Donna Raymond. I thank Karen Kodys and Donna Catalano for their tireless effort and friendship. It is due to the foundation they have laid that I, and others, have been able to achieve so much.

I am deeply grateful to have had Shashi Bala as a mentor, colleague, friend, and bay-mate. I am, and always will be, humbled by her knowledge, kindness, and dedication to fostering a love of science. I wish to thank many post-docs from lab, both past and present: Jan Petrasek, Terence Bukong, Aditya Ambade, Michal Ganz, and Timea Czsak. They have supplied me with guidance and examples of scientific achievement to aspire to. Additionally, I would like to thank my partners in crime from lab: Patrick Lowe AKA “Brain Boy”, Benedek Gyongyosi AKA “Gut Guy”, and Arvin Iracheta-Vellve AKA “Liver Lad II”. Their contributions to this project go beyond the science and I am proud to call them colleagues and friends.

I am grateful for the previous work done by Dr. Barath Nath, a former MD/PhD student from lab; his efforts aided in establishing the foundation of my work.

I would like to thank members of the Mandrekar Lab, Melissa Fulham and Arlene Lim, for their technical and moral support.

The work presented here was supported by an F30 fellowship funded by the National Institutes of Alcohol and Alcoholism (NIH/NIAAA F30 AA022283). I thank the members of the selection committee, particularly Dr. Svetlana Radaeva, for this award and their belief in the science and in me. Additionally, I would like to thank Lori Randal for her assistance with this grant application.

Throughout my years at UMass, I have benefited from mentorship by members of the graduate and medical schools, particularly Dr. Jean-Marie Houghton, Dr. John Harris, Dr. Egil Lien, and Dr. Paulo Martins. They all have provided me with advice, guidance, support, and opportunities to further my medical education and career. Specifically, I would like to thank Dr. Houghton for her effort and support in development of the MD/PhD clinical review course.

I thank Dr. David Hatem for his continued support of my medical education. He has been a pillar of support since I began medical school.

I would like to extend my gratitude to Dr. Sylvia Corvera, Dr. William Schwartz, and Anne Michelson for their support of the MD/PhD Program.

I feel privileged to have gone through this program with fellow MD/PhD students. In particular, I would like to thank those in my matriculating class, Anouch Matevossian, Evelyn Guerra, Kristina Prachanronarong, Suzanne Czerniak, and Dmitry Ratner for their support, occasional distractions, and friendship. I would also like to thank Cindy Lai, Brian Quattrochi, and Thomas Akie for their scientific input and advice in traversing the wandering path of an MD/PhD Student.

I want to thank my friends from the medical school class of 2013, Mary Le, Inna Baran, Alex Shapeton, Nathalee Kong, Chris Gibson, Phanicharan Sistla, and David Ong; and many more whose names I don't have space to list. I thank them for being more than friends; for being family.

For my family, immediate and in-laws, I do not know if I can adequately express my gratitude. It is only because of their selflessness and dedication that I am here today. My mother and father have been the invisible hands supporting me throughout my years. Their examples of hard work, passion, respect, and sincere desire to make the world a better place have not only inspired me, but all of their children, to reach for the stars and be their best selves.

Most of all, to my wonderful wife Hiral, this achievement is as much hers as it is mine. It is because of her love, support, and encouragement (by way of occasional kick in the rear) that I have been able to accomplish all that I have. I am thankful for all the days we have shared and all those yet to come.

ABSTRACT

Chronic alcohol use results in accelerated liver injury, leading to alcoholic steatohepatitis, cirrhosis, and hepatocellular carcinoma. However, due to the complex nature of this disease process, a central, druggable mechanism has remained elusive. microRNAs are potent post-transcriptional regulators of gene expression. A single miRNA has the ability to regulate hundreds of pathways simultaneously, defining cellular fate and function. microRNA-122 (miR-122), the most abundant miRNA in hepatocytes, has a demonstrated role as an tumor suppressor, regulator of hepatocyte metabolism, and hepatic differentiation.

In this dissertation I demonstrate the role of miR-122 on alcoholic liver disease (ALD) pathogenesis over four parts. In chapter II, I will demonstrate chronic alcoholic patients, free of neoplastic changes, have a reduction of miR-122 and that this miRNA regulates HIF-1 α , a determinant of ALD pathogenesis. In chapter III, using hepatocyte-tropic adeno-associated virus 8 (AAV8) vector, I demonstrate that miR-122 inhibition mimics ALD pathogenesis, and furthermore, using hepatocyte-specific HIF-1 α -null (HIF1hepKO) mice that this phenomenon is HIF-1 α dependent. Given this finding, in chapter IV, I demonstrate that ectopic expression of miR-122 *in vivo* can reverse alcohol-induced liver damage, steatosis, and inflammation by directly targeting HIF-1 α . Finally, in chapter V, I present evidence that alcohol-induced dysregulation of grainyhead-like proteins 1 and 2 (GRHL2), mediate the inhibition of miR-122 at the transcriptional level. These findings dissect a novel mechanistic regulatory axis of miR-122 and indicate a potential opportunity for restoration of miR-122 as a therapy in early ALD.

TABLE OF CONTENTS

DEDICATION	IV
ACKNOWLEDGEMENTS	V
ABSTRACT.....	VIII
TABLE OF CONTENTS	IX
LIST OF FIGURES	XII
LIST OF TABLES.....	XIV
LIST OF ABBREVIATIONS USED COMMONLY IN THIS TEXT.....	XV
PREFACE.....	XVII
CHAPTER 1: INTRODUCTION.....	18
ALCOHOLIC LIVER DISEASE: EPIDEMIOLOGY & CLINICAL PROGRESSION.....	18
<i>Epidemiology</i>	<i>18</i>
<i>Disease Spectrum.....</i>	<i>18</i>
<i>Steatosis</i>	<i>19</i>
<i>Alcoholic Hepatitis, fibrosis, and cirrhosis</i>	<i>19</i>
<i>Fibrosis</i>	<i>22</i>
OVERVIEW OF MOLECULAR MECHANISMS IN ALD PATHOPHYSIOLOGY	24
<i>Oxidative Stress.....</i>	<i>24</i>
<i>Lipid Accumulation</i>	<i>26</i>
<i>Hypoxia & Hypoxia inducible factors.</i>	<i>28</i>
<i>Inflammation</i>	<i>33</i>
MICRORNA BIOGENESIS AND MECHANISM OF ACTION	37
<i>Background and Overview.....</i>	<i>37</i>
<i>Genomic loci</i>	<i>38</i>
<i>Transcription of pri-miRNA and pre-miRNA processing</i>	<i>38</i>
<i>Nuclear export.....</i>	<i>42</i>

<i>Dicer, Argonats, & RISC</i>	43
MICRORNA-122: BIOGENESIS & FUNCTION	46
<i>Background and Overview</i>	46
<i>miR-122 Biogenesis</i>	47
<i>miR-122 in the serum</i>	48
<i>miR-122 in HCV</i>	53
<i>miR-122 in HBV</i>	55
<i>miR-122 in NASH</i>	56
<i>miR-122 in HCC</i>	57
<i>Mutations associated with miR-122</i>	58
MIRNA MODULATION AND THERAPEUTICS.....	59
CHAPTER 2: ALCOHOL, MIR-122 AND HIF-1ALPHA.....	65
SUMMARY.....	65
ACKNOWLEDGEMENTS	66
INTRODUCTION	67
METHODS.....	69
RESULTS	77
CONCLUSIONS AND DISCUSSION	93
CHAPTER 3: MIR-122 MEDIATES ALCOHOLIC LIVER DISEASE	
PATHOGENESIS VIA HIF-1A <i>IN VIVO</i>	95
SUMMARY.....	95
ACKNOWLEDGEMENTS	96
INTRODUCTION	97
METHODS.....	99

RESULTS	107
CONCLUSIONS AND DISCUSSION	128
CHAPTER 4: THERAPEUTIC RESTORATION OF MIR-122 REVERSES ALCOHOL-INDUCED LIVER INJURY VIA HIF-1ALPHA <i>IN VIVO</i>	131
SUMMARY	131
ACKNOWLEDGEMENTS	132
INTRODUCTION	133
METHODS.....	138
RESULTS	144
CONCLUSIONS AND DISCUSSION	145
CHAPTER 5: ALCOHOL REGULATES MIR-122 THROUGH ALTERNATIVE SPLICING OF GRAINYHEAD PROTEINS	159
SUMMARY	159
INTRODUCTION	161
METHODS.....	170
RESULTS	174
CONCLUSIONS AND DISCUSSION	193
CHAPTER 6: FINAL SUMMARY, DISCUSSION, & FUTURE DIRECTIONS .	202
BIBLIOGRAPHY	215

LIST OF FIGURES

FIGURE 1.1: SCHEMATIC REPRESENTATION OF ALD PATHOGENESIS	20
FIGURE 1.2: GENERAL SCHEMATIC OF HIF-1A SIGNALING	31
FIGURE 1.3: GENERAL SCHEMATIC OF mRNA BIOGENESIS.....	39
FIGURE 1.4: SCHEMATIC REPRESENTATION OF KEY REGULATORY FUNCTIONS OF M R-122 IN HEPATOCYTES AND TOTAL BODY PHYSIOLOGY AND DISEASE.....	50
FIGURE 1.5: MECHANISMS FOR mRNA MODULATION.....	60
FIGURE 2.1: HUMAN LIVER M R-122 EXPRESSION.	79
FIGURE 2.2: CHARACTERISTICS OF CHRONIC ALCOHOL FEEDING MODEL.....	81
FIGURE 2.3: H&E LIVER HISTOLOGY FROM WILD-TYPE PARR- AND ETHANOL-FED MICE.....	84
FIGURE 2.4: CHRONIC ALCOHOL IS ASSOCIATED WITH REDUCED M R-122 IN MURINE HEPATOCYTES.....	86
FIGURE 2.5: INVERSE CORRELATION BETWEEN M R-122 AND HIF-1A IN CHRONIC ALCOHOL.....	89
FIGURE 2.6: M R-122 REGULATES HIF-1A VIA 3'UTR SILENCING.....	91
FIGURE 3.1: CHARACTERISTICS OF CHRONIC ALCOHOL FEEDING MODEL.....	108
FIGURE 3.2: M R-122 MEDIATES HIF-1A STEATOSIS AND LIVER INJURY THROUGH HIF-1A IN VIVO	114
FIGURE 3.3: M R-122 MEDIATED LIVER INJURY IS HIF-1A DEPENDENT	116
FIGURE 3.4: ALCOHOL AND M R-122 MEDIATED HEPATOCYTE STEATOSIS IS HIF-1A DEPENDENT.....	118
FIGURE 3.5: ALCOHOL AND M R-122 MEDIATED HEPATOCYTE INFLAMMATION IS HIF-1A DEPENDENT	122
FIGURE 3.6: ALCOHOL AND M R-122 MEDIATED HEPATOCYTE INFLAMMATION IS HIF-1A DEPENDENT	124
FIGURE 3.7: M R-122 LOSS MEDIATES EARLY FIBROTIC CHANGES THROUGH HIF-1A	126
FIGURE 4.1: DESIGN OF M R-122 TREATMENT MODEL.....	147
FIGURE 4.2: M R-122 EXPRESSION IN AAV8-M R-122-OX TREATED MICE.....	149
FIGURE 4.3: RESTORATION OF M R-122 IN BATS ALCOHOL-INDUCED INCREASES OF HIF-1A	151
FIGURE 4.4: TREATMENT WITH RAAV8-M R-122-OX REVERSES ALCOHOL-INDUCED LIVER INJURY AND STEATOSIS.....	153
FIGURE 4.5: TREATMENT WITH RAAV8-M R-122-OX REVERSES ALCOHOL-INDUCED INFLAMMATION.....	155

FIGURE 5.1: SCHEMATIC REPRESENTATION OF GRHL1 & 2 FULL LENGTH AND SPLICED PROTEINS 167

FIGURE 5.2: CHRONIC ALCOHOL INHIBITS PROMOTER-122 180

FIGURE 5.3: EXPRESSION OF HNF-4A AND HNF6B IN MURINE LIVERS 182

FIGURE 5.4: M R-122 PROMOTER CONTAINS A CONSERVED GRN HEAD BINDING SITE 184

FIGURE 5.5: GRN HEAD-LIKE 1 AND 2 IMMUNOHISTOCHEMISTRY 186

FIGURE 5.6: CHRONIC ALCOHOL INCREASES GRHL2 EXPRESSION IN MURINE HEPATOCYTES 188

FIGURE 5.7: EXPRESSION OF GRN HEAD-LIKE PROTEINS IN MURINE AND HUMAN LIVERS 190

FIGURE 5.8: CHRONIC ALCOHOL INDUCES ALTERNATIVE SPLICING OF GRHL1 AND GRHL2 194

FIGURE 5.9: ROLE OF GRN HEAD SOFRTS ON M R-122 EXPRESSION 196

FIGURE 6.1: PROPOSED MODEL OF FINDINGS 203

LIST OF TABLES

TABLE 2.1 QPCR AND CLONING PRIMERS USED IN THIS STUDY 72

TABLE 2.2: HUMAN LIVER SAMPLES; DEMOGRAPHIC AND CLINICAL DATA..... 78

LIST OF ABBREVIATIONS USED COMMONLY IN THIS TEXT

miRNA, microRNA, miR-122, microRNA-122-5p, pri-miR; primary miRNA transcript; pre-miRNA, precursor-miRNA transcript; XPO5, exportin 5; miRISC, miRNA-induced silencing complex; ALD, Alcoholic liver disease; ALT, alanine aminotransferase; AMPK, Adenosine monophosphate-activated protein kinase; CYP2E1, cytochrome P450 2E1; ERK, extracellular signal regulated kinase; HIF1^{hepKO}, hepatocyte-specific homozygous deletion of the HIF-1 α gene; HIF1^{dPA}, mouse mutant degradation-resistant HIF-1 α ; HIF-1 α , Hypoxia Inducible Factor-1-alpha; HIF-2 α , Hypoxia Inducible Factor-2-alpha; IFN, interferon; IL, interleukin; KC, Kupffer Cells; LPS, lipopolysaccharide; MAPK, mitogen activated protein kinase; MCP-1, Monocyte Chemoattractant Protein; MYD88, myeloid differentiation primary response gene 88; poly I:C, polyinosinic/ polycytidylic double-stranded RNA; PPAR, peroxisome proliferator-activated receptor; ROS, reactive oxygen species; RXR, retinoic acid receptor; SREBP, Sterol-regulatory element binding protein; SIRT1, sirtuin 1; STAT3, signal transducer and activator of transcription 3; TLR, Toll-like receptor; TNF- α ", tumor necrosis factor- α "; IFN β , interferon- β ; WT, Wild-type, GRH, Drosophila Grainyhead protein; GRHL, mammalian grainyhead-like protein; HCV, Hepatitis C Virus; HBV, Hepatitis B Virus; PAMP, pattern associated molecular patterns; DAMP, damage associated molecular patterns; RPII, RNA polymerase II; LNA, Locked nucleic acid; ASO, anti-sense oligonucleotide; TuD, Tough Decoy; Cat-1, cationic amino acid transferase-1; HRE, hypoxia responsive element; PPRE, PPAR response element; VHL, Von Hippel-Lindau protein; CPT, Carnitine palmitate transferase; FA, fatty acid; GSH,

glutathione; ROS, reactive oxygen species; NASH, non-alcoholic steatohepatitis, NAFLD, non-alcoholic fatty liver disease; AH/ASH-alcoholic hepatitis/alcoholic steatohepatitis; PTX, pentoxiphylline; PDE, phosphodiesterase; SREBP, sterol regulatory element binding protein; 122LKO, hepatocyte specific miR-122 knockout mice; FFPE, formalin-fixed paraffin embedded; EMSA, electromobility shift assay

PREFACE

Data for some figures in these chapters were generated in collaboration with members of the Szabo laboratory. In particular, *in vitro* HIF-1 α data from Chapter II of this dissertation was previously published in Csak et al, *Liver International*, 2015.

Additionally, AAVs were designed and generated in collaboration with Dr. Xie, Jai Li, and Dr. Li Zong of the UMass Vector Core under the direction of Dr. Gao.

CHAPTER 1: INTRODUCTION

Alcoholic Liver Disease: Epidemiology & Clinical Progression

Epidemiology

The pathologic effect of chronic alcohol abuse has been cited for thousands of years.¹ Approximately two-thirds of the US population consume alcohol, with the incidence of abuse and/or dependence nearing 7%, it is the cause of 44% of all liver related deaths.² In fact, morbidity and mortality from alcoholic cirrhosis far exceeds than that of non-alcoholic cirrhosis.^{3,4}

World-wide, clinically diagnosed alcoholic liver disease is among the top 20 causes of death, and constitutes a significant social and economic burden to drinkers and society.¹ The World Health Organization's Global Alcohol Database has estimated alcohol will contribute to 9.2% of disability-adjusted life years the world over.⁵ While these numbers are staggering, given the prevalence of consumption and the extra hepatic manifestations of excessive alcohol consumption such as cardiovascular diseases, fetal alcohol syndrome, and diabetes mellitus, to name a few, it is widely believed that the morbidity and mortality estimates associated with excessive alcohol consumption are vastly underreported.

Disease Spectrum

Alcoholic liver disease (ALD) is a term used to describe a spectrum of clinical manifestations classically described as occurring in three stages; steatosis, alcoholic hepatitis, and cirrhosis (Figure 1.1).⁶ These independent characterizations, are a

manifestation of histological descriptions and are not exclusive events, rather they are concurrent events in ALD pathogenesis.

Steatosis

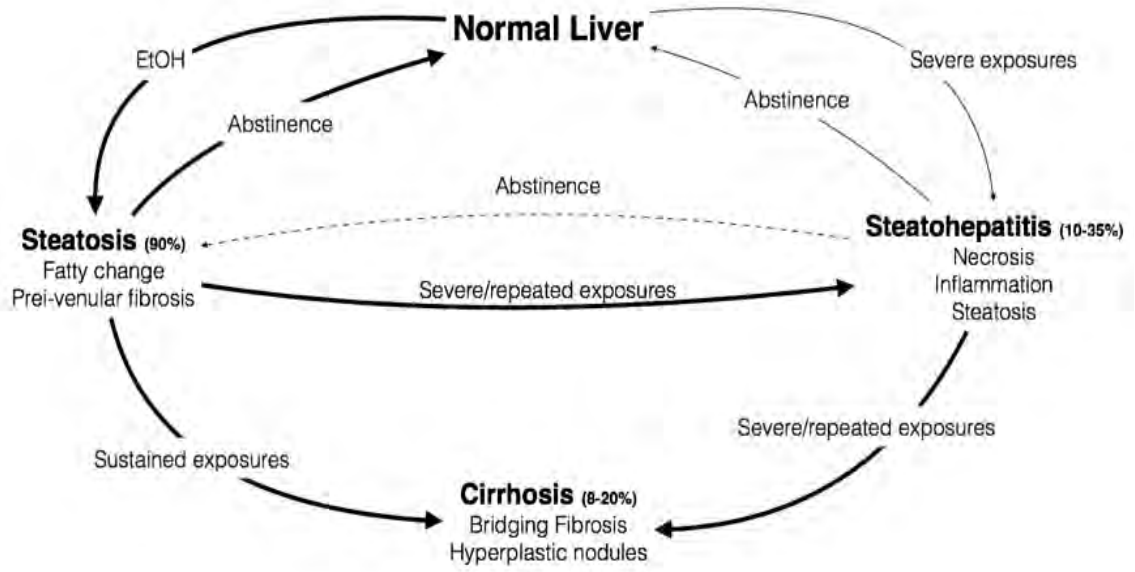
Macro- and microvesicular steatosis, also known as alcoholic fatty liver disease (AFLD) occurs in as many as 90% of individuals who drink excessively.⁶⁻⁸ This asymptomatic process is typically reversible with abstinence and lifestyle modification. However, it has been suggested that 5-15% of patients still progress to fibrosis or cirrhosis, regardless of abstinence. This risk doubles to 30-37% with continued consumption of >40g/day.⁶⁻⁸

Alcoholic Hepatitis, fibrosis, and cirrhosis

Alcoholic hepatitis or steatohepatitis (AH or ASH) occurs in 10-35% of patients with ALD and can range from mild injury to acute hepatic decompensation superimposed on chronic liver disease.⁹ Histologically, AH presents with considerable hepatocyte death, neutrophilic infiltration, Mallory body formation, and fibrosis.⁶⁻⁸ Liver biopsy remains the definitive diagnostic tool for alcoholic hepatitis, however, it is often unnecessary and unwarranted given a carefully obtained patient history.^{10,11} In addition to a thorough history, laboratory findings may hold vital hints as to liver disease etiology. Patients with AH will often have elevated AST and ALT with a ratio of AST to ALT of >2.^{10,12} This distinguishing characteristic can be used diagnostically to define alcoholic hepatitis when non-alcoholic hepatitis, or drug-induced liver injury is suspected.^{10,12} ALT, is enriched within peri-portal hepatocytes in zone 1 of the liver lobule, an oxygen rich environment, while AST demonstrates elevated expression in zone 3. Being at a

Figure 1.1: Schematic Representation of ALD pathogenesis.

Thicker arrows indicate traditional course of disease. Percentages indicate likelihood of developing disease with continued exposure to alcohol. Adapted from medchrome.com.



lower oxygen tension, zone 3 hepatocytes are more susceptible to alcohol-induced liver injury and thus upon release more AST into circulation. Additionally, patients typically present with decreased albumin production, severe jaundice, hypertriglyceridemia, hyperuremia, hypokalemia, leukocytosis, and thrombocytopenia. In this context the elevation of serum creatinine is indicative of acute renal failure, also known as hepatorenal syndrome, and is a poor prognostic indicator. Prediction of disease severity and mortality can be calculated using one of many methods, including Maddery's Discriminant Function (DF), MELD, or Glasgow scores.¹⁰⁻¹² Typically, patients who present with symptomatic disease are at an advanced stage with evidence of cirrhosis and those with severe alcoholic hepatitis (DF>32, MELD>18) have a 40-50% 6-month mortality.¹⁰⁻¹² At this stage of disease, even with abstinence from alcohol, 73% will progress to cirrhosis or have persistent alcoholic hepatitis.¹³

Fibrosis

Fibrosis is the increased deposition of collagen within the liver parenchyma. Characteristically, alcoholic fibrosis begins with perivenular fibrosis and extends in a pericellular distribution, commonly referred to as "chicken-wire" fibrosis.⁶⁻⁸ These findings, superimposed with those of alcoholic hepatitis confers a 40% risk of cirrhosis within 5 years.^{10,14,15} The resulting cirrhosis significantly increases the risk of hepatocellular carcinoma (HCC). Worldwide, primary liver cancers are the 3rd leading cause of cancer mortality, 80% of which are due to HCC.¹⁴⁻¹⁶ While there are many risk factors for cirrhosis and HCC development, alcohol consumption of 80 g/day constitutes

a five-fold increase in risk, while concurrent HCV infection increases that risk 100-fold.^{17,18 14,15}

Overview of molecular mechanisms in ALD pathophysiology

The broad characterizations of ALD represents varying degrees of hepatic parenchymal and non-parenchymal dysfunction. These changes are driven by direct and indirect effects of alcohol on the metabolic and inflammatory processes within the liver. Steatosis, which is marked by increased hepatic lipid accumulation within hepatocytes was originally attributed to redox shifts within hepatocytes due to alcohol metabolism and mobilization of peripheral adipose stores to the liver. However, an abundance of literature has demonstrated that alterations within hepatocytes that promote cell death, lipogenesis, decreased triglyceride (TG) export, and decreased fatty acid oxidation (FAO) are not only directly due to alcohol, but are also extensively influenced by innate immune signaling pathways. This portion of the introductory chapter will serve to briefly summarize the essential pathways in ALD.

Oxidative Stress

A well-established mechanism for hepatic injury due to alcohol is that of increased oxidative stress from a variety of sources. Hepatocytes, are extremely metabolically active and must constantly buffer against reactive oxygen species (ROS) production.¹⁹ Their buffering capacity stems from a combination of enzymatic species such as superoxide dismutase and catalase, to non-enzymatic species such as glutathione (GSH), and vitamins A, C and E.²⁰⁻²⁴ However, chronic alcohol consumption, severe malnutrition and vitamin deficiencies significantly deplete the ROS buffer capacity of the liver. Furthermore, the metabolism of alcohol produces acetaldehyde, hydrogen peroxide (H₂O₂), and superoxide anions (O₂⁻) which result in lipid peroxidation of biological

membranes, protein adduct formation, and DNA mutations triggering cell death pathways.^{20-23,25-27} Treatments with various antioxidants such as N-acetylcysteine (NAC) and S-Adenosyl-L-methionine (SAM) have been shown to inhibit steatosis and liver injury.²⁸⁻³²

The pathogenic effect of chronic alcohol is due to the direct and indirect effects of ethanol itself and the intermediates from its metabolism. The oxidation of ethanol to acetaldehyde and then acetate is catalyzed by the enzymes alcohol dehydrogenase (ADH) and aldehyde dehydrogenase (ALDH), respectively.³³⁻³⁶ Both enzymes utilize NAD⁺ as a cofactor, converting it to its reduced form, NADH. This nets a large increase in NADH levels in the liver, and a reduction of the NAD⁺/NADH ratio. The consequence of this is a dramatic shift in metabolic pathways including the inhibition of gluconeogenesis, the TCA cycle, and fatty acid oxidation as well as a shift to lipogenesis.³³⁻³⁵ Two alternative pathways of ethanol metabolism are also present; the enzyme catalase, and the microsomal ethanol oxidation system enzyme, cytochrome P450-2E1 (CYP2E1).³⁷⁻³⁹ Catalase, has been shown to have negligible expression in the liver and does not significantly contribute to alcohol metabolism, but does serve as an ROS buffer by degrading H₂O₂. CYP2E1 on the other hand accounts for 10% of ethanol metabolism in the normal liver. This high kd enzyme is only utilized upon ADH saturation and unlike ADH, is inducible by its many substrates. In chronic alcoholics, ADH is quickly saturated forcing CYP2E1 to be used.³⁷⁻³⁹ This increases its accumulation in the perivenous zone (zone 3) of the hepatic lobule. However, CYP2E1, unlike ADH, uses NADPH and molecular oxygen during the oxidation of ethanol, dramatically increasing the oxygen

demand of perivenular hepatocytes.⁴⁰ The simultaneous inhibition of TCA cycle leaves only the mitochondria respiratory chain available to regenerate NAD⁺ from NADH, further increasing oxygen demand. Taken together, it is widely accepted these processes result in increased oxygen consumption creating a hypoxic microenvironment in the liver prone to ROS-induced injury, particularly in zone 3.⁴⁰

Lipid Accumulation

As mentioned above, the metabolism of alcohol decreases the NAD⁺/NADH ratio, causing shifting hepatic metabolic end-points towards *de novo* triglyceride synthesis rather than β -oxidation. Additionally, it has been found that alcohol promotes steatosis via dysregulation of a number of nuclear factors that control lipid metabolism including; sterol regulatory element binding protein-1c (SREBP1c), liver retinoid acid X receptors (LXR and RXR), and peroxisome proliferator-activated receptors (PPARs).⁴¹⁻⁴⁴

PPARs are considered to be master regulators of metabolic function. Generally, they are directly regulated by many lipid-derived products such as prostaglandins, free fatty acids (FFAs), and as described later, pharmacological agents. Upon activation by its ligand, PPARs form heterodimers with RXR which then, in-turn bind its genomic peroxisome-proliferator responsive elements (PPREs). Within the umbrella of the PPAR family, there are three distinct isoforms, PPAR α , PPAR β/δ , and PPAR γ which have varied expression patterns with overlapping. Globally, the role PPARs/RXR are central to regulation of hepatic β -oxidation and *de novo* lipogenesis, primarily through SREBP1c.^{41,45}

While less studied in alcoholic liver disease, studies into the function of PPARs, and specifically, the roles of PPAR α and PPAR γ , have primarily been performed in models of non-alcoholic fatty liver disease (NAFLD).^{46,47} In models of NAFLD, it has been shown that while PPAR α expression decreases significantly, and this is associated with a corresponding increase in PPAR γ .^{46,48}

In models of chronic alcohol, the reduction of PPAR α expression and transcriptional activity in the liver has been well characterized, particularly due to its high level of hepatic expression when compared to other tissues.^{41,45} PPAR α functions to stimulate mitochondrial β -oxidation of fatty acids (FA) via carnitine palmitoyl transferase-1 (CPT-1) which is responsible for FA transport into the mitochondrial inner membrane.^{49,50} This inhibition of PPAR α results in decreased CPT-1 expression, decreased β -oxidation and the accumulation of toxic FFA within the liver.^{51,52} Importantly, both RXR-null and PPAR α -null mice, had worsened liver injury due to chronic alcohol. Pharmacologically, PPAR α agonists are within a class of amphipathic carbocyclic acids or fibrate drugs (fenofibrate). Initial indications included hypercholesterolemia, however, they are also being used for treatment of hypertriglyceridemia as well by stimulation of β -oxidation and inhibition of de novo lipogenesis.⁴⁶ Given the reduction in activity noted in ALD, studies have shown that PPAR α agonists may be able to reverse liver injury due to chronic alcohol.^{45,53}

As mentioned above, regulation of SREBP-1c is central to hepatic cholesterol and lipid homeostasis in NAFLD and ALD. While many factors have been shown to regulate SREBP-1c expression, few more so than PPAR- γ /RXR. PPAR- γ , is expressed at

significantly lower levels in the liver when compared to PPAR- α and in adipose tissue.⁵⁴⁻

⁵⁶ In models of NAFLD, it has been found that PPAR- γ directly activates SREBP-1c via binding to a PPRE within the SREBP-1c promoter, stimulating its expression. The increase in SREBP-1c drives *de novo* lipogenesis. Importantly rosiglitazone, a PPAR- γ specific agonist, enhances glucose uptake in response to insulin while also increasing SREBP-1c-mediated lipogenesis, enhancing hepatic steatosis.⁴⁸

Finally, insulin resistance is a significant factor in ALD progression. Alcohol consumption associated with metabolic syndrome has been shown to accelerate disease progression and mortality.⁵⁷⁻⁵⁹ Insulin resistance in animal models of chronic alcohol is well documented and results in increased macrophage infiltration within adipose tissue.^{57,59} The subsequent release of pro-inflammatory cytokines leads to a reduction in adiponectin, AMPK, and PPAR α , promoting FA synthesis.

Hypoxia & Hypoxia inducible factors.

As mentioned above, alcohol metabolism significantly increases oxygen demand within the liver, effecting zone 3 hepatocytes more than others in zone 3. Interestingly, the arteriovenous oxygen gradient within the liver is very different when compared to other capillary systems. Typically, oxygenated blood contains a partial pressure 74-104 mm Hg on the arterial side, and 34-46 mm Hg on the venous. In the liver this gradient is strikingly different. Zone 1, where oxygenated blood enters via the hepatic artery and is mixed with portal blood, the partial pressure of oxygen is 60-65 while the venous side, (perivenular, zone 3) is 34-46 mm Hg.⁶⁰⁻⁶³ As a reflection the difference in oxygen tension, there appears to be a difference in the metabolomics in hepatocytes depending

where they are along this gradient. Those in zone 1 hepatocytes typically express higher levels of enzymes relating to urea formation, glutathione conjugation, and glucose production enzymes.⁶⁰

Conversely, the zone 3 perivenous zone contains hepatocytes more suited to glucose uptake, glycolysis, and xenobiotic metabolism.^{60-62,64} Beyond differences in metabolic function, the differences in relative anoxia in these zones, mediates their susceptibility to hypoxic stressors. Hepatocytes incubated at periportal oxygen tensions were more resilient to cell death when compared to those cultured in perivenous oxygen environments.⁶⁵ Taken together, perivenular hepatocytes live at a threshold oxygen tension where they are susceptible to hypoxic or oxidative injury such as alcohol.

Indeed, as one would expect, given the inherent oxygen gradient in the liver, perivenular hepatocytes demonstrate substantially higher mRNA and protein expression of aptly named hypoxia-inducible factors (HIF) when compared to negligible expression in zones 1 and 2.

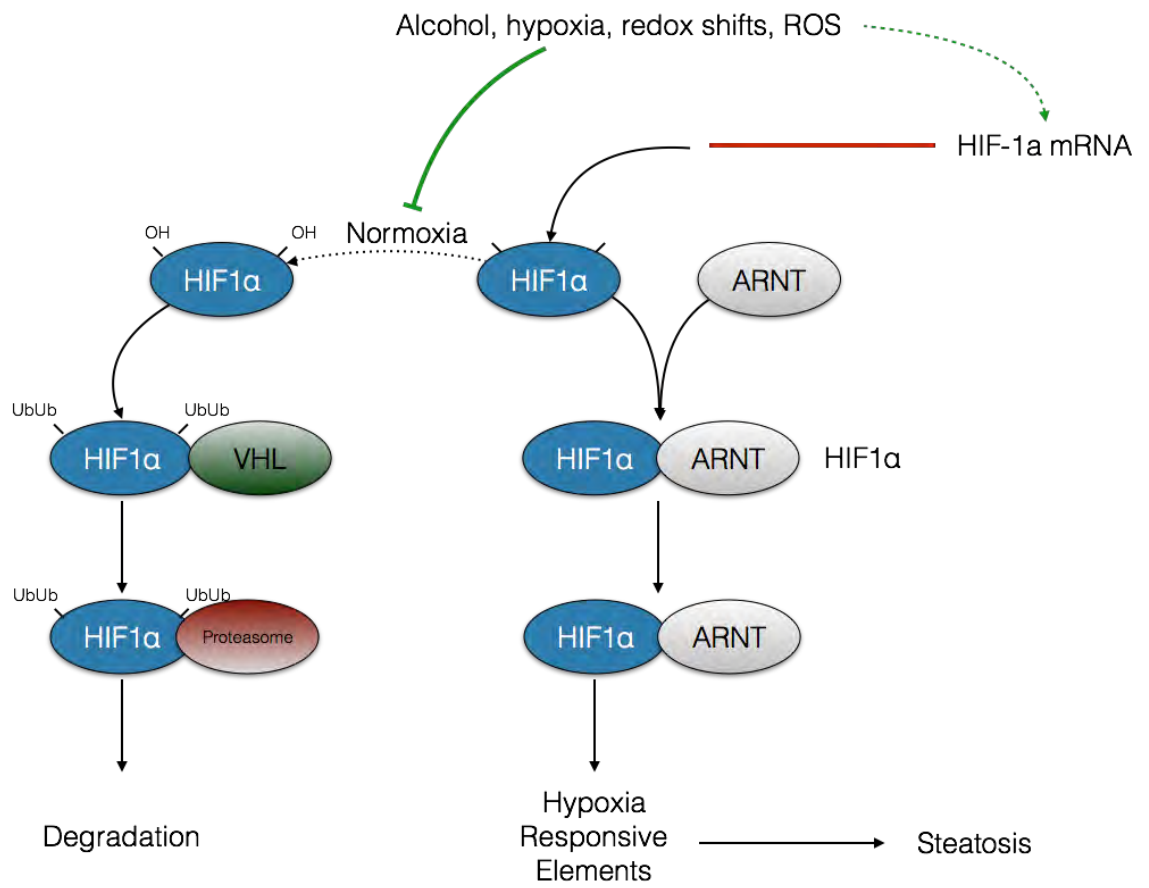
As a family, these transcriptional regulators function as heterodimers, containing an alpha and a beta subunit which bind to hypoxia-responsive elements (HREs) found within the promoter regions of the genes they regulate. Within the family of HIF proteins, there are 3 alpha subunits; HIF-1 α , and HIF-2 α , and HIF-3 α which are well conserved among multiple species. Additionally, there is a single beta subunit, HIF-1 β also referred to as aryl-hydrocarbon-nuclear receptor (ARNT).⁶⁰ Since there is only one common subunit, the active heterodimer is commonly referred to by their alpha subunit, (e.g. the HIF-1 α /ARNT heterodimer is called HIF-1 α), (Figure 1.2).⁶⁰

Under normoxic conditions, the alpha subunits of HIF are subjected to rapid hydroxylation by prolyl hydroxylases (PHDs) accompanied by a complex of scaffolding proteins, critically containing the Von Hippel-Lindau (VHL) protein. The binding of this complex leads to ubiquitination and subsequent proteasomal degradation.⁶⁶ In conditions of hypoxia or redox imbalances, the HIF proteins are able to escape hydroxylation, translocate to the nucleus to heterodimerize with ARNT, exerting their transcriptional activity.⁶⁷ It is key to mention, that while most hypoxic models have demonstrated that HIF-1 α mRNA either does not, or only slightly changes, and that regulation of its activity is only post-translational, it has been found that this can vary by cell type, frequency, and duration of the insult.^{68,69}

The association between hypoxia inducible factors and lipid accumulation has been described in a variety of tissues. Of note, overexpression of HIF-1 α in cardiomyocytes increased lipid accumulation and was noted to suppress PPAR α , while enhancing PPAR γ .⁷⁰ While a direct link has not been established for PPAR α , Krishnan et al determine that the PPAR γ promoter contains a conserved HRE ~1Kb upstream of the TSS.⁷¹ Furthermore, using mice homozygous for a mutated degradation resistant form of HIF1- α (HIF1dPA) mice they noted enhanced PPAR γ expression and FA uptake.

Figure 1.2: General schematic of HIF-1 α signaling

Under conditions of normal oxygen tension and balanced redox status, HIF-1 α subunits are rapidly hydroxylated at proline and asparagine residues. Hydroxylation facilitates complexation with the Von Hippel-Lindau (VHL) tumor suppressor, resulting in polyubiquitination at the hydroxylated sites followed by rapid degradation by the proteasome. However, conditions which result in overt hypoxia, shifts in cellular redox states, and exposure to toxic stimuli such as alcohol, the alpha subunits escape hydroxylation and degradation. As these proteins accumulate, they dimerize with the Aryl Hydrocarbon Nuclear Translocator (ARNT also known as the β subunit). The now active heterodimer, translocates to the nucleus activating target genes which contain hypoxia responsive elements in their upstream promoter region. In chronic alcohol, our lab has demonstrated that not only is there an accumulation of HIF-1 α protein, but alcohol also increases in HIF-1 α mRNA. Furthermore, this increase in HIF-1 α drives steatotic changes within hepatocytes.



In the liver, deletion of VHL, which leads to accumulation of all HIF subunits in hepatocytes is associated with significant steatosis.^{72,73} Mice homozygous for the HIF-dPA gene in hepatocyte develop hepatic steatosis as well, albeit to a lesser degree than VHL-knockouts, or degradation resistant HIF-2 α (HIF2dPA) mice which exhibited a steatotic phenotype similar to that of VHL knockout mice.⁷⁴ Subsequent studies using simultaneous knockouts of VHL and HIF-1 α or VHL and HIF-2 α , demonstrated that HIF-2 α may be stronger driver of lipid accumulation.⁷³

In alcoholic liver disease, there have been two studies into the role of HIF-1 α in alcoholic liver disease with conflicting results. Our lab has previously reported that alcohol increases HIF-1 α expression in hepatocytes and hepatocyte-specific HIF-1 α knockout mice (HIF1hepKO) were protected from chronic alcohol. Furthermore, HIF1dPA mice had evidence of steatosis in the control group that was augmented alcohol-induced liver injury. Collectively, the loss or increase in HIF-1 α was inversely correlated with Ppar α expression.⁷⁵ However, contrary to these findings and the role of HIF-1 α regulation of PPAR γ described above, Nishyama et al. in 2012 reported that HIF-1 α played a protective role and could suppress steatosis by enhancing β -oxidation in chronic alcohol by inhibiting SREBP-1c via its inhibitor, differential embryochondrocyte 1 (DEC1).⁷⁶ While the activation of DEC1 by HIF-1 α has been shown, these findings are contradictory to other studies demonstrating that HIF-1 α directly increases PPAR γ expression, a direct transcriptional activator of SREBP-1c, and a very well characterized enhancer of FA synthesis.^{54,71,77} This discrepancy of HIF-1 α has not been fully resolved.

Inflammation

Innate immune signaling due to activation of resident liver macrophages (kupffer cells, KCs) and infiltrating lymphocytes is critical to ALD pathogenesis. It is widely accepted that chronic alcohol exposure impairs the barrier function of the gut resulting in translocation of bacteria, and bacterial components into portal circulation and thus into the liver.^{78,79} In both humans and mice, chronic alcohol exposure is associated with increased circulating concentrations of lipopolysaccharide (LPS) which also correlates with the severity of liver injury.⁷⁹⁻⁸² While the interaction between LPS and toll-like-receptor 4 (TLR4) is the most studied in ALD, other bacterial components, collectively referred to as pathogen-associated molecular patterns (PAMPs), are also elevated in portal circulation.^{83,84} In the liver, LPS binds to pattern-recognition receptors (PRRs), specifically TLR4 on parenchymal and non-parenchymal cells of the liver. However, it is key to mention that once sensitized by alcohol, hepatocytes and immune cells within the liver readily respond via other innate immune receptors such as NODs 1/2, and TLRs 2/4 as well. TLR2 has been shown to recognize prokaryotic unmethylated CpG DNA (CpG DNA) while TLRs 2 and 6 recognize bacterial lipopeptides.^{83,84} Additionally, while I am describing the effects of alcohol on TLR and innate immune signaling pathways within immune cells, hepatocytes, and hepatic stellate cells have both been shown to express PRRs and respond to PAMPs as well.⁸⁵ In fact, hepatocytes specifically, in response to LPS, significantly up regulate a key cytokine in ALD pathogenesis, monocyte chemoattractant protein 1 (MCP1 or CCL2).⁸⁶⁻⁸⁸ Additionally, it has been shown that hepatocytes exposed to alcohol and infected with HCV, have

unregulated expression, and constitutive activation, of TLR4 driving neoplastic changes.⁸⁹

In kupffer cells, LPS, via TLR4, signal through MyD88 dependent and independent pathways to result in activation of MAP-kinases ERK1, ERK2, and JNK, as well as NFkB and AP-1. The activated KCs release pro-inflammatory cytokines TNF- α , IL-1B, and IL-6. KCs also contribute to the redox imbalance in the liver by producing ROS, via NAPDH oxidase.^{88,90-94}

Hepatocytes are traditionally resistant to the to the pro-apoptotic effect of TNF- α . However, chronic alcohol exerts a priming effect on hepatocytes for TNF- α -mediated cell death pathways.⁹⁵⁻⁹⁹ As mentioned before, depletion of mitochondrial GSH and SAM reduce mitochondrial integrity favoring mitochondrial transition pore formation.⁹⁷⁻¹⁰² Furthermore, it has been noted in mouse models and patients that chronic alcohol consumption increases TNF- α -receptor (TNFR).⁹⁵ A result of the increase in cell death is the release of sterile stimuli (immune ligands not derived from microbial pathogens), from damaged parenchymal and nonparenchymal cells. Collectively these are known as damage-associated molecular patterns (DAMPs).¹⁰³⁻¹⁰⁵ Multiple DAMPs, in coordination with alcohol and PAMPs, have been implicated in the pathogenesis of ALD, leading to the assembly of the inflammasome and activation of the serine protease, caspase-1, leading to the cleavage of pro-IL-1B to cleaved (active) IL-1B.^{84,103,104,106,107}

Peripheral leukocytes contribute to hepatic inflammation as well. As stated earlier, the histological characterization of steatohepatitis is the infiltration of lymphocytes, particularly neutrophils, into the liver parenchyma.⁷ Attracted by PAMPs

and cytokines, infiltrating neutrophils also respond strongly to PAMPs and DAMPs, enhancing liver injury. However, it is key to mention that the infiltration of leukocytes is beyond that of just phagocytic cells. A combination of cytotoxic T-cells, natural killer T-cells and circulating monocytes enter the liver to contribute to the pro-inflammatory state within the liver.⁸⁸

microRNA Biogenesis and Mechanism of Action

Background and Overview

Since their discovery of microRNAs (miRNAs) in 1993, over 500 have been discovered in the human genome.¹⁰⁸ These small molecules are 21-24 nucleotide (nt) RNA molecules that generally repress the expression of genes via Watson-Crick base-pairing to complementary sequences within target mRNAs.¹⁰⁹⁻¹¹¹ With each of these small molecules able to simultaneously inhibit hundreds of genes, and in many cases, through imperfect complementarity, studies have implicated them in the regulation of virtually every cellular pathway.¹¹¹⁻¹¹⁴ The expression patterns within different cells types are are equally as diverse. In many cases, individual miRNAs are “specific” or enriched within in a particular cell type or stage of development.

Their involvement in diseases has been well documented. Let-7, one of the first miRNAs described, functions as a tumor-suppressor where its loss promotes cancer cell growth.¹¹⁵⁻¹¹⁷ miRNAs have also been associated with mediating inflammatory responses from cytokine production to cellular differentiation; miR-155 induction can both directly stabilize TNF- α mRNA as well as promote inflammatory responses by targeting suppressor of cytokine signaling 1 (SOCS1), and M1/M2 macrophage polarization is regulated by miR-27a.¹¹⁸⁻¹²¹ In contrast to alterations in expression, microRNA-122 (miR-122), a highly abundant, liver-expressed miRNA is utilized by HCV as a host factor to promote viral replication. miR-122 binds to two closely spaced target sites in the 5' noncoding region (NCR) of the HCV genome, stabilizing viral RNA.¹²²⁻¹²⁴

The maturation of miRNAs is a complex process involving 5 major steps that are tightly regulated; transcription of miRNA primary transcript (pri-miRNA), the cleavage of the pri-miRNA into a pre-miRNA, export of the pre-miRNA from the nucleus to the cytoplasm, cleavage of the pre-miRNA to form a mature miRNA duplex, and finally its loading into the active RNA silencing complex. Given the complexity and multiple steps involved, any changes due to stressors or mutations can alter the functions or abundance of specific miRNAs leading to human disease (Figure 1.3).

Genomic loci

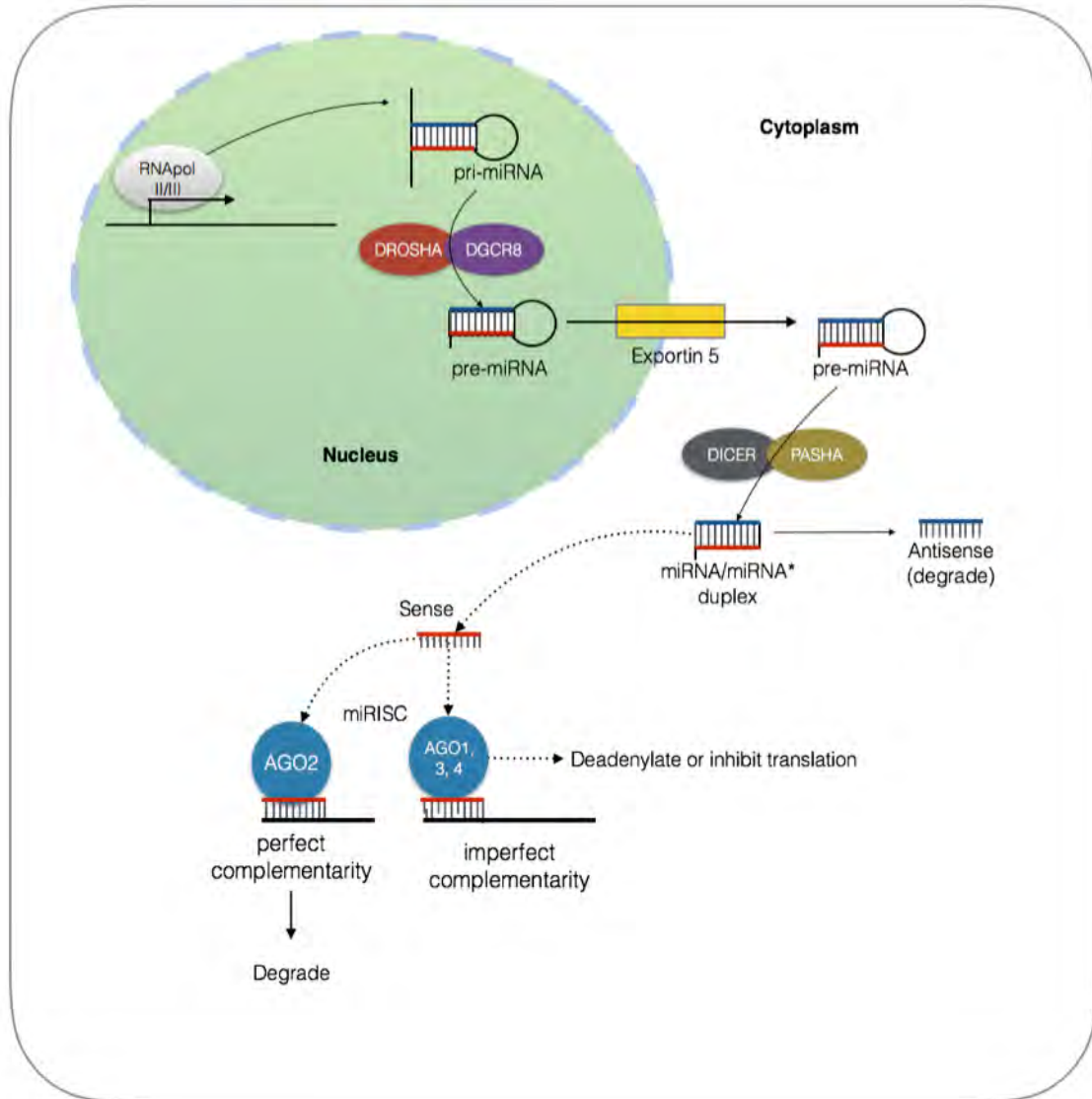
MiRNAs in animals are found in diverse genomic locations. Seventy percent of all miRNAs are derived from intronic regions, typically within a protein-coding gene, but they may also be found in exonic regions.¹²⁵ The remaining 30% are transcribed as independent ncRNA transcripts by RNA polymerase II (RNA pol II).^{125,126} These independently transcribed miRNAs can either code for individual miRNAs or clusters which contain anywhere from 2-7 miRNA genes.^{112,127} These clusters may, but not always, contain multiple miRNAs that have highly similar seed sequences, (nucleotides 2-7), the primary determinant of target recognition.¹¹⁴ For the purposes of this review, I will primarily focus on the mechanism and regulation of independently transcribed miRNAs derived from ncRNA transcripts.

Transcription of pri-miRNA and pre-miRNA processing

Most miRNAs are transcribed in an RNA pol II dependent fashion resulting in a primary transcript (pri-miRNA), which can vary in length from a few hundred

Figure 1.3: General Schematic of miRNA biogenesis

Most miRNAs are transcribed in an RNA pol II dependent fashion resulting in a primary transcript (pri-miRNA). The pri-miRNA transcript is very short lived, and is quickly processed into the pre-miRNA stem-loop which can even occur co-transcriptionally. This process is mediated by the microprocessor complex consisting of the RNase III enzyme DROSHA and the dsRNA binding protein, DGRC8. Once formed the pre-miRNA is transferred to the cytoplasm by exportin 5 (XPO5) hydrolyzing GTP to GDP in the process. This is considered to be a rate-limiting step in miRNA biogenesis, and if saturated, may be toxic to the cell. Once in the cytoplasm, the pre-miRNA is further cleaved by an enzyme complex containing the RNase II enzyme DICER and its binding partner PASHA. Subsequent to Dicer formation of the mature miRNA duplex, one of the strands (more thermodynamically stable) is loaded onto an Argonaute protein thus forming the miRNA-induced silencing complex (RISC or miRISC). The anti-sense, “passenger” or star (*) strand is quickly degraded. Guided by their seed region (nucleotides 2-8) of the miRNA, the RISC complex binds to target mRNAs leading to direct AGO2-mediated slicing or deadenylation/translational repression.



nucleotides to many thousands, with a 5' methylated cap and a 3' poly-A tail (Figure 1.3).

The result is a double-stranded short hairpin RNA (shRNA).¹²⁸⁻¹³⁰ Multiple studies have shown that the pri-miRNA transcript is very short lived, and that processing into the pre-miRNA stem-loop can even occur co-transcriptionally.¹³¹⁻¹³³ These transcripts contain promoter and enhancer elements similar to other RNA pol II regulated genes.^{110,111,134,135} Taken together, these studies indicate that pri-miRNA formation is solely controlled by RNA pol II processivity and the transcriptional regulatory environment in a particular cell.

Pre-miRNAs are ~66nt hairpins that have been liberated from their respective pri-miRNAs, in many cases co-transcriptionally, by a microprocessor complex which minimally contains an RNase III enzyme, Drosha, and DGCR8 (DiGeorge syndrome critical region gene 8).^{131-133,136-139} Drosha itself contains two RNase III domains and a double-stranded RNA binding domain (dsRBD).^{140,141} DGCR8 also has two additional dsRBDs which are also essential for binding to the pri-miRNA substrate.^{138,140} The result of the microprocessor complex cleavage of the pri-miRNA is a ~66nt stem-loop that contains a two-nucleotide overhang at the 3' end characteristic of RNase III enzymes.

Processing by the Microprocessor complex, Drosha/DGCR8, is subjected to complex regulation by positive and negative factors. Briefly, two additional proteins, p68 and p72 have been co-precipitated with Drosha and are essential for processing of specific miRNAs.¹⁴² It has been shown that p68/p72 may act as a bridge for other regulatory factors such as p53 and SMAD to fine-tune the maturation of specific

miRNAs.¹⁴³⁻¹⁴⁵ p53 is a transcription factor and tumor suppressor often activated during stress responses. Its function is to inhibit cell cycle progression while promoting apoptotic pathways.¹⁴³ p53 has been shown to stimulate transcription of certain miRNAs (pri-miRNA formation) in the miR-34 family, as well as directly stimulate microprocessor activity for other miRNAs via p68/p72.¹⁴⁶⁻¹⁴⁸ SMAD proteins, downstream of TGF- β signaling, can regulate miRNAs in two distinct ways.^{145,149} First, SMAD proteins have been shown to bind promoter elements at SMAD-binding elements (SBEs) activating or repressing transcription. Additionally, SMAD has been shown to bind similar SBEs found in the stem region of pri-miRNAs (r-SBEs). The binding of SMAD, recruits and stabilizes the interaction between p68, Drosha, and the pri-miRNA molecule, enhancing processing.^{144,150}

Nuclear export

To function and be processed as a mature miRNA, pre-miRNAs generated by DROSHA cleavage must be transported out of the nucleus to be processed by Dicer. As with most RNA nuclear transporters, the process uses the cofactor Ran-GTP.¹⁵¹ Once the RNA is transferred to the cytoplasm, GTP is hydrolyzed to GDP and the RNA is released.¹⁵¹ Once such exporter, exportin 5 (XPO5), preferentially recognizes structures of pre-miRNA products.¹⁵²⁻¹⁵⁵ XPO5 specifically distinguishes the 2 nucleotide overhang found on the 3' end after DROSHA cleavage, a loop of at least 5 nucleotides, and base pairings within the stem region of at least 15 nucleotides.¹⁵⁶⁻¹⁵⁸ In addition to its function as an exporter, it has been shown that XPO5 is also able to stabilize pre-miRNAs from exonuclease digestion.¹⁵⁸ Export of pre-miRNAs is presumed to be the rate limiting step

in miRNA biogenesis and its expression is closely tied with that of Dicer. Saturation of XPO5 by expression of synthetic shRNAs has been shown to saturate the transporter resulting in significant toxicity and represents a barrier to therapies seeking to increase miRNAs.^{155,159} This finding is of particular importance when considering miRNA therapeutics that utilize endogenous maturation pathways.

Dicer, Argonaunts, & RISC

Dicer, another RNase III enzyme is the final step in the formation of miRNA maturation.¹⁶⁰⁻¹⁶² Similar to DROSHA, Dicer also contains two RNase III domains, a dsRNA binding domain, however Dicer also contains a PAZ and a helicase domain.¹⁶³ The PAZ domain recognizes the 2-nt overhang left by DROSHA. Once recognized and loaded, Dicer simultaneously removes the both ends of the pre-miRNA loop structure, gauging this site by measuring 21-24-nucleotides from the 5' mono-phosphorylated end.¹⁶⁴

Dicer function can be regulated in many ways. Global miRNA maturation can be effected by endogenous targeting of Dicer mRNA by miRNAs themselves.^{161,165} In humans, let-7 has been shown to have three binding sites within the Dicer coding sequence and facilitate its degradation.¹⁶⁶ While Dicer is capable of cleaving pre-miRNA substrates without the use of cofactors, HIV-1 TAR RNA binding protein has been shown to enhance the reaction rate in mammalian cells through stabilization of Dicer.¹⁶⁷ Other proteins such as monocyte chemoattractant protein 1-induced protein 1 (MCP1P1), was shown to suppress miRNA maturation by degradation of pre-miRNA molecules.¹⁶⁸ MCP1P1 is induced during inflammatory responses and facilitates cleavage of pre-

miRNAs within the loop region blocking Dicer activity and inducing rapid degradation of the cleaved fragments.¹⁶⁸

Subsequent to Dicer formation of the mature miRNA duplex, one of the strands is loaded onto an Argonaute protein thus forming the miRNA-induced silencing complex (RISC).¹⁶⁹ There are two sub-categories of Argonaute proteins, Ago and Piwi, that are defined by the presence of PAZ (Piwi-Argonaute-Zwille) and PIWI domains.^{170,171} Of the eight total Argonaute proteins encoded within the human genome, Argonautes 1-4 are within the Ago-sub-category. All four Ago proteins are able to bind a mature miRNA to form a RISC complex, however, only Ago2 is capable of catalytically cleaving target mRNAs.^{170,171}

Often, Dicer cleavage will result in the release of a mature miRNA duplex. The strand that is loaded into miRISC is referred to as the “guide” strand while the other the “passenger” or star (*) strand.¹⁷² Initially, it was thought that these unloaded star strands were rapidly degraded, however, they too can be loaded into Argonautes and facilitate direct targeting and inhibition of complementary mRNAs.^{172,173}

Traditionally, the miRNA-Ago complex binds to the 3' untranslated region (UTR) of an mRNA silences its expression. Once bound to the target mRNA, Ago2 “slices” the loaded mRNA after the nucleotide paired to the 10th base of the small RNA guide. While efficient miRNA-mediated slicing requires complementarity between guide strand and the mRNA, in actuality, most miRNAs only partially base pair with their target mRNA. Specifically, nucleotides 2-8 of the miRNA (seed sequence) are required for miRISC assembly and slicing. In other cases, if sufficient complementarity is lacking throughout

the length of the miRNA rather than direct slicing, Ago interacts with cofactors that deadenylate and degrade the mRNA (Figure 1.3).¹⁷⁴ Additionally, miRNAs may also bind to the mRNA and block its translation into a protein, leaving the mRNA intact.^{113,170,171,175,176}

A less well understood stage in the life cycle of miRNAs is the stability of its mature form. The half-life of a mature miRNAs is directly related to the number of available targets. When loaded in the miRISC and bound to a target mRNA, mature miRNAs are protected from degradation.¹⁷⁷ However, contrary to this, perfect base pairing can also lead to increased rates of miRNA decay. Upon binding with perfect complementarity, Ago not only slices the target mRNA but the guide strand as well. In addition, the 3' end of mature miRNAs can be modified with the addition of either adenosines or uridines. One such instance is that of microRNA-122 (miR-122) and the cytoplasmic poly(A) polymerase GLD-2, which adds a single adenosine to the 3' end of 22-nt mature miR-122 resulting in a 23-nt product. The addition of this single nucleoside to miR-122 prevents exonuclease degradation.¹⁷⁸

microRNA-122: Biogenesis & Function

Background and Overview

In a study from 2002, Tuschl et al systematically cloned small RNAs from adult murine tissues. They found a number of miRNAs that exhibited high expression levels in certain tissues but negligible expression in others, none more so than miR-122.¹¹² When aligned to known sequence databases, miR-122 was linked to a woodchuck genomic sequence designated *hcr* (gi:51212) discovered in 1989 by Moroy et al.¹⁷⁹ In their study of HBV-induced liver tumors they found that most exhibited mutations or altered expression of known oncogenes, however, one tumor, W64, exhibited a unique chromosomal translocation.¹⁷⁹ They identified that the 5'-end of an unknown gene recombined with *c-myc*, increasing its expression 50-fold.^{180,181} The translocated segment aligned to a 4.5kb unspliced, polyadenylated non-coding RNA normally present in the woodchuck liver. They determined that this transcript had a small 37aa ORF at the 5'-end followed by a large 3'UTR which contained a 200-nt region upstream of the poly(A) site that was subjected to extensive endonucleolytic cleavage, with most of the transcript remaining within the nucleus.¹⁸¹ As it was later determined, the small 200-nt region within the 3'UTR was the miR-122 hairpin.^{112,182}

microRNA-122 (miR-122) was one of the first microRNAs to be identified as a “tissue specific”, constituting 70% of all hepatic microRNAs.¹⁸² In mice, miR-122 reaches maximum expression on embryonic day 17 (E17), at 50,000 copies per mature hepatocyte. Surprisingly, primary human hepatocytes were found to have 130,000 copies per cell while even a well differentiated (Huh-7) human hepatocellular carcinoma cell

line has 16,000 copies per cell. Taken together, this suggested that high miR-122 expression is a feature of a differentiated hepatocyte.¹⁸²

miR-122 Biogenesis

The miR-122 ncRNA gene is located on chromosome 18 in both mice and humans. Its transcription follows canonical miRNA RNA pol II-driven miRNA biogenesis pathways outlined above. The resulting ncRNA is ~4.5kb in size which is then processed into a 66nt pre-miR-122. While the full pri-miR-122 sequence is poorly conserved, the precursor hairpin and mature miR-122 has been found to be conserved in 18 vertebrate species, including zebrafish. No known orthologs have been discovered in species that do not have livers (i.e. drosophila or *C. elegans*).^{182,183}

As noted above, the expression of miR-122 sharply increases during embryonic liver maturation in both mice and humans, which suggested an essential role of miR-122 in hepatic development. Xu et al. were the first to characterize a conserved binding site for the liver enriched transcription factors (LETFs), hepatocyte nuclear factors (HNF) HNF1 α , HNF3 β , HNF4 α , and CCAAT/enhancer-binding protein (C/EBP) α within the promoter region and demonstrate its ability to enhance miR-122 transcription.¹⁸⁴ They determined miR-122 directly targets CUTL-1, a transcription factor which inhibits terminal differentiation of hepatocytes.¹⁸⁴ Subsequent work by Laudadio et al identified a unique role for yet another LETF member, HNF6 α , in miR-122 regulation.¹⁸⁵ This complex circuit, including HNF1 α , HNF3 β , HNF4 α , HNF6 α and C/EBP β , collectively function as master regulators of hepatic transcriptional activity.^{135,186-189} Dysregulation of this circuit was demonstrated in HNF6 α -knockout mice, which showed alterations in

hepatobiliary development, as well as significant decreases in miR-122 and many LETF components.¹⁸⁵

Further evidence to support this link was elucidated in the study of HCC tumors, which demonstrated a significant loss of multiple components of the LETF network with a concurrent reduction of miR-122.¹⁸⁴ Collectively, this complex circuit functions as a master regulator of hepatic transcriptional activity.

Interestingly, it was also found by that miR-122 transcription may be intricately involved with circadian rhythms. Gatfield et al determined that miR-122 transcription was regulated in a circadian manner by REV-ERB α .¹⁹⁰ Using REV-ERB α knockout mice, they demonstrated that miR-122 transcription was inhibited by REV-ERB α . While WT mice exhibited circadian fluctuations in pri- and pre-miR-122 levels, they found no change in mature miR-122.¹⁹⁰ This surprising finding could be due to its stability and long half-life maintained by the cytoplasmic poly(A) polymerase, GLD-2, which through the addition of an adenine to the 3' end, increase the half-life of miR-122.¹⁹¹ They also found that miR-122 can regulate Nocturnin, a clock-regulated deadenylase which post-transcriptionally regulates mRNAs through poly(A) tail removal, and Smarcd1 a Ppar-beta/gamma co-activator – both essential genes involved in regulation of hepatic lipid metabolism.^{190,192} However, given that the mature levels of miR-122 are unchanged throughout the day, it is unclear how miR-122 may regulate these genes in the normal liver. It has been suggested that modifications to the miR-122 structure such as those by GLD-2 described above may be the functional species that regulates these targets.¹⁹²

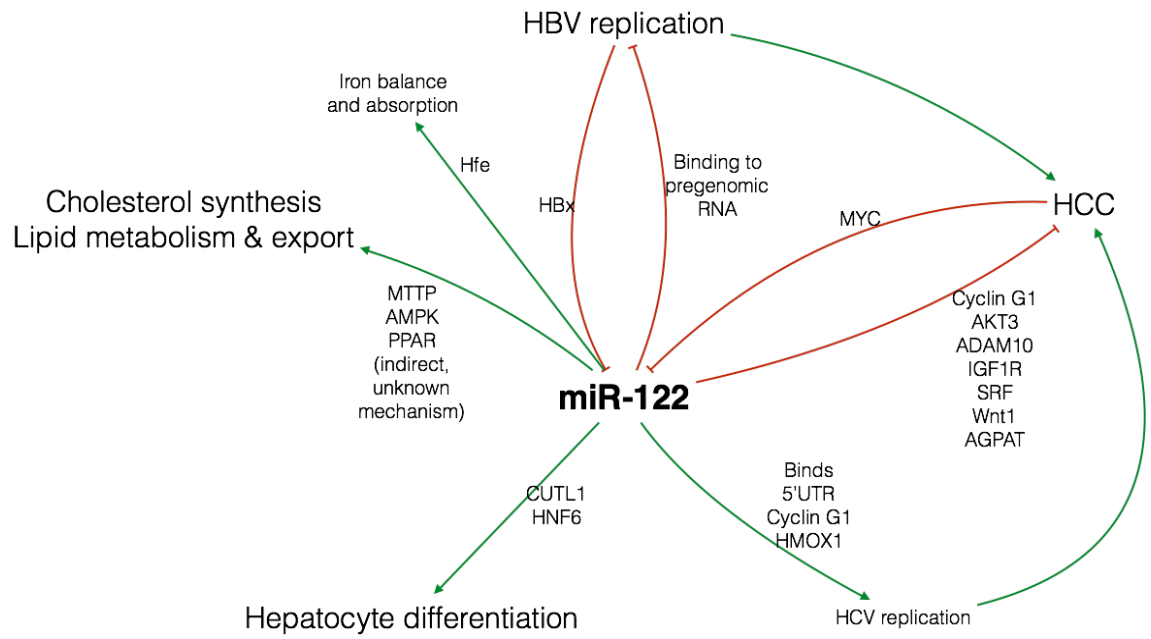
miR-122 in the serum

The pursuance for non-invasive biomarkers, particularly for the liver, has been an active field of work. miRNAs have demonstrated the presence of miRNAs in the circulation, urine, saliva, and various other body fluids.¹⁹³⁻¹⁹⁸ Increased miR-122 in the serum has been found in HCC, acetaminophen overdose, NASH, ALD, as well as HCV and HBV infection.^{193,195,196,199-208} In many of these studies, miR-122 has been shown to be a more sensitive and specific marker than traditional liver enzymes tests. These circulating miRNAs are either found in association with RISC proteins such as GW182 and Ago2, or within exosomes or microvesicles.²⁰⁹⁻²¹³ Of particular interest has been the presence of miR-122 in exosomes. These small 50-100 nm particles are released from every cell type in the body and more so during times of cellular stress.^{214,215} They have the ability to transfer functional miRNA, mRNA and protein laden cargo to target cells providing novel pathway for inter-cell communication. It has been shown that in response to APAP and LPS that exosomes from hepatocytes can transfer miR-122 to macrophages.²¹⁵ Furthermore, exosomes from chronically infected HCV patients can transfer replication-competent viral RNA, transmitting infection without a viral capsid.¹⁹⁹ The functions of miR-122 in the liver are schematically represented in Figure 1.4.

Given its abundance and specificity in the liver, it is unsurprising that miR-122 has diverse and pleiotropic effects on hepatic and even total body homeostasis. The first target of miR-122 identified was cationic amino acid transporter-1 (CAT-1). Chang et al

Figure 1.4: Schematic representation of key regulatory functions of miR-122 in hepatic and total body physiology and disease.

Green arrows indicate activation or positive regulation. Red blunted lines indicate inhibitory function. Adapted from Bandiera et al, 2014.²¹⁶



found that its expression was inversely correlated with increasing expression of miR-122 during fetal liver development. Furthermore, in the adult mouse, CAT-1 is detectable in nearly every tissue, but showed no discernable expression in the liver. It is key to note that the regulation of CAT-1 by miR-122 is uniquely complex. Upon exposure to a stressor, such as serum starvation the repression of CAT-1 by miR-122 can be released by the protein HuR. HuR serves to bind to CAT-1's 3'UTR, causing displacement from the miRISC and protecting it from degradation.

As discussed above, during hepatic development miR-122, coordinating with the LETFs in hepatocyte differentiation via CUTL1. The *ectopic* expression of miR-122 *in vitro* in isolated human and murine embryonic fetal liver and adipose-derived stem cells leads to differentiation and a hepatocyte phenotype. These findings correlate well in patients with acute liver failure, where those who survive were found to have higher hepatic miR-122 than non-survivors.²¹⁷ Further studies will have to be done to determine whether the noted increased miR-122 in surviving patients is maintaining hepatic function or a marker of a differentiated hepatocyte.

While being specific to the liver, miR-122 has profound effects on total body homeostasis. Systemic iron levels are regulated through the peptide hormone, hepcidin, which is produced in the liver. Castoldi et al demonstrate that knocking down miR-122 in the liver using a locked-nucleic acid (LNA), mice became iron deficient and anemic. They found that miR-122 regulated two key transcription factors which regulate the transcription of hepcidin, hemochromatosis (HFE) and hemojuvelin (HJV).²¹⁸

As discussed above, miR-122 has also been implicated in the regulation of the circadian control of metabolic genes in the liver through Noctrunin and Smarcd1. These studies however, were not the first to discover that found that knockdown of miR-122 could result in dramatic shifts in lipid and cholesterol metabolism. In 2005, Krutzfeldt et al utilized a cholesterol-conjugated 2'-O-methyl phosphorothioate ASO to knockdown miR-122 in the liver. They observed a 40% decrease in serum cholesterol and a coordinated decrease in genes involved in cholesterol biosynthesis.²¹⁹ Their findings initiated a succession of studies into the effect of miR-122 on hepatic and systemic lipid and cholesterol metabolism. Esau et al. published another study using 2'-O-methoxyethylphosphorothioate ASOs in mice fed a high-fat diet which revealed reduced serum cholesterol and hepatic triglycerides.²²⁰ Subsequent studies utilizing various techniques for miRNA inhibition such as AAV-delivered tough decoys (TuDs) and locked-nucleic acid (LNA) anti-miRs have confirmed these findings in rodents and non-human primates without any off-target or toxic effects.²²¹⁻²²³ This overwhelming evidence supported the claim that anti-miR-122 therapy to reduce serum triglycerides and cholesterol may be a potent cardio-protective therapy in patients suffering from metabolic disease.

miR-122 in HCV

One of the most revelatory findings of miR-122 has been its rather complicated role in stimulating HCV infection. HCV is a hepatotropic, sense strand RNA virus which chronically infects nearly 180 million people world-wide. As mentioned previously, HCV is a major risk factor for cirrhosis and HCC both independently and with alcohol.^{17,224,225}

Its approximately 10kb positive-sense RNA genome contains a single open reading frame with a flanking UTRs.²²⁶ In 2005, Jopling et al discovered two miR-122 binding sites within the 3'- and 5'-UTRs. Their study demonstrated that miR-122 base-pairing within the 5'UTR was required for viral RNA accumulation, and further that anti-miR sequestration of miR-122 led to a loss of HCV replicative ability.²²⁷ Two studies by Chang et al, and Narbus et al showed that expression of miR-122 could sustain active viral replication in HEK-293, and HepG2 cells, which have no detectible miR-122 and are typically not permissive to HCV infection.^{182,228,229} Further studies revealed that there are actually two binding sites for miR-122 in the 5'-UTR.²³⁰ When bound, miR-122 induces conformational changes to the HCV genome revealing an internal ribosome entry site, thereby increasing translation of the viral RNA. The stabilization of a target mRNA is uncharacteristic of miRNA-mRNA binding which typically leads to degradation of the target mRNA. It was shown that while Ago2 associates with the miR-122-HCV genome complex, the miRISC-complex actually protects the mRNA from exonuclease digestion.²³¹ Our lab has also shown that this stabilized complex can be released into serum within exosomes which can then transfer infectious viral RNA to target cells independent of a viral capsid.¹⁹⁹

It is also key to mention that there appears to be reciprocal regulation of miR-122 by HCV. miR-122 transcription was shown to be inhibited by interferon-beta (IFN- β). IFN- β , as part of the interferon system, is an integral part of a host's response against viral challenge suggesting that the inhibition of miR-122 by IFNs may be a defensive

response to HCV infection.²³² While the significance of these findings remains elusive, they speak to the complexity of the relationship between miR-122 and HCV infection

Together, these findings led Lanford et al to treat HCV infected chimpanzees with an 8-mer anti-miR-122 LNA against the miR-122 seed region led to a 300-fold reduction of miR-122 and a 2-log decrease in viral RNA in the serum and liver.²²² They also noted reduced liver injury by serum ALT and no observable viral resistance.²²² At present, the anti-miR-122 LNA, also known as miravirsin, is the first miRNA-targeted drug that has undergone successful phase 2a clinical trials to treat HCV infection.²³³

miR-122 in HBV

While also a hepatotropic virus, contrary to that of HCV, it has been found that miR-122 can inhibit HBV infection. Worldwide, there are twice as many people chronically infected with HBV than HCV, (350 vs 180 million) and also carries an increased risk of cirrhosis and HCC. Chen et al, found that transfection of a miR-122 mimic inhibits HBV expression while anti-miR-122 lead to increased HBV production in vitro. The result indicates that in contrast to HCV, miR-122 actually inhibits replication of the hepatotropic virus HBV, suggesting that therapies that increase miR-122 may be an effective strategy to limit HBV replication.²³⁴ It was determined that miR-122 down-regulates its target cyclin G1, thereby removing the interaction between Cyclin G1 and p53, and allowing p53 to bind to and inhibit the enhancer elements within the HBV genome.²³⁵

In patients they found that expression in the liver is significantly decreased in patients with HBV infection when compared to healthy, uninfected controls and the miR-

122 levels were negatively correlated with viral loads.²³⁵ Finally, it was shown by Song et al that HBV protein X protein specifically complexes with PPAR- γ and that this dimer inhibits the miR-122 transcription.²³⁶

miR-122 in NASH

As mentioned previously, the transient knockdown of miR-122 in the liver using ASOs has been shown to reduce serum cholesterol, implicating miR-122 in the regulation of cholesterol and lipid metabolism.²²¹ However, a dichotomy in the data emerged. One previous study has shown that ASO knockdown in the livers of high-fat diet fed mice reversed hepatic steatosis.²³⁷ It was found that miR-122 was reduced in murine models of non-alcoholic steatohepatitis (NASH). To better define the causal link between NASH and miR-122, two groups utilized germline and liver-specific knockouts of miR-122.

^{238,239}

While these knockout mice studies recapitulated the reduction of serum triglycerides and cholesterol seen in ASO-knockdown of miR-122, both germline and liver-specific knockout mice developed spontaneous, progressive steatohepatitis.^{238,239} Hsu et al, utilizing hepatocyte-specific knockouts (122LKO) determined that this was due to an increase in a large swath of genes associated with triglyceride synthesis such as *Agpat1*, a direct miR-122 target, *mogat1*, *agpat3*, *agpat9*, *Ppap2a*, and *Ppap2c*. Furthermore, they found up-regulation of *Cidec*, another miR-122 target and a protein that inhibits lipolysis while also enhancing triglyceride accumulation.²³⁸

Also finding the same phenotype of spontaneous steatosis, Tsai et al explored the role of microsomal triglyceride transfer protein (MTTP) which was reduced in their

germline miR-122 knockout (122aKO) mice. MTTP typically enhances lipoprotein assembly for export. As confirmation, ectopic expression MTTP reversed the reduced serum triglycerides and cholesterol seen in the knockout mice as well as reversed the NASH phenotype. However, MTTP is not a direct target of miR-122 and the mechanism by which it is regulated has yet to be determined.²³⁹

Notably, knockout mice from both groups spontaneously developed steatosis, inflammation and eventually progressed to liver fibrosis and HCC.^{238,239} They also showed significantly increased infiltration of F4/80⁺ macrophages and CD11b^{hi}Gr1⁺ populations of immune cells producing IL-6 and TNF- α which they suggested drove hepatic stellate cell (HSC) activation. In addition, they proposed that the increase in KLF6 in HSCs, secondary to an increase in TGF- β , a miR-122 target, may play a role in driving fibrosis.²³⁸ However, Hsu and colleagues suggested that this was mediated by a chemokine, Ccl2 (MCP-1 or macrophage chemoattractant protein 1), which they found to be a weak, but direct target of miR-122.²³⁹ Interestingly, upon restoration of Mttp in 122KO mice, they observed not only a resolution steatosis but reduced inflammation and fibrosis as well.²³⁹ Therefore, these studies imply that there may be minor effects on stellate cells and immune cells from the loss of miR-122 in hepatocytes, their activation is secondary to the hepatocyte steatosis and injury.

miR-122 in HCC

The first paper published on the discovery of miR-122 by Chang et al. in 2004, showed decreased miR-122 copies in cancer cell lines.¹⁸² It was not until 2006 that a survey of primary rodent and human HCCs found a reduced level of miR-122 when

compared to matched normal tissue.²⁴⁰ A wealth of studies that followed have confirmed the role miR-122 as a tumor suppressor, regulator of EMT, and angiogenesis.^{122,216,241,242} In vitro experiments have also showed that ectopic expression of miR-122 can also sensitize tumor cells to the multi-kinase inhibitor Sorafenib and the DNA intercalating agent Doxorubicin.^{243,244}

However, the most direct evidence resulted from the aforementioned 122aKO and 122LKO mice, which not only developed progressive spontaneous steatohepatitis, but metastatic HCC after a year of life. Furthermore, using a potent hepatic carcinogen, diethylnitrosamine (DEN), 122LKO mice were found to be predisposed to pre-neoplastic hepatobiliary cysts as early as 8 weeks after exposure.²⁴⁵ Using an AAV8-miR-122, Hsu et al were able to reduce, but not negate, tumor burden in 122LKO mice. Subsequent human studies have shown that that reduced levels of miR-122 is correlated increased HCC metastasis and poorer prognosis.^{16,246,247}

Mutations associated with miR-122

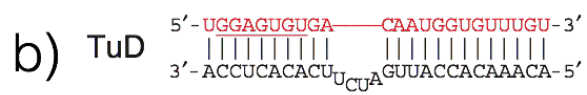
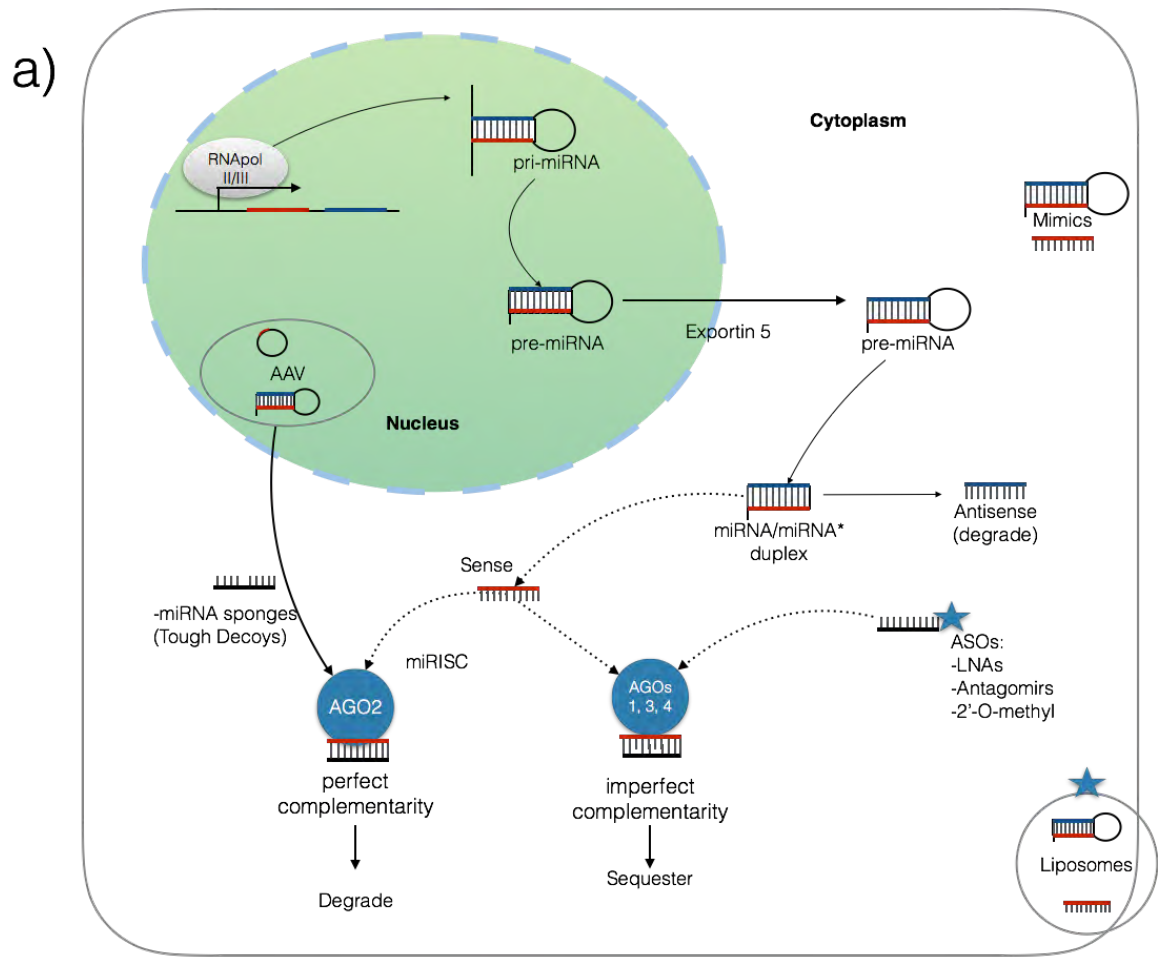
There have been no known single nucleotide polymorphisms (SNPs) detected with the mature miR-122 sequence. However, two SNPs, rs4309483 and rs4503880, were detected in the 5' regulatory region of human Mir-122 gene in patients of Han Chinese decent. The former SNP has been suggested to increase the risk of HCC in HBV infected patients.²⁴⁸ The ENCODE project has also identified another SNP, rs41292412, a C to T, that is located on the miR-122-3p (antisense or miR-122*) strand, though its significance is unknown.

miRNA modulation and therapeutics

As described above, many of the studies into the function of microRNAs in cellular processes requires modulation of miRNA abundance or function in vivo and in vitro. Currently there are two main classes of miRNA inhibitors; antisense oligonucleotides (ASOs) or miRNA sponges. Antisense oligonucleotides themselves are broadly characterized as a short nucleic acid sequence complimentary to their target RNA molecule, where in their traditional use were used to inhibit mRNA translation or facilitate RNase H-mediated degradation.²⁴⁹ Within the classification ASOs there are antagomirs, locked nucleic acids (LNAs), and tiny LNAs. Antagomirs are single stranded RNA molecules that are fully complementary to their target miRNA.²⁵⁰ Chemical modifications at the 2'-carbon such as additions of -O-methyl, 2'-methoxyethyl, 2'-fluoro (in order of increasing stability), as well as a partial phosphorothioate backbone have significantly increased stability.²⁵¹ Furthermore, the addition of a cholesterol moiety to the 3' carbon has facilitated increased uptake of these antagomirs.²¹⁹ However, the greatest leap in ASO stability has been the synthesis of locked nucleic acids (LNAs).^{223,252} These modified 13-22-nt long antgomiRs contain a methane bridge connecting the 2'-oxygen to the 4'-carbon of their ribose ring.²⁵³ This modification maintains the C3'-endo conformation, which promotes RNA:RNA interaction, and prevents a conformational change to its C2'-endo state, which does not. Given that the of the specificity of an antagomir is covered primarily by its seed region, it was

Figure 1.5: Mechanisms for miRNA modulation.

miRNA biogenesis and therapeutic delivery. miRNA function can be inhibited by using chemically modified antisense oligonucleotides (ASO) such as lock nucleic acid (LNA), antagomirs, 2'-O-methyl typically resulting in sequestration of the target miRNA. To increase stability and tissue specific delivery both ASOs and liposomes have chemical modifications to backbone chemistry have increased stability ASOs while conjugating of molecules such as GalNac and PEG to liposomes and ASOs alike have facilitated enhanced target cell specificity. Use of ASOs, Nanoparticles, or adeno-associated vectors (AAV) can be used for tissue-specific anti-miRNA and miRNA mimic delivery through modification of the outer surface of the lipid bilayer. For overexpression of a particular miR, miRNA mimics can be used directly however, delivery of a miRNA containing transgene via AAV results in specific and sustained mimic expression. Furthermore, depending on complementarity of sense strand to target gene, either the target miRNA is degraded or sequestered. (b) Schematic representation of anti-miR-122 tough decoy (TuDs). AAVs are also capable of delivering modified miRNA inhibitors, tough decoys (TuDs). Rather than perfect 1:1 binding to their target miRNA, TuDs contain a four-nucleotide insert at the Ago2 cleavage site protecting the TuD from nuclease cleavage. Image adopted from Xie. et al. 2012.



discovered that truncation of the LNA to be only 8 nucleotides long and complimentary to nucleotides 2-8 of the target miRNA, corresponding to its 5' seed region was sufficient to maintain robust, and specific inhibition.^{223,254}

While LNAs have been shown to strongly and specifically inhibit their targets, these modalities require repeated intravenous doses leading to systemic distribution and uptake in multiple organ systems. As the issue of cell and organ specificity still remains, much work has been put into conjugation and packaging strategies for targeted delivery. Recently, it has been shown that the addition of a N-acetylgalactosamine (GalNac) conjugation results in robust delivery to hepatocytes via sub-cutaneous delivery.²⁵⁵ Alternatively, the use of liposomes and lipids, have gained attention. These particles consist of cationic lipid bilayers able to bind their anionic cargo resulting in a positively charged liposome able to bind the anionic surface of target cells.^{256,257} Further, the addition of surface modifications such as polyethylene glycol (PEG), or peptides can facilitate cell or organ specific delivery. Once attached, the head groups of these lipids can be modified to facilitate release in either the nucleus, cytoplasm, or endosome.²⁵⁸⁻²⁶⁰

miRNA sponges, or decoys, are RNA pol II driven transcripts that produce a product containing multiple sites for a specific miRNA which were designed to sequester these target miRNAs.²⁶¹ Subsequently, miRZips and tough-decoy RNAs (TuDs) were developed which were transcribed either by H1 or U6 based RNA pol III promoters respectively, and optimized to facilitate efficient nuclear export.^{261,262} Once in the cytoplasm, The H1-driven miRZip contained a single hairpin complimentary to the target miRNA leading to degradation of both target and miRZip. Like traditional miRNA

decoys, TuDs express a transcript with multiple perfectly complementary miRNA binding sites along its length, however, TuDs contain a four-nucleotide insert at the Ago2 cleavage site protecting the TuD from nuclease cleavage (Figure 1.5b).^{221,261} This modification allows for long-term inhibition of a target miRNA after a single treatment. Recently, Xie et al demonstrated that a single intravenous dose rAAV9-delivered anti-miR-122 TuD robustly inhibited miR-122 in murine livers for over 25 weeks.^{221,261,262}

Unlike that of antimiR approaches, the restoration of a miRNAs can be accomplished with either miRNA mimics or pri-miRNAs encoded within expression vectors. miRNA mimic molecules are double-stranded synthetic miRNA oligonucleotides that, when transfected into cells, are processed into a mature miRNA. However, their use *in vivo* is limited by their stability and inefficient delivery, requiring the use of nanoparticles, or liposomes.^{259,263} Most effective has been the use of recombinant adeno-associated virus (rAAV) delivery of pri-miRNA expression vectors.²³⁸ These non-replicating viruses have been effectively used to express genes or miRNAs in the liver. Through discovery and manipulation many serotypes have been found that exhibit varying degrees of cellular tropism and immunological memory in the population.^{264,265} While many AAVs have been discovered and engineered, with respect to the liver, AAV8 holds the greatest promise for use *in vivo*.²⁶⁶⁻²⁶⁸ In fact, recent clinical trials in the UK using rAAV8 vectors to treat Hemophilia B deficiency has demonstrated that a single peripheral-vein dose can safely and effectively achieve sustained transgene expression for 5 years after treatment.^{264,265,269} Vectors can also be used to increase specificity by engineering cell specific promoters that limit non-specific expression. It is key to

mention that the over expression of short hairpin RNA in rats has been shown to cause hepatotoxicity, organ failure, and death.¹⁵⁹ This has been associated caused by the saturation of exportin-5 which appears to limit miRNA production in cells to tolerable levels.^{159,270-272} However, accurately titrating doses, optimization of the promoter, as well as designing transgenes to produce pri-miRNAs that more accurately mimic endogenous transcripts may mitigate these toxic effects.

CHAPTER 2: ALCOHOL, MIR-122 AND HIF-1ALPHA

Summary

The loss of miR-122 has been clearly demonstrated in stages of advanced NASH and HCC correlating with poor prognoses. However, its role in acquired, pre-neoplastic liver disease and specifically alcoholic liver disease, has not been explored. Previous studies have demonstrated the inverse correlation between miR-122 and its putative primary target, HIF-1 α . The increase in HIF-1 α due to chronic alcohol, and its role in ALD pathogenesis has been studied. In this chapter I offer evidence to suggest that miR-122 is reduced in patients with alcoholic cirrhosis, and mice fed chronic alcohol. Further, I find that this reduction is specific for hepatocytes and not only inversely correlates with HIF-1 α expression but that HIF-1 α is directly regulated by miR-122.

Acknowledgements

Thank you to Karen Kodys for the procurement of human liver samples, to Timea Csak and Shashi Bala for assistance in miR-122-HIF-1 α in vitro experiments. I would also like to thank Ying-Chao Hsueh for his help with the HIF-1 α 3'UTR studies. I am also grateful to services provided by DERC morphology (H&E sections) and CFAR (Primer Synthesis) core facilities at UMASS Medical School.

Introduction

Liver disease is a major cause of death in the United States and has been increasing in recent years. Chronic alcohol consumption accounts for nearly 50% of these cases and few specific therapies exist for patients.¹¹ While the early steatosis in ALD is reversible, chronic, excessive alcohol consumption is the single greatest risk factor of hepatocellular cancer (HCC).^{14,15,273}

Alcohol-triggered hepatocyte steatosis and cell death results in the activation and infiltration of immune cells within the liver leading to advanced hepatic injury. The subsequent release of inflammatory cytokines causes further hepatocyte cell death resulting in a feedback mechanism, driving ALD pathogenesis.^{11,14,15} The standard of care with steroid treatment has little benefit and recent clinical trials using pentoxifylline showed little efficacy. Thus, identification of novel therapeutic targets is a major need in ALD.²⁷⁴

Hepatic microRNAs (miRNAs) have crucial roles in maintaining total body homeostasis, mitochondrial function, and oncogenesis. miR-122 constitutes 70% of all miRNAs in mature hepatocytes, or approximately 130,000 copies per cell, with negligible expression in other tissues.¹⁸² It has been found to regulate key pathways in lipid metabolism. Germline deletions of miR-122 display steatosis at birth, spontaneous progression to fibrosis, and HCC.²³⁸ In humans, miR-122 expression inversely correlates with HCC survival and metastasis while miR-122 inhibition reduces HCV viremia, serum triglycerides, and cholesterol.^{16,228,275} These observations suggest that miR-122 may have diverse and pleiotropic effects on hepatocytes and liver diseases warranting further

exploration of its role in alcoholic liver disease. Specifically, given that the loss of miR-122 results leads to hepatic steatosis and injury patterns similar to ALD pathogenesis, I hypothesized that the loss of miR-122 due to alcohol may regulate ALD pathogenesis.

Our lab and others have demonstrated the essential role of HIF-1 α in driving hepatic steatosis and hepatic injury in high-fat diet, alcohol, and hypoxic liver injury. Specifically, our lab has previously determined that chronic alcohol administration in mice leads to an up-regulation of both HIF-1 α mRNA and protein in hepatocytes, which drives lipogenesis. Stimuli that induce HIF-1 α activity classically result in stabilization of the HIF-1 α protein and not due to changes at the mRNA level. Briefly, during normoxia, HIF-1 α is quickly proline hydroxylated, ubiquitinated, and subsequently degraded by the proteasome. During hypoxia HIF-1 α is not hydroxylated and therefore protected from degradation, increasing its half-life. The accumulation allows for dimerization with its constitutively expressed beta subunit, ARNT. The HIF-1 α /ARNT complex translocates to the nucleus acting its target genes, driving steatosis.

Using seed matching algorithms, I have determined that HIF-1 α is a putative target of miR-122. I hypothesized that the increase in HIF-1 α mRNA noted in chronic alcohol could be due to a decrease in miR-122. Furthermore, I hypothesized that miR-122 regulates HIF-1 α through canonical miRNA pathways via bindings its 3'UTR.

In this chapter I characterize the expression patterns of miR-122 and HIF-1 α in the livers of patients with alcoholic cirrhosis when compared to healthy controls and HCV-infected patients and in mice exposed to chronic alcohol. Furthermore, using HIF-

1 α 3'UTR-luciferase, my data indicates that miR-122 regulates HIF-1 α through 3'UTR-mediated miRNA silencing mechanisms.

Methods

Procurement of Human Specimens

Paraffin embedded blocks and flash frozen human liver tissue was obtained from healthy controls, alcoholic cirrhosis, and HCV cirrhosis, were obtained through the Liver Tissue Cell Distribution System, Minneapolis, Minnesota, which was funded by NIH Contract # N01-DK-7-0004/HHSN26700700004C.

Animal Studies

All animals received care in compliance with protocols approved by the Institutional Animal Use and Care Committee (IACUC) of the University of Massachusetts Medical School. Wild-type (WT) mice (C57/B16), Alb-Cre, and HIF-1 α ^{flox/flox} mice were purchased from Jackson Laboratories (Bar Harbor, ME) and backcrossed onto a C57/B16 background. 6-8 week old mice were gradually acclimated to a Lieber-DeCarli liquid diet with 5% ethanol (vol/vol) over a period of 1 week, then maintained on the 5% diet for 4 weeks (total of 5 weeks). Consumption was recorded daily and isocaloric amounts of a control diet (in which dextran-maltose replaced calories from ethanol) were dispensed to pair-fed (PF) animals. Weights were recorded weekly. At the conclusion of the 5-week feeding, mice were weighed, blood collected, and euthanized. Livers were dissected, weighed and divided into lipid nitrogen for protein and biochemical assays, fixed in 10% phosphate-buffered formalin for histological analysis,

preserved in OCT frozen section preparation solution, or soaked in RNALater (Qiagen, Hilden, Germany, Hilden, Germany).

Blood was allowed to clot and serum obtained using gel-based serum separator tubes.

Isolation of primary mouse hepatocytes and LMNCs

Anesthetized animals were perfused by way of portal vein with saline solution, followed by enzymatic digestion, as previously described.⁷⁵ The hepatocytes were separated by centrifugation, and LMNCs were purified by centrifugation in Percoll gradient followed by CD45+ microbead selection using MACS LS columns (MACS). In vitro experiments. Primary hepatocytes were cultured in low-glucose DMEM supplemented with 10% fetal bovine serum, 1% Anti-Anti, 1% gentamycin, 1% insulin, transferrin, selenium solution. Primary hepatocytes were seeded in 6-well collagen-coated plates (Biocoat, Becton Dickinson). Before starting stimulation experiments, hepatocytes were rested for 4 hours.

RNA extraction and real-time PCR

Total RNA was extracted using the Quiagen miRNeasy kit (Qiagen, Hilden, Germany, Hilden, Germany) according to the manufacturer's instructions. Briefly, tissue samples were lysed in QIAzol Lysis reagent (Qiagen, Hilden, Germany, Hilden Germany), homogenized with stainless steel beads in TissueLyser II (Qiagen, Hilden, Germany) followed by miRNA isolation following manufacturer's instructions and

DNase 1 Digest. RNA was quantified using Nanodrop 2000 (Thermo Scientific, Waltham, MA). Complementary DNA (cDNA) synthesis was performed by reverse transcription of 1 ug total RNA using the iScript Reverse Transcription Supermix (Bio-rad, Hercules, CA). Real-time quantitative PCR was performed using Bio-Rad iTaq Universal SYBR Green Supermix and a CFX96 real-time detection system (Bio-Rad Laboratories, Foster City, CA). Primers were synthesized by IDT, Inc. The primer sequences are listed in Table 2.1. Relative gene expression was calculated by the comparative cycle threshold (Ct) method. The expression level of target genes was normalized to the house-keeping gene, 18S rRNA, in each sample and the fold-change in the target gene expression between experimental groups was expressed as a ratio. Melt-curve analysis was used to confirm the authenticity of the PCR products.

miRNA Analysis

Reverse transcription (30 min - 16°C; 30 min - 42°C; 5 min - 85°C) was performed in Eppendorf Mastercycler (Eppendorf, New York, USA) using 10 ng RNA, TaqMan primers and miRNA Reverse Transcription Kit (Applied Biosystems,) followed by quantitative RT- in CFX96 (Bio-rad, Hercules, CA) using TaqMan Universal Probes Master Mix (Bio-rad, Hercules, CA). All samples were normalized to snoRNA202, or U6 expression based on Normfinder (<http://moma.dk/normfinder-software>) analysis of loading control stability. hsa-miR-122-FAM, U6-FAM, and sno202-FAM primer sets were purchased from Applied Biosystems.

HIF-1 α 3'UTR

All cells were seeded into 96 well plate 24 hours ahead of Lipofectamine 3000 (Thermo Fisher)-based transfection. HIF-1 α 3'UTR-luciferase reporter (Origene) and with renilla luciferase plasmid were co-transfected, miR-122 mimic or scrambled mimic

Table 2.1 qPCR and cloning primers used in this study

Table 1:	Primers used in this study	
Gene	Forward Primer – 5'-3'	Reverse primer – 5'-3'
mTNF α	CACCACCATCAAGGACTCAA	AGGCAACCTGACCACTCTCC
mMCP-1	CAGGTCCCTGTCATGCTTCT	CAGGTCCCTGTCATGCTTCT
mActa2	GTCCCAGACATCAGGGAGTAA	TCGGATACTTCAGCGTCAGGA
mCollagen1a1	GCTCCTCTTAGGGGCCAT	CCACGTCTCACCATTGGG
mHIF1 α	CAAGATCTCGGC GAAGCA A	GGTGAGCCTCATAACAGAAGCTTT
mHNF4	AGCTCGAGGCTCCGTAGTGTTT	GAAAATGTGCAGGTGTTGACCA
mF4/80	TGCATCTAGCAATGGACAGC	GCCTTCTGGATCCATTTGAA
mCD68	CCCACAGGGCAGCACAGTGGAC	TCCACAGCAGAAGCTTTGGCCC
mIL-1B	CTTTGAAGTTGACGGACCC	TGAGTGATACTGCCTGCCTG
mHNF6	TTCCAGCGCATGTCGGCGCTC	GGTACTAGTCCGTGGTTCTTC
mPPAR- γ	GGAAGACCACTCGCATTCTT	TCGCACTTTGGTATTCTTGGAG
m/h18s	GTAACCCGTTGAACCCATT	CCATCCAATCGGTAGTAGCG
hGRHL2	GAAAGTCCAGTTTCACCAGAGG	GGCACTAAGGCCACTAGTCTTTT
mGRHL2	GGATGTGAACGAGGAGGCAAAG	CTGGCAGTATGCTCTGTGGATG
hGRHLmut	GAGAAAGGGAAGTTGGGGTTCTGAGGGG	TTAACGTTCTCACGGGAAGACTG

(ThermoFisher Scientific) into HEK293T cells for 36 hours, followed by Dual Luciferase Assay (Promega) according to manufacturer's instruction.

miR-122 regulation of HIF-1 α

For overexpression of miR-122, primary murine hepatocytes were isolated from chow fed female mice. Cells were transfected with either pre-miR-122, or pre-miR-negative control #1 (10nM) (Ambion) using Lipofectamine RNAiMAX transfection reagent (ThermoFisher Scientific). To inhibit miR-122 function, primary murine hepatocytes were transfected with either anti-miR-122 or anti-miR-negative control #1.

Biochemical Assays

Serum alanine aminotransferase (ALT) levels were determined using a commercially available reagent (Advanced Diagnostics Inc) as described. Serum alanine aminotransferase (ALT) was determined using a commercially available reagent (Advanced Diagnostics Inc, Plainfield, NJ). 15ul of serum was mixed 1:10 with assay reagent diluted according to the instructions of the manufacturer, and UV absorbance at 37 degrees Celsius was measured over three minutes. The average change in absorbance per minute interval is then multiplied by a conversion factor to yield ALT levels.

Liver triglycerides were extracted using a 5% NP-40 lysis solution buffer. Triglycerides were quantified using a commercially available kit (Wako Chemicals) followed normalization to protein amount.

Protein concentration was determined by by BCA protein assay (ThermoFisher Scientific) by using 10 uL of 1:10 or serially diluted lysate and incubating in assay reagent for 30 minutes at 37 degrees C. Absorbance was measured at 562nm on a 96 well

plate using a plate reader. Concentrations were interpolated using 4-PL regression derived from a standard curve generated using bovine serum albumin standard (Pierce).

Nuclear Extraction

50mg of snap-frozen liver tissue was washed in 10-fold excess volume TKM-0.32 buffer (0.32M sucrose, 50mM Tris-HCl, 25mM KCl, 5mM MgCl, 5mM PMSF), with protease inhibitor tablets 1 per 10 mL, (Roche) and homogenized using a hand-held homogenizer. Homogenates were transferred to microcentrifuge tubes and centrifuged (1000rpm for 10 minutes at 4 degrees C). Pelleted material was resuspended in TKM-2.0 buffer (2M sucrose, 50mM Tris- HCl, 25mM KCl, protease inhibitor cocktail) and homogenized again by handheld homogenizer. Pellets were collected by centrifugation (14000rpm for 30 minutes at 4 degrees C) and resuspended in 500ul Buffer A (10mM Hepes/KOH, pH 7.9, 2mM MgCl, 1mM EDTA, 10mM KCl, 1mM DTT, 5mM PMSF, 1 protease inhibitor tablet). Pellets were again collected by centrifugation (14000rpm for 30 minutes at 4 degrees C) and resuspended in 50ul Buffer B (10mM Hepes/KOH pH 7.9, 2mM MgCl, 1mM EDTA, 50mM KCl, 300mM NaCl, 2mM DTT, and 5mM PMSF with protease inhibitor tablets 1 per 10 mL, (Roche), 10% glycerol. Pellet was resuspended was sonicated at 40% duty cycle 1 second on/off cycle, frozen at -80 degrees overnight, and thawed with gentle agitation at 4 degrees celcius. Supernatant containing nuclear extract was collected after centrifugation (14000rpm for 30 minutes at 4 degrees C) and assayed for protein concentration.

Electrophoretic Mobility Shift Assay

The DNA binding activity of HIF-1 α was assessed by electrophoretic mobility shift assay as described previously (Nath B., *Hepatology*. 2011 May;53(5):1526-3).⁷⁵ A consensus double-stranded Hypoxia Response Element (HRE) (Santa Cruz Biotech, CA) oligonucleotide was used for EMSA. End-labeling was accomplished by treatment with T4 kinase in the presence of [P32]ATP. Labeled oligonucleotides were purified on a polyacrylamide copolymer column (Bio-rad, Hercules, CA). Five micrograms of liver or hepatocyte nuclear protein was added to a binding reaction mixture containing 50 mM Tris-HCl, pH 7.5, 5 mM MgCl₂, 2.5 mM EDTA, 2.5 mM DTT, 250 mM NaCl, 20% glycerol, 20 &g/ml BSA, 2 & poly(dI-dC) and 50,000 cpm γ ³²P-labeled HIF-1 α consensus oligonucleotide. Cold competition was done by adding a 20-fold excess of specific unlabeled double-stranded probe to the reaction mixture. Samples were incubated at room temperature for 30 min. Reactions were run on a 4% polyacrylamide gel and the dried gel was exposed to an X-ray film at -80°C overnight. Band density was quantified using ImageJ64 image analysis.

Histopathological analysis

Sections of formalin-fixed, paraffin-embedded livers were stained with hematoxylin and eosin (H&E), or Sirius Red and assessed for histological features of steatosis, inflammatory cell invasion, and fibrosis. The H&E and Sirius Red stained sections were independently examined by 2 pathologists, Dr. Garlick and Dr. Jin-Kyu Park in a blinded manner (see acknowledgments). Immunohistochemistry staining for

GRHL2 (Atlas antibodies, HPA004820) were performed on formalin-fixed, paraffin-embedded livers according to the manufacturer's instructions. ImageJ (NIH) was used for image analysis.

Statistical Analysis

Statistical significance between two groups was determined using two-tailed t-test. Two-way ANOVA and Dunnett's multiple comparison post-test were used to compare the means of multiple groups. Outliers were determined using ROUT method with a q of 1%. Data are shown as mean \pm SEM and were considered statistically significant at $P < 0.05$. GraphPad Prism 6.02 (GraphPad Software Inc.) was used for analysis.

Results

Characterization of miR-122 expression in human alcoholic cirrhosis

The role of miR-122 in preneoplastic conditions such as alcoholic liver disease, is unknown. I hypothesized that alcohol may inhibit miR-122, driving the hepatic dysfunction. I obtained frozen liver specimens from normal controls, alcoholic cirrhosis, and HCV-infected patients. Demographic and clinical data are listed in (Table 2.2). The healthy patient control samples are age and gender matched to the alcohol and HCV patients. Total RNA was extracted from patient liver samples and quantitative real-time PCR (qPCR) for miR-122 was performed using Taqman based probe system. In this and subsequent experiments, three small RNA species were tested as internal controls; sno202, U6, and RNU48. Once Ct values were obtained, the data for all samples were entered into NORMFINDER software to determine the most stable control. Using this method I found that miR-122 expression was reduced approximately 50% in livers from patients with alcoholic cirrhosis, when compared to HCV cirrhosis or healthy controls, suggesting that chronic alcohol may promote liver injury by inhibiting miR-122 (Figure 2.1).

Establishment of mouse model of ALD

To dissect the specificity of the reduction of miR-122, I sought to reproduce human ALD in a murine model of chronic alcohol-induced liver injury. Six-to-eight week-old C57/Bl6 mice were acclimated to the Lieber DeCarli liquid. (Figure 2.2a) diet for two days. During each subsequent day, the alcohol concentration was increased by 1%/day to a maximum of 5% vol/vol, or 36% of the total caloric intake, for

Table 2.2: Human Liver Samples; Demographic and Clinical Data.

	<i>Alcoholic Patients</i>	<i>Hepatitis C Patients</i>
<i>N</i>	10	12
<i>Age, years</i>	51 (39 - 66)	56 (41 - 69)
<i>Sex, Male/Total</i>	9/10	6/12
<i>Race</i>	White (10/10)	White (9/12), Black (1/12), Hispanic (1/12), American Indian or Alaskan (1/12)
<i>MELD</i>	31 (22 - 40)	28 (12 - 39)
<i>Prothrombin Time (INR)</i>	2.49 (1.50 - 3.24)	2.1 (1.23 - 3.18)
<i>Total Bilirubin (mg/dl)</i>	5.15 (1.50 - 20.60)	3.70 (1.50 - 42.20)
<i>Creatinine</i>	2.13 (1.01 - 4.04)	1.29 (0.63 - 5.34)
<i>AST, IU/L</i>	41.50 (30.00 - 1425.00)	80.00 (40.00 - 286.00)
<i>ALP, IU/L</i>	163.50 (84.00 - 326.00)	105.00 (60.00 - 219.00)
<i>Albumin, g/dL</i>	3.30 (2.70 - 4.70)	2.70 (2.00 - 3.60)
<i>Years since abstinence</i>	0.67 (0.083 - 2)	12 (4 - 20)
<i>Months since last drink</i>	8.00 (1 - 24)	0 (0 - 240)
<i>Collection type</i>	Transplant (10/10)	Transplant (10/10)
<i>Primary diagnosis</i>	Alcoholic cirrhosis (10/10)	Chronic active hepatitis, type C (10/10)
<i>HAV, IgG+ /Tot available</i>	4/10	7/10
<i>HBV core, IgG+ /Tot available</i>	0/10	4/11
<i>HBV surface, IgG+ /Tot available</i>	2/10	4/11
<i>HCV, IgG+ /Tot available</i>	0/10	12/12
<i>HIV 1 and 2, IgG+ /Tot available</i>	1/10	0/10
<i>CMV, IgG+ /Tot available</i>	5/10	11/12
<i>EBV, IgG+ /Tot available</i>	10/10	12/12
<i>Pathology report: Evidence of Dysplasia</i>	0/10	0/10

Figure 2.1: Human Liver miR-122 expression.

miR-122 expression determined by quantitative real-time PCR from the livers of healthy controls, alcoholic cirrhosis, and HCV cirrhosis patients. miR-122 expression is decreased in the livers of patients with alcoholic cirrhosis when compared to healthy controls and patients with HCV cirrhosis.

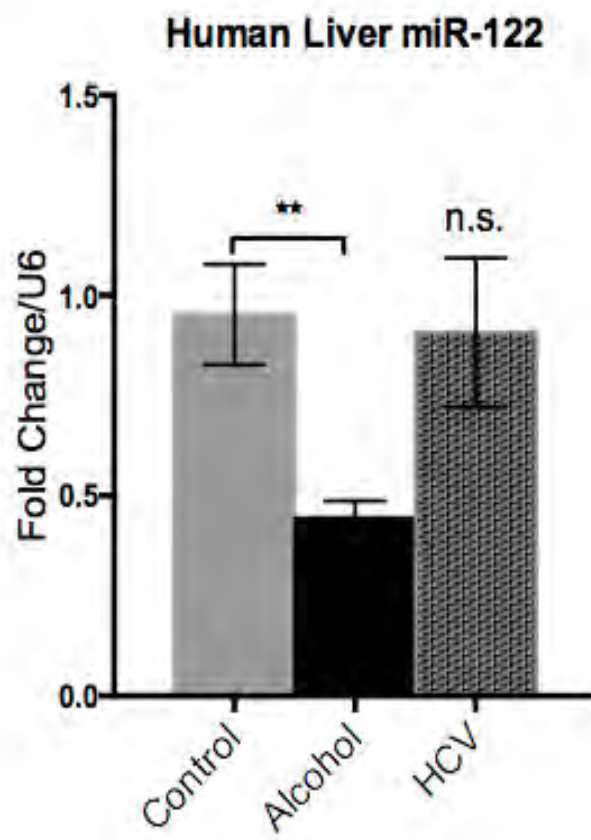


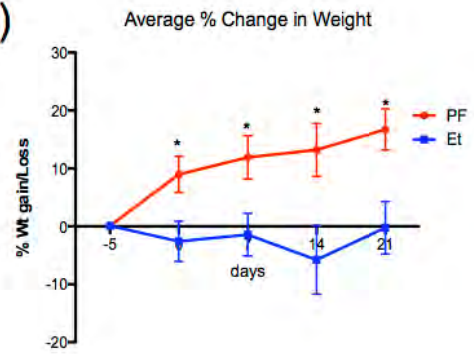
Figure 2.2: Characteristics of chronic alcohol feeding model.

(a) Schematic representation of a five-week alcohol feeding model. Mice were gradually acclimated to a Lieber-DeCarli liquid diet with 5% ethanol (vol/vol) over a period of 1 week, then maintained on the 5% diet for 4 additional weeks. Consumption was recorded daily and isocaloric amounts of a control diet (in which dextran-maltose replaced calories from ethanol) were dispensed to pair-fed (PF) animals. Weights were recorded weekly. Mice were (b) weighted and bleed weekly to monitor health. Alcohol-fed mice exhibited no weight gain during the course of the feeding while pair-fed mice consistently gained weight. (c) Alcohol-fed mice exhibited significant increases in serum ALT at the end of the five-week feeding compared to PF controls. (d) Alcohol-fed mice exhibited increased hepatic triglyceride accumulation. * $P < 0.05$, ** $P < 0.005$, *** $P < 0.0005$ by two-way Anova.

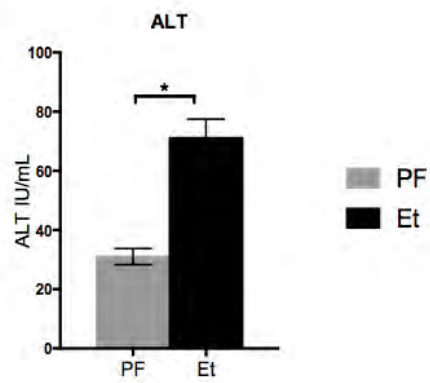
a)



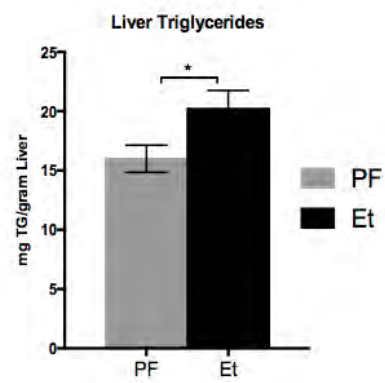
b)



c)



d)



four additional weeks (EtOH-fed or Et). Consumption was recorded daily, and a control diet was dispensed to pair-fed (PF) mice substituting maltose-dextran for ethanol calories. Over the course of the feeding I noted consistent weight gain in PF-mice while Et-fed mice failed to gain any weight (Figure 2.2b).

Upon completion of the five-week feeding, serum and livers were collected and analyzed for serum alanine amino transferase (ALT), a serum marker specific for hepatic injury. (Figure 2.2c) Indeed, 4 weeks of chronic alcohol increased serum ALT enzyme activity in alcohol-fed mice when compared to PF controls Liver injury in ALD is the result of hepatic steatosis. To determine lipid accumulation in the liver I extracted triglycerides from fresh frozen tissue using a 5% NP-40 lysis solution. For normalization, a BCA protein assay was performed to determine protein concentration of the lysate. Subsequently, triglyceride assay revealed that alcohol significantly increased triglyceride concentration within the liver. (Figure 2.2d) Histological examination of formalin-fixed paraffin embedded liver tissue was stained with hematoxylin and eosin revealed evidence of steatotic changes and glycogen depletion within hepatocytes in Et-fed mice. (Figure 2.3) In contrast, pair-fed mice showed normal liver parenchyma, and no evidence of fatty change.

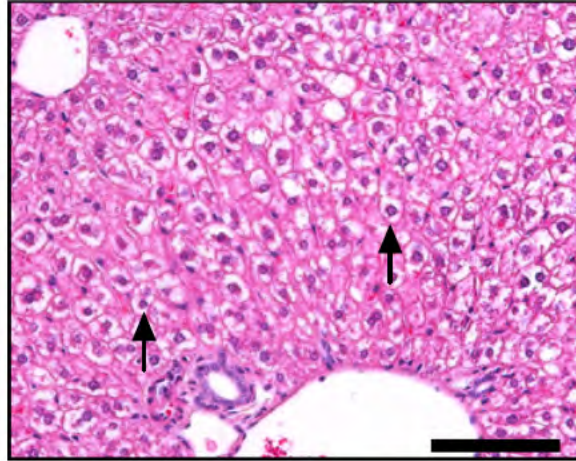
Characterization of miR-122 expression in murine ALD

Utilizing taqman probes specific for the mature miR, I found that that miR-122 expression was significantly reduced in the livers of alcohol-fed mice compared to pair-fed controls (Figure 2.4a), equivalent to that seen in the human patient samples.

Figure 2.3: H&E liver histology from wild-type pair- and ethanol-fed mice

Pair-fed mice exhibit no evidence of steatosis. Ethanol-fed mice display extensive lipid accumulation within hepatocytes (short arrows), increased inflammatory infiltrate (asterisk), and depletion of glycogen stores (long arrows). Scale bars =100 μ m.

Pair-fed



Ethanol

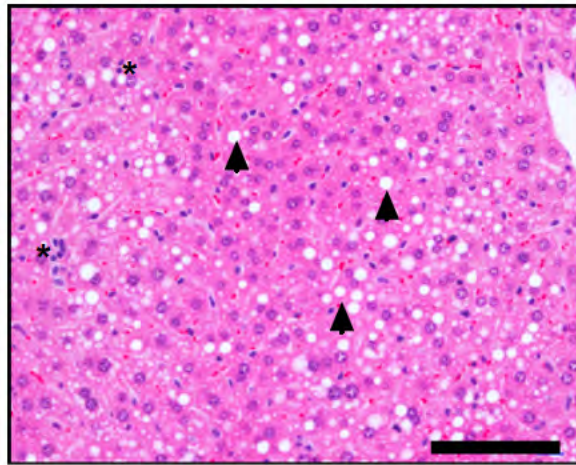
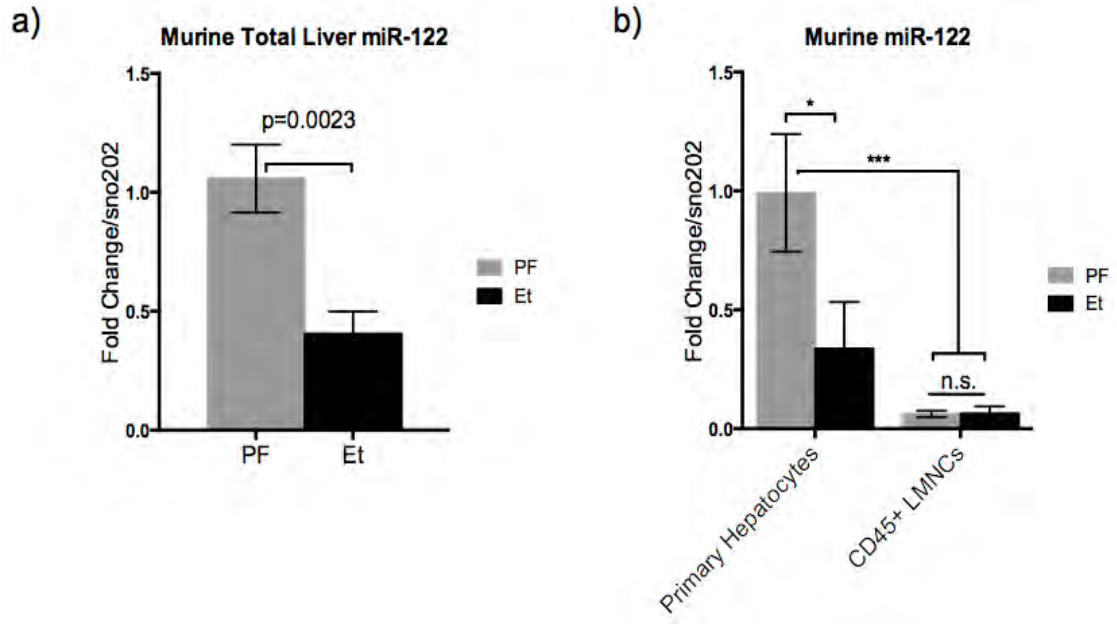


Figure 2.4: Chronic alcohol is associated with reduced miR-122 in murine hepatocytes.

miR-122 is reduced in (a) total murine livers (n=8-14) and (b) hepatocytes (n=5) of alcohol-fed mice when compared to pair-fed controls. CD45+ liver mononuclear cells (LMNCs, n=5) show 10-fold lower expression of miR-122 and is not effected by alcohol.

*P < 0.05, **P<0.005, ***P<0.0005 by Student's t test (a) or two-way ANOVA (b).



To determine the cell specificity of the miR-122 reduction, I isolated primary hepatocytes and liver mononuclear cells (LMNCs) from Pair- and alcohol-fed mice. Briefly, mice were anesthetized, perfused with collagenase solution, livers excised, and single-cell suspension was differentially centrifuged to separate non-parenchymal and parenchymal cells. Parenchymal cells were directly lysed and RNA isolated. However, even with percoll gradient separation of LMNCs, given the relative enrichment of miR-122 in hepatocytes, even slight contamination within liver could drastically effect miR-122 expression analysis. Therefore, to further purify the immune cells, I used a MACS bead system to positively select for CD45+ non-parenchymal cells. qPCR revealed that miR-122 was selectively decreased in hepatocytes and not in CD45+ LMNCs from alcohol-fed mice (Figure 2.4b) when compared to pair-fed controls. Additionally, CD45+ LMNC expression of miR-122 is approximately 10-fold lower than that found in hepatocytes (Figure 2.4b). This supported our hypothesis that alcohol-induced changes in miR-122 in the total liver are hepatocyte-specific.

Correlation between miR-122 and its putative target HIF-1 α

Using a miRNA target prediction algorithm, based on seed recognition, I identified HIF-1 α as a putative target of miR-122. Our present analysis of the livers of alcoholic cirrhosis patients and hepatocytes of alcohol-fed mice also revealed an increase of HIF-1 α mRNA (Figure 2.5a,b) that showed a significant inverse correlation with miR-122 expression (Figure 2.5a,b). This correlation suggested that HIF-1 α increases noted by alcohol may be miR-122 dependent.

Figure 2.5: Inverse correlation between mir-122 and HIF-1 α in chronic alcohol.

Expression of HIF-1 α and correlation to miR-122 expression in (a) human livers (n=9-12), and (b) murine hepatocytes (n=8-14). miR-122 and HIF-1 α exhibit a significant inverse correlation in the hepatocytes of alcohol-fed mice and the liver of patients with alcoholic cirrhosis. *P < 0.05, **P<0.005, ***P<0.0005 by Student's t test or two-way ANOVA (n=8-14). Regression analysis determined using Spearman's Correlation.

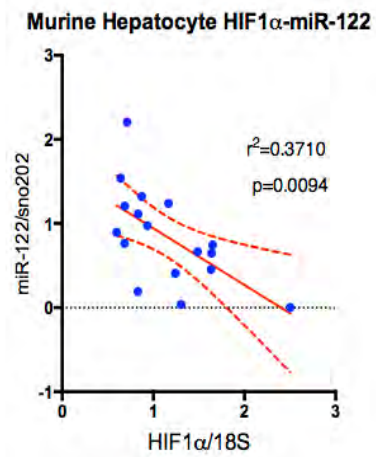
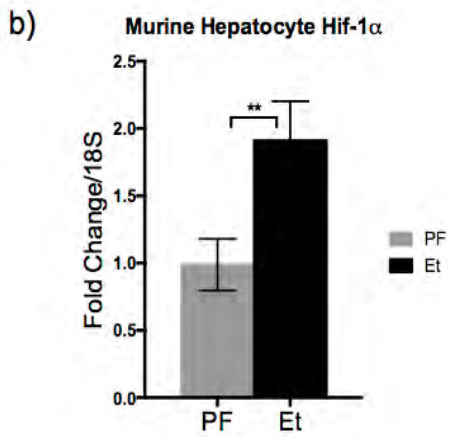
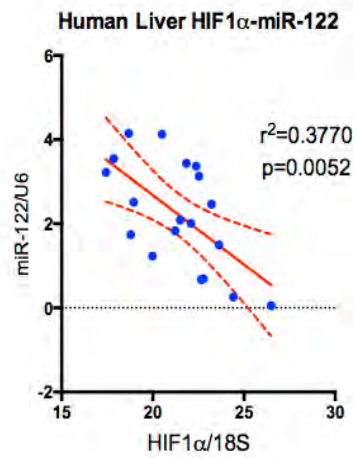
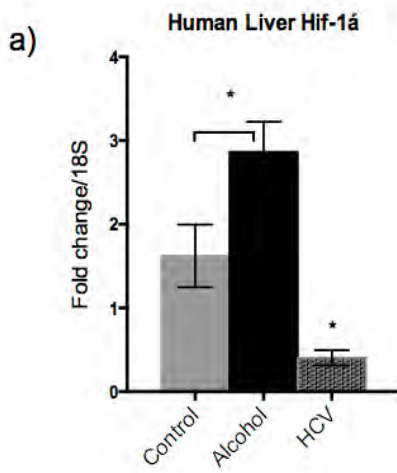
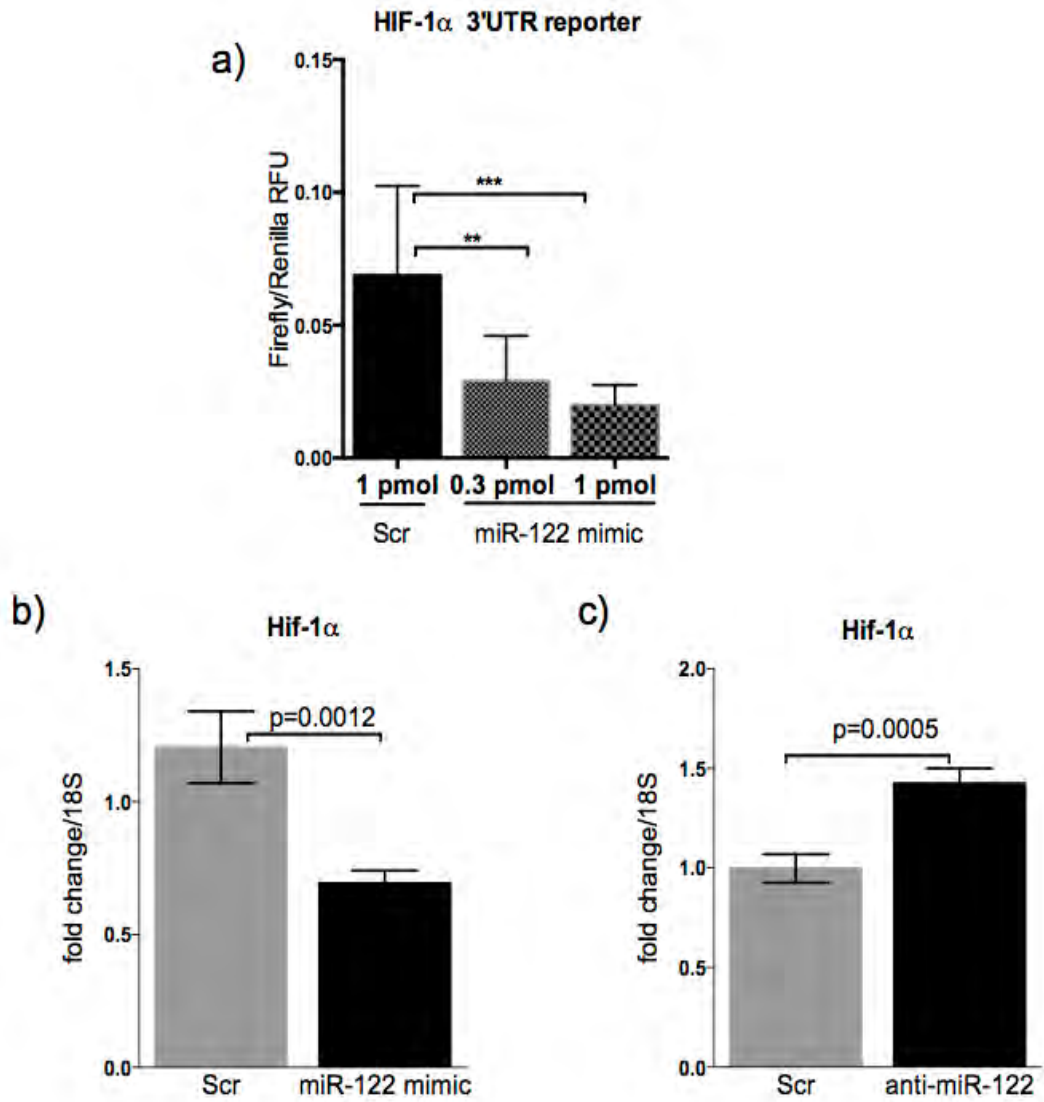


Figure 2.6: miR-122 regulates Hif-1 α via 3'UTR silencing.

(a) The effect of miR-122-5p or scrambled oligonucleotide on luciferase activity from pmirCHECK-transfected HEK293T cells expressing the WT (3'UTR) of HIF-1 α (n=8). Hif-1 α mRNA expression is inhibited and enhanced in murine hepatocytes treated with either (c) miR-122 mimic or (d) anti-miR-122 inhibitor respectively. (n=12). (c) *P < 0.05, **P<0.005, ***P<0.0005 by Student's t test.



miR-122 regulates HIF-1 α through canonical miRNA silencing mechanism

To establish that miR-122 directly regulates HIF-1 α through canonical miRNA pathways, I co-transfected a plasmid containing the HIF-1 α 3'UTR-luciferase reporter (HIF-3'luc, Origene), with scrambled or miR-122 mimic into HEK293T cells. The miR-122 mimic strongly repressed HIF-3'luc activity in a dose-dependent manner (Figure 2.6a). As further evidence of this regulatory pathway, I found that transfection of either a miR-122 mimic or an inhibitor into primary murine hepatocytes results in decreased or increased HIF-1 α mRNA, respectively (Figure 2.6b,c).

Conclusions and Discussion

Given the essential role of miR-122 in mediating lipid homeostasis and differentiation of hepatocytes, I hypothesized that chronic alcohol may modulate, and specifically, reduce miR-122 expression. In this chapter I sought to characterize the relationship between miR-122 expression and its putative target, HIF-1 α , in alcoholic liver disease. As I hypothesized, miR-122 expression is reduced in patients with alcoholic cirrhosis when compared to healthy controls. However, it is key to note that the tissue obtained were from resected livers during transplantation due to end-stage cirrhosis - a terminal stage in ALD. Additionally, reduced miR-122 was noted in a bile duct ligation model of liver injury and cirrhosis. Therefore, to determine if this finding was alcohol-specific, or due to cirrhosis I obtained patient samples from cirrhotic patients also undergoing transplant due to end-stage cirrhosis due to chronic HCV infection. Importantly, the decrease in miR-122 found in alcoholic patients was not noted in HCV-induced cirrhosis, suggesting that this decrease is alcohol specific. Although this data is

convincing, it has been shown that HCV utilizes miR-122 as part of its viral replication cycle and the virus itself, as well as immune reactions to active viral infection, have been known to effect miR-122 expression.

In order to first, perform further mechanistic studies, and second, determine if the reduction of miR-122 occurs in the early stages of ALD in the absence of end-stage cirrhosis, I sought a murine model which reproduces the earlier stages of human ALD. I chose to utilize the Lieber DeCarli chronic alcohol model which allows mice ad libitum access to a liquid alcohol diet, while control mice are administered a calorie-matched amount. This model accurately reproduced the phenotype associated with chronic alcohol consumption in humans as noted by hepatic steatosis and serum ALT as well as decreased weight gain in alcohol-fed mice when compared to pair-fed controls.

qPCR analysis of miR-122 and HIF-1 α expression revealed that alcohol specifically reduced miR-122 in murine hepatocytes and inversely correlated with HIF-1 α expression-as I observed in the alcoholic-cirrhosis patient samples. *In vitro* assays knocking down and overexpressing miR-122 in the primary murine hepatocytes increased and decreased HIF-1 α mRNA respectively. However, these studies only demonstrated an inverse association between miR-122 and HIF-1 α , and not a causal one. Utilizing a luciferase reporter system with the 3'UTR of HIF-1 α , I found that miR-122 regulates HIF-1 α post-transcriptionally through canonical miRNA silencing pathways.

These results confirmed that miR-122 directly inhibits HIF-1 α expression in hepatocytes, and may do so *in vivo*.

CHAPTER 3: MIR-122 MEDIATES ALCOHOLIC LIVER DISEASE PATHOGENESIS VIA HIF-1A *IN VIVO*

Summary

Our findings suggest that miR-122 regulates HIF-1 α . I hypothesized that loss of miR-122 contributes to ALD. In this study, our goals were to assess; the role of miR-122 in the pathogenesis of ALD through its regulation of HIF-1 α . To determine whether the loss of miR-122 can mediate alcoholic liver injury through HIF-1 α , I used wild-type 8-week-old, C57/B16 mice or hepatocyte specific HIF-1 α knockout (HIF1hepKO) mice. Both WT and HIF1hepKO mice were injected intravenously with AAV8 containing anti-miR-122 TuD (TuD) to knockdown miR-122 in the liver, or scrambled (Scr) vector followed by a Lieber-DeCarli (LDC) alcohol diet (Et) or PF control diet for 4 weeks. Anti-miR-122 TuD treatment alone resulted in significant increases in liver injury (ALT), steatosis, inflammation, and fibrosis in PF mice compared to Scr-treated controls. The co-administration of miR-122 TuD and alcohol resulted in a synergistic effect, further increasing liver injury, inflammation and fibrosis. The hepatic expression and DNA-binding activity of HIF-1 α , a miR-122 target, was increased in TuD+PF mice equivalent to that of alcohol feeding alone. HIF1- α activity was the highest in TuD+Et mice compared to all other groups. HIF-1 α deficiency in hepatocytes protected mice from liver damage, inflammation and fibrosis induced either by alcohol or miR-122 knockdown. Our findings suggested miR-122 reduction in alcohol potentiates the steatosis, inflammation and early fibrosis seen in ALD through its downstream target HIF-1 α .

Acknowledgements

I particularly would like to acknowledge the work of three individuals, Donna Catalano for her diligence in maintenance of the mouse colonies used here as well as Sitara Rao and Nicita Mehta for their technical assistance and dedication to this work, they were directly involved in performing all qPCR, ELISA, and triglyceride assays. I would also like to thank Shashi Bala, Aditya Ambade, Benedek Gyongyosi, and Patrick Lowe for their stimulating intellectual discussions and scientific input. I thank Dr. David Garlick of Cancer Biology Department at UMASS and Dr. Jin-Kyu Park DVM, PhD, a former lab member, for histopathological examination of liver tissue sections. I am grateful to services provided by Mass Histology for tissue sectioning and staining, My collaborators at the UMass Vector Core and Gao lab (AAV production) and CFAR (Primer Synthesis) core facilities at UMASS Medical School.

Introduction

In the previous chapter I demonstrated that chronic alcohol reduces miR-122 expression in the livers, and specifically the hepatocytes, of patients with alcoholic cirrhosis and mice administered chronic alcohol. Furthermore, I found that not only is there a significant inverse association between miR-122 and HIF-1 α in alcohol-fed mice, but HIF-1 α is a direct target of miR-122. Our lab has previously reported that alcohol increases HIF-1 α expression in hepatocytes and hepatocyte-specific HIF-1 α knockout mice (HIF1hepKO) were protected from chronic alcohol, while transgenic mice, expressing degradation-resistant HIF-1 α (HIF1dPA) in murine hepatocytes, had augmented alcohol-induced liver injury.⁷⁵ Other groups have also reported similar findings of steatosis and cellular injury when overexpressing HIF signaling partners or knocking out key elements involved in HIF degradation. Taken together, this suggests that the reduction in miR-122 by alcohol may directly lead to the increase of HIF-1 α mRNA and therefore ALD pathogenesis.

To investigate the effect of miR-122 on ALD, I required the use of a knockdown system that; first, would target hepatocytes specifically, and second, could maintain a robust knockdown of miR-122 throughout the five-week feeding. Many modalities for miRNA inhibition, particularly for targeting miR-122, have been shown. However, anti-sense oligonucleotides, and LNAs lack organ specificity and the sustained inhibition needed for our studies. Our collaborators in the Gao lab, have developed a self-complimentary adeno-associated virus 8 (rAAV8) vector system expressing a U6-driven anti-miR-122 Tough Decoy (TuD) which they have shown to have tropism for

hepatocytes and maintain sustained inhibition of miR-122 in murine livers after a single intravenous dose.²²¹ While their studies utilized AAV serotype 9 (AAV9), we chose to use serotype 8 which has been shown to have a tropism for hepatocytes, thereby minimizing any off-target effects in other organs or cell types. Furthermore, AAV8-mediated gene therapy has been deemed a safe and effective vector system in humans following clinical trials delivering a Factor IX transgene to patients with Hemophilia B.

I hypothesized that the reduction of miR-122, by either alcohol or AAV-mediated knockdown, would alleviate its inhibition of HIF-1 α , driving hepatic steatosis. Importantly, the role of immune cells in driving steatohepatitis is a key pathogenic mechanism of ALD. Chronic alcohol induces a hyper-responsive state in liver immune cells, whereby upon stimulation by PAMPs and DAMPs, they release inflammatory mediators such as TNF- α and IL-1 β . These cytokines, in turn, activate cell death pathways in hepatocytes, which due to their steatotic state, have a diminished capacity to endure these inflammatory insults. Therefore, I also expected that the increase in steatosis due to miR-122 reduction, and HIF-1 α activation, in WT mice would not only induce increased steatosis, but also significant inflammation as well.

As sated above, our lab has previously utilized hepatocyte specific HIF-1 α knockout mice to demonstrate its role in ALD. To establish a causal link between HIF-1 α , miR-122, and ALD pathogenesis, I utilized these HIF1hepKO mice. Given my findings that miR-122 can regulate HIF-1 α , I hypothesized that these knockout mice would not only be protected from chronic alcohol-induced steatosis and inflammation as previously shown, but also from miR-122 inhibition when compared to WT mice.

In accordance with our hypothesis, the knockdown of miR-122 in WT mice recapitulated the steatosis and inflammation associated with ethanol alone. Interestingly, the combination of miR-122-TuD and alcohol yielded an additive effect on liver injury and fibrosis. Furthermore, HIF1hepKO mice exhibited decreased steatosis, inflammation and fibrosis when compared to WT mice treated with either miR-122-TuD, alcohol, or their combination. I conclude that the loss of miR-122 in ALD mediates disease progression through its primary target, HIF-1 α , and that restoration of miR-122 in hepatocytes may have therapeutic significance.

Methods

Animal Studies

All animals received care in compliance with protocols approved by the Institutional Animal Use and Care Committee (IACUC) of the University of Massachusetts Medical School. Wild-type (WT) mice (C57/B16), Alb-Cre, and HIF-1 $\alpha^{\text{flox/flox}}$ mice were purchased from Jackson Laboratories (Bar Harbor, ME) and backcrossed onto a C57/B16 background. The HIF-1 α floxed allele has been described by Kim et al.⁶⁷ Hepatocyte specific HIF-1 α knockout mice (HIF1hepKO) obtained from the F1 generation of a cross between HIF-1 $\alpha^{\text{flox/flox}}$ mice and Alb-Cre homozygous mice. 6-8 week old mice were gradually acclimated to a Lieber-DeCarli liquid diet with 5% ethanol (vol/vol) over a period of 1 week, then maintained on the 5% diet for 4 weeks (total of 5 weeks). Consumption was recorded daily and isocaloric amounts of a control diet (in which dextran-maltose replaced calories from ethanol) were dispensed to pair-fed (PF) animals. Weights were recorded weekly. At the conclusion of the 5-week feeding, mice

were weighed, blood collected, and euthanized. Livers were dissected, weighed and divided into lipid nitrogen for protein and biochemical assays, fixed in 10% phosphate-buffered formalin for histological analysis, preserved in OCT frozen section preparation solution, or soaked in RNALater (Qiagen, Hilden, Germany, Hilden, Germany). Blood was allowed to clot and serum obtained using gel-based serum separator tubes.

Isolation of primary mouse hepatocytes and LMNCs

Anesthetized animals were perfused by way of portal vein with saline solution, followed by enzymatic digestion, as previously described.⁷⁵ The hepatocytes were separated by centrifugation. In vitro experiments. Primary hepatocytes were cultured in low-glucose DMEM supplemented with 10% fetal bovine serum, 1% Anti-Anti, 1% gentamycin, 1% insulin, transferrin, selenium solution. Primary hepatocytes were seeded in 6-well collagen-coated plates (Biocoat, Becton Dickinson). Before starting stimulation experiments, hepatocytes were rested for 4 hours.

RNA extraction and real-time PCR

Total RNA was extracted using the Quiagen miRNeasy kit (Quiagen, Hilden, Germany, Hilden, Germany) according to the manufacturer's instructions. Briefly, tissue samples were lysed in QIAzol Lysis reagent (Quiagen, Hilden, Germany), homogenized with stainless steel beads in TissueLyser II (Quiagen, Hilden, Germany) followed by miRNA isolation following manufacturer's instructions and DNase 1 Digest. RNA was quantified using Nanodrop 2000 (Thermo Scientific, Waltham, MA). Complementary

DNA (cDNA) synthesis was performed by reverse transcription of 1 ug total RNA using the iScript Reverse Transcription Supermix (Bio-rad, Hercules, CA). Real-time quantitative PCR was performed using Bio-Rad iTaq Universal SYBR Green Supermix and a CFX96 real-time detection system (Bio-Rad Laboratories). Primers were synthesized by IDT, Inc. Relative gene expression was calculated by the comparative cycle threshold (Ct) method. The expression level of target genes was normalized to the house-keeping gene, 18S rRNA, in each sample and the fold-change in the target gene expression between experimental groups was expressed as a ratio. Melt-curve analysis was used to confirm the authenticity of the PCR products.

miRNA Analysis

Reverse transcription (30 min - 16°C; 30 min - 42°C; 5 min - 85°C) was performed in Eppendorf Mastercycler (Eppendorf, New York, USA) using 10 ng RNA, TaqMan primers and miRNA Reverse Transcription Kit (Applied Biosystems, Foster City, CA) followed by quantitative RT- in CFX96 (Bio-rad, Hercules, CA) using TaqMan Universal Probes Master Mix (Biorad, Hercules, CA). All samples were normalized to snoRNA202, or U6 expression based on Normfinder (<http://moma.dk/normfinder-software>) analysis of loading control stability. hsa-miR-122-FAM, U6-FAM, and sno202-FAM primer sets were purchased from Applied Biosystems (Foster City, CA).

Construction of miR-122 antagonist and overexpression plasmids

The scAAV-anti-miR-122 TuD and scAAV-anti-SCR TuD constructed were made as previously described Xie et al., 2012.²²¹ The BamHI fragment carrying anti-miR-122 TuD was replaced with the pri-miR-122 sequence amplified from C57/Bl6 mouse genome DNA to generate scAAV-pri-miR-122 construct. Mice were treated by tail vein injection with AAV vectors at 6×10^{11} genome copies/mouse or approximately 3×10^{13} genome copies/kg.²²¹

Biochemical Assays

Serum alanine aminotransferase (ALT) levels were determined using a commercially available reagent (Advanced Diagnostics Inc) as described. Serum alanine aminotransferase (ALT) was determined using a commercially available reagent (Advanced Diagnostics Inc, Plainfield, NJ). 15 uL of serum was mixed 1:10 with assay reagent diluted according to the instructions of the manufacturer, and UV absorbance at 37 degrees Celsius was measured over three minutes. The average change in absorbance per minute interval is then multiplied by a conversion factor to yield ALT levels.

Liver triglycerides were extracted using a 5% NP-40 lysis solution buffer. Triglycerides were quantified using a commercially available kit (Wako Chemicals) followed normalization to protein amount.

Protein concentration was determined by by BCA protein assay (ThermoFisher Scientific) by using 10 uL of 1:10 or serially diluted lysate and incubating in assay reagent for 30 minutes at 37 degrees C. Absorbance was measured at 562nm on a 96 well

plate using a plate reader. Concentrations were interpolated using 4-PL regression derived from a standard curve generated using bovine serum albumin standard (Pierce).

Nuclear Extraction

50mg of snap-frozen liver tissue was washed in 10-fold excess volume TKM-0.32 buffer (0.32M sucrose, 50mM Tris-HCl, 25mM KCl, 5mM MgCl, 5mM PMSF), with protease inhibitor tablets 1 per 10 mL, (Roche) and homogenized using a hand-held homogenizer. Homogenates were transferred to microcentrifuge tubes and centrifuged (1000rpm for 10 minutes at 4 degrees C). Pelleted material was resuspended in TKM-2.0 buffer (2M sucrose, 50mM Tris- HCl, 25mM KCl, protease inhibitor cocktail) and homogenized again by handheld homogenizer. Pellets were collected by centrifugation (14000rpm for 30 minutes at 4 degrees C) and resuspended in 500ul Buffer A (10mM Hepes/KOH, pH 7.9, 2mM MgCl, 1mM EDTA, 10mM KCl, 1mM DTT, 5mM PMSF, 1 protease inhibitor tablet). Pellets were again collected by centrifugation (14000rpm for 30 minutes at 4 degrees C) and resuspended in 50ul Buffer B (10mM Hepes/KOH pH 7.9, 2mM MgCl, 1mM EDTA, 50mM KCl, 300mM NaCl, 2mM DTT, and 5mM PMSF with protease inhibitor tablets 1 per 10 mL, (Roche), 10% glycerol. Pellet was resuspended was sonicated at 40% duty cycle 1 second on/off cycle, frozen at -80 degrees overnight, and thawed with gentle agitation at 4 degrees celcius. Supernatant containing nuclear extract was collected after centrifugation (14000rpm for 30 minutes at 4 degrees C) and assayed for protein concentration.

Electrophoretic Mobility Shift Assay

The DNA binding activity of HIF-1 α was assessed by electrophoretic mobility shift assay as described previously (Nath B., *Hepatology*. 2011 May;53(5):1526-3).⁷⁵ A consensus double-stranded Hypoxia Response Element (HRE) (Santa Cruz Biotech, CA) oligonucleotide was used for EMSA. End-labeling was accomplished by treatment with T4 kinase in the presence of [P32]ATP. Labeled oligonucleotides were purified on a polyacrylamide copolymer column (Bio-rad, Hercules, CA). Five micrograms of liver or hepatocyte nuclear protein was added to a binding reaction mixture containing 50 mM Tris-HCl, pH 7.5, 5 mM MgCl₂, 2.5 mM EDTA, 2.5 mM DTT, 250 mM NaCl, 20% glycerol, 20 &g/ml BSA, 2 & poly(dI-dC) and 50,000 cpm γ ³²P-labeled HIF-1 α consensus oligonucleotide. Cold competition was done by adding a 20-fold excess of specific unlabeled double-stranded probe to the reaction mixture. Samples were incubated at room temperature for 30 min. Reactions were run on a 4% polyacrylamide gel and the dried gel was exposed to an X-ray film at -80°C overnight. Band density was quantified using ImageJ64 image analysis.

Whole Cell Lysate

Approximately 50 mg of liver tissue was washed in ice cold PBS and homogenized in lysis buffer (9.5ml RIPA buffer, 1mM NaF, 2mM Na₃VO₄, 1 protease inhibitor tablet, 5mM PMSF) with stainless steel beads in TissueLyser II (Qiagen, Hilden, Germany, Hilden, Germany). After 10 minutes of incubation on ice, homogenates

were centrifuged at 14,000xg for 10 minutes at 4 degrees C. The supernatant (clarified whole cell lysate) was collected and stored in aliquots at -80 degrees C.

ELISA

Cytokine levels were monitored in 25 mg of liver whole cell lysates diluted in assay diluent following manufacturer instructions. MCP-1 and TNF α were measured by use of specific anti-mouse ELISA from BioLegend. IL-1 β was measured by use of specific anti-mouse ELISA (R&D Systems) that recognizes both pro- and cleaved- IL-1 β .

Histopathological analysis

Sections of formalin-fixed, paraffin-embedded livers were stained with hematoxylin and eosin (H&E), or Sirius Red and assessed for histological features of steatosis, inflammatory cell invasion, and fibrosis. The H&E and Sirius Red stained sections were independently examined by a 2 pathologists, Dr. Garlick and Dr. Jin-Kyu Park in a blinded manner (see acknowledgments).

Statistical Analysis

Statistical significance between two groups was determined using two-tailed t-test. Two-way ANOVA and Dunnett's multiple comparison post-test were used to compare the means of multiple groups. Outliers were determined using ROUT method with a q of 1%. Data are shown as mean \pm SEM and were considered statistically

significant at $P < 0.05$. GraphPad Prism 6.02 (GraphPad Software Inc.) was used for analysis.

Results

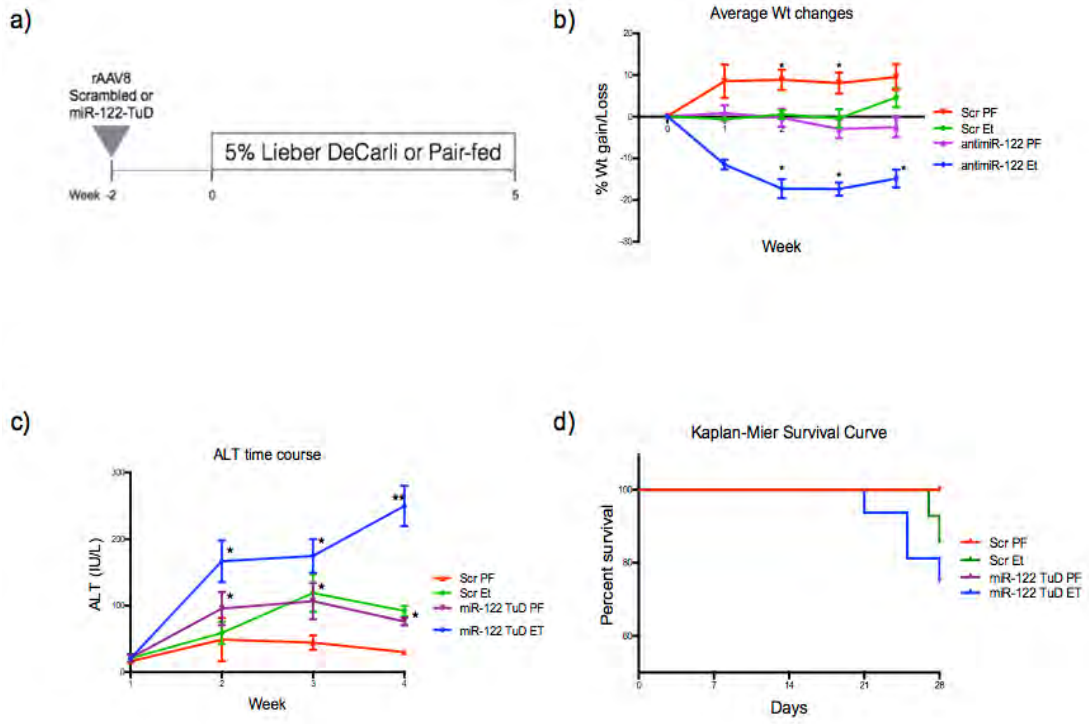
Characterization of miR-122 knockdown on ethanol feeding parameters in WT mice

Previous data has suggested that self-complimentary AAV vectors require approximately 2-3 weeks to fully express their transgene and recover from any initial cytotoxicity. Therefore, I chose to administer the viral vectors to six week old mice, two-weeks prior to the start of a five-week Liber DeCarli feeding. This timing would allow near full vector expression during the week-long alcohol ramp-up and ensure that all groups were within the eight week-old age range used for previous studies. WT mice were administered 6×10^{11} genome copies/mouse carrying either transgenes encoding a U6-driven, scrambled tough decoy (Scr) or anti-miR-122-TuD (anti-miR-122-TuD or TuD). After two weeks on chow diet, mice were randomized into either ethanol (Et) or pair-fed (PF) groups after a one-week acclimation period. (Figure 3.1a)

Weights and serum was collected weekly to monitor the overall health and specifically time-course of liver injury of mice in each group. To avoid over-stressing and over-bleeding, no individual mouse had serum collected two weeks in a row (n=3-4/group/week). Similar to our findings in chapter 2, scrambled+PF mice gained weight as expected, while ethanol-fed mice did not over the course of the feeding (Figure 3.1b). This was associated with an increase in serum ALT in the Scr+Et group (Figure 3.1c). In both weight gain and serum ALT, I observed similar patterns in both the miR-122-TuD+PF group and Scr+Et. Surprisingly, the knockdown of miR-122 with alcohol (TuD+Et) resulted in dramatic weight loss and increases in serum ALT throughout the

Figure 3.1: Characteristics of chronic alcohol feeding model.

(a) Schematic representation of alcohol feeding model with rAAV administration. WT mice were treated with 6×10^{11} genome copies rAAV8 particles containing either scrambled or anti-miR-122 TuD two weeks prior to the start of a 5-week alcohol feeding. Mice were (b) weighted and bleed weekly to monitor health and (c) serum ALT. TuD+PF and TuD+Et mice demonstrated significantly decreased weight gain and increased serum ALT when compared to their respective scrambled controls. (d) While there was a trend towards increased mortality in TuD+Et mice, this was not statistically significant when compared to the mortality in Scr+Et mice. * $P < 0.05$, ** $P < 0.005$, *** $P < 0.0005$ by two-way Anova.



feeding, greater than either knockdown or alcohol alone. Some mortality was observed in the alcohol group of both Scr and TuD-treated mice during the 4th week of the feeding (Figure 3.1d). Considering the significant weight loss and increasing ALT in the TuD+Et group, I halted the feeding at a total of 4 weeks (28 days) total.

In vivo regulation of HIF-1 α by miR-122

First I sought to verify that the inhibition of miR-122 was effectively maintained throughout our alcohol feeding model.

In chapter 2 of this dissertation I demonstrated that HIF-1 α was indeed a target of miR-122 *in vitro*. Based on the discovery that miR-122 inhibits HIF-1 α in hepatocytes, I hypothesized that firstly, AAV-mediated reduction of miR-122 in hepatocytes will increase its primary target, HIF-1 α , resulting in liver injury equivalent to that of alcohol alone. Secondly, I hypothesized that the inhibition of miR-122 alone will sensitize the liver alcohol-induced injury, resulting in greater hepatic injury than either alcohol or miR-122 inhibition alone. The rAAV8 miR-122 TuD achieved a robust and sustained knockdown of miR-122, in both pair-fed and alcohol-fed mice (Figure 3.2a).

Interestingly, in TuD+Et mice, I found an even further decrease in miR-122 compared to TuD+PF mice (Figure 3.2a). Alcohol and knockdown of miR-122 in the livers of WT mice increased HIF-1 α mRNA individually and additively (Figure 3.2b). To determine if this increase in mRNA was associated with an increase in HIF-1 α activity within hepatocytes, a subsequent feeding was performed and at the time of sacrifice, mice were perfused and primary hepatocytes isolated by differential centrifugation. Hepatocyte nuclear extracts were obtained and assayed by electromobility shift assay

(EMSA) using a P32 labeled HIF-1 α consensus oligonucleotide. Our results showed that TuD-mediated inhibition of miR-122 resulted in increased HIF-1 α DNA binding at baseline, equivalent to alcohol-feeding alone (Figure 3.2c). Furthermore, the combination of alcohol and miR-122-TuD-inhibition yielded a synergistic increase of HIF-1 α mRNA (Figure 3.2b) and DNA-binding activity (Figure 3.2c), confirming that miR-122 indeed regulates HIF-1 α in hepatocytes *in vivo*.

miR-122 regulates alcohol induced-steatosis, inflammation, and fibrosis via HIF-1 α

Given the increase in HIF-1 α mRNA and DNA binding noted when knocking down miR-122 *in vivo*, I hypothesized that HIF1hepKO mice would be protected from miR-122-mediated liver injury. I generated hepatocyte specific HIF-1 α knockouts by crossing HIF-1 α (flox/flox) and Alb-Cre homozygous mice. As described above these mice were also administered 6×10^{11} viral particles of either rAAV8-scrambled (Scr) or rAAV8-anti-miR-122-TuD (miR-122 TuD), randomized and administered an alcohol or pair-fed diet.

As seen in wild-type mice, both alcohol and TuD+PF treatment in HIF1hepKO mice resulted in efficient knockdown of miR-122 (

Figure 3.3: miR-122 mediated liver injury is HIF-1 α dependent). Interestingly, I also noted a further 50% reduction in TuD-treated knockout mice when they were given alcohol. However, contrary to the findings in WT mice, HIF1hepKO mice exhibited no mortality or weight loss. Serum collected at the end of the feeding revealed that HIF1hepKO mice had significantly lower hepatic injury from either alcohol, TuD-mediated miR-122 knockdown, or their combination when compared to wild-type mice (

Figure 3.3b). While these reductions were significant when compared to WT mice, it is notable that even HIF1hepKO had increased serum ALT when treated with a combination of TuD and alcohol.

In this and subsequent sections analysis of histological sections were scored for steatosis, inflammation, and fibrosis by two independent veterinary pathologists and myself, blinded to sample numbers, genotype, and treatments. H&E sections revealed that in wild-type mice, TuD-mediated inhibition of miR-122 alone resulted in a significant increase in and hepatic steatosis equivalent to that induced by the alcohol-diet, (Figure 3.4a). The combination of alcohol and miR-122-TuD treatment resulted in a synergistic effect, further increasing hepatic lipid accumulation which correlated with increasing HIF-1 α expression in hepatocytes, (Figure 3.4b). Indeed, I found that HIF1hepKO mice were protected from steatosis induced by alcohol, TuD-mediated miR-122 inhibition, or their combination. In order to validate and quantify the histological findings of lipid accumulation in the liver I performed a triglyceride assay from NP-40 lysates, as sated in the previous chapter. This assay confirmed that alcohol significantly increased triglyceride concentration within the liver (Figure 3.4c). Together these data suggested first, that the loss of miR-122 in hepatocytes directly triggers an increase of HIF-1 α , resulting in steatosis and hepatocyte injury. Second, alcohol further decreases miR-122, synergistically inducing HIF-1 α and its pathogenic effect.

Figure 3.2: miR-122 mediates HIF-1 α steatosis and liver injury through HIF-1 α in vivo

(a) miR-122 and (b) HIF-1 α mRNA in the total livers of scrambled or miR-122-TuD treated mice after 5 weeks of control (PF) or alcohol (Et) diet. Alcohol (c) HIF-1 α Electro-Mobility Shift Assay (EMSA) of hepatocyte nuclei isolated from Scr or miR-122-TuD treated WT mice after 5 weeks of PF or Et diet. rAAV8-delivered anti-miR-TuD effectively inhibits miR-122 expression in PF and Et-fed mice. Chronic alcohol further reduces miR-122 expression when compared to TuD treatment alone. The loss of miR-122 due to alcohol, TuD, or their combination is associated with an increase in HIF-1 α mRNA and DNA binding activity. *P < 0.05, **P<0.005, ***P<0.0005 by two-way ANOVA (n=6-14).

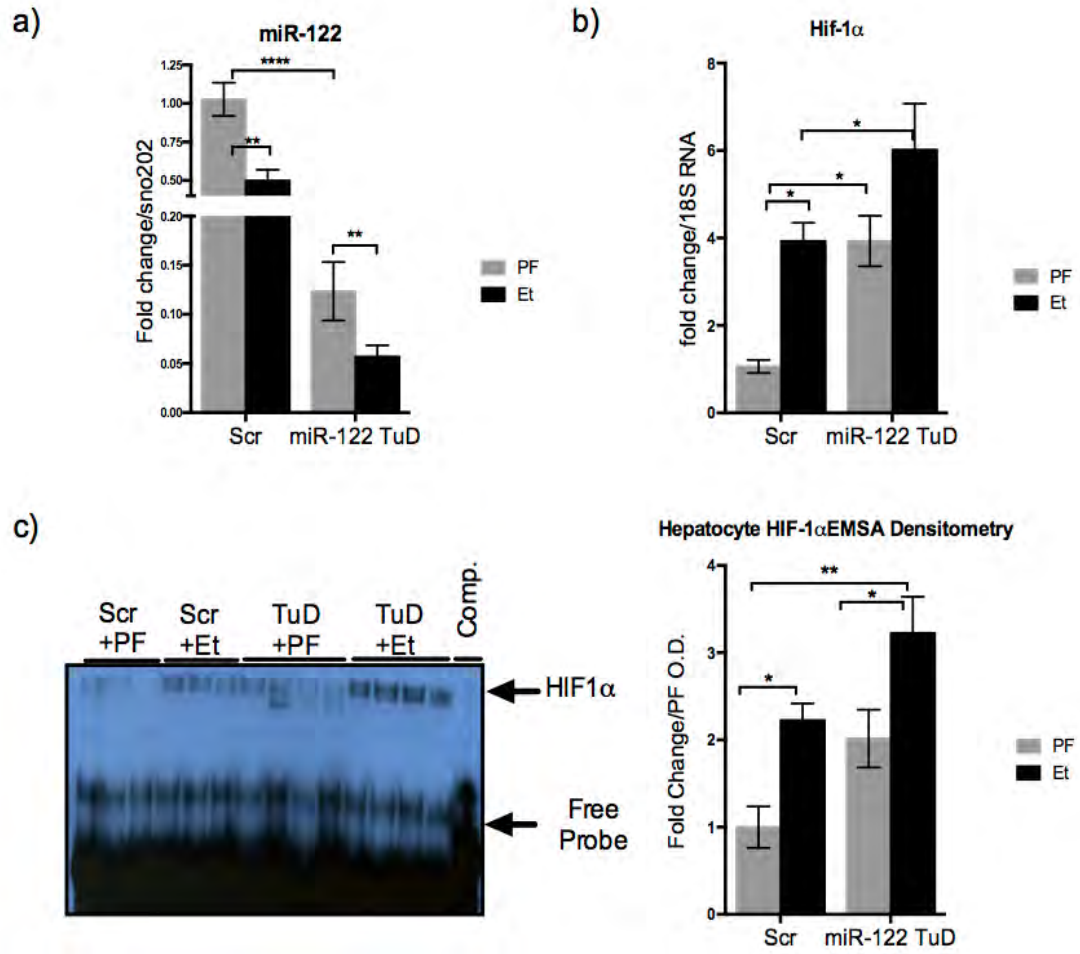
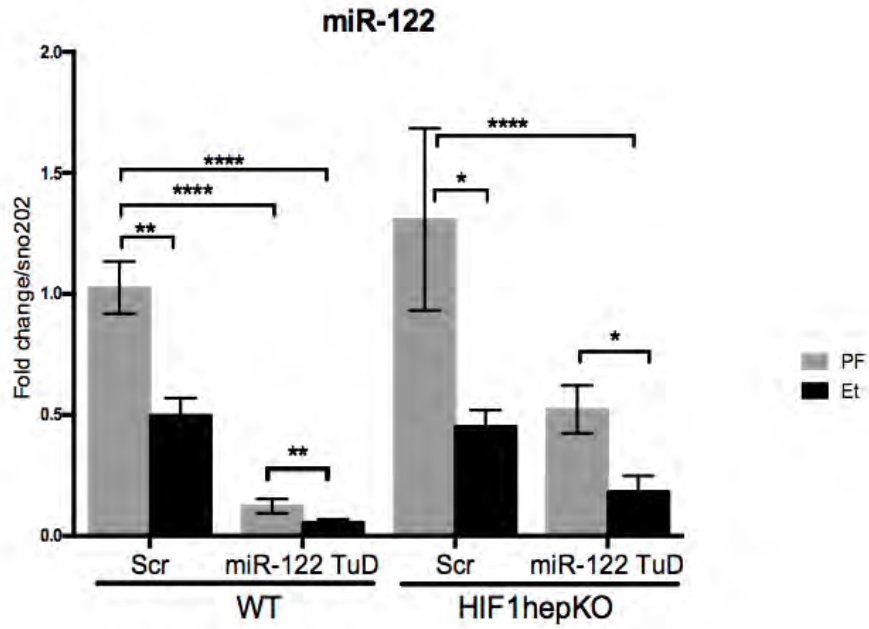


Figure 3.3: miR-122 mediated liver injury is HIF-1 α dependent

(a) miR-122 expression and (b) serum ALT in the total livers of WT and HIF1hepKO mice administered scrambled or miR-122-TuD after 5 weeks of control (PF) or alcohol (Et) diet. Alcohol resulted in a 50% reduction in both WT and HIF1hepKO mice. TuD treatment effectively inhibited miR-122 in WT and HIF1hepKO mice, given either alcohol or PF diet. While the loss of miR-122 is correlates with increased serum ALT in Wt mice, HIF1hepKO mice are protected from liver injury due to alcohol, antimiR-122-TuD, or their combination. *P < 0.05, **P<0.005, ***P<0.0005 by two-way ANOVA (n=6-14). Scale bars; 100 μ m.

a)



b)

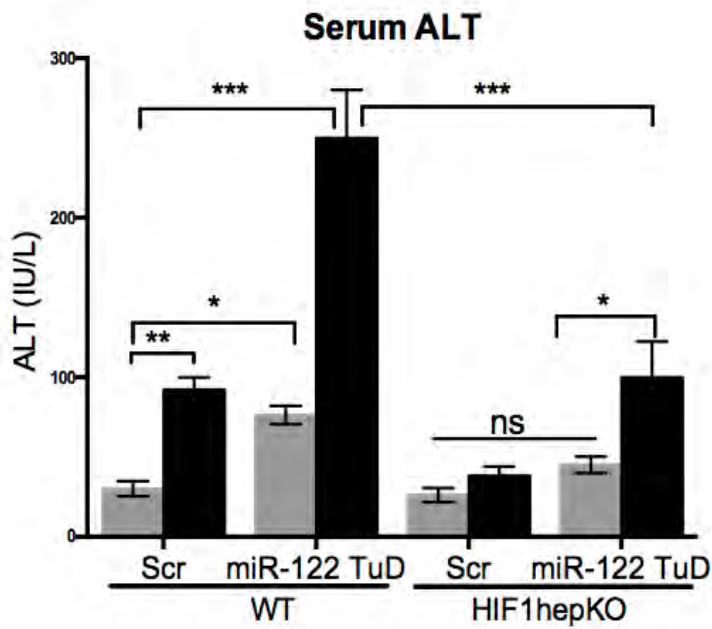
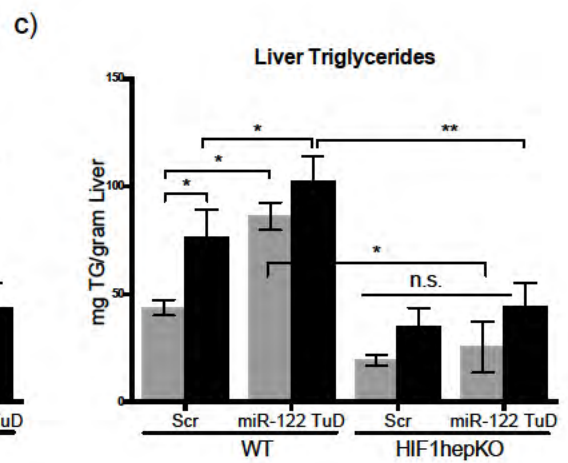
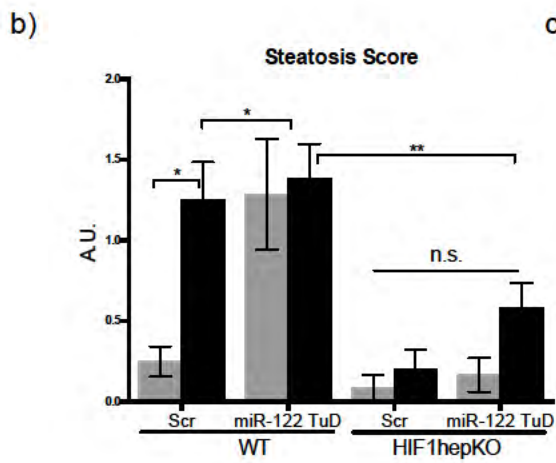
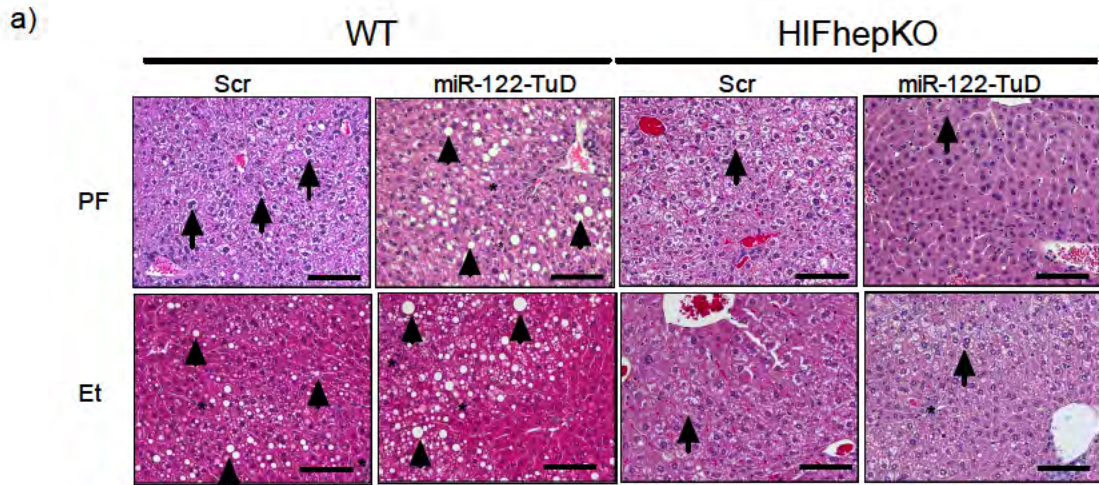


Figure 3.4: Alcohol and miR-122 mediated hepatic steatosis is HIF-1 α dependent

Histological assessment of steatosis and hepatocyte injury of (a) H&E staining of formalin-fixed, paraffin-embedded (FFPE) livers. (b) Scoring of histological sections for severity of steatosis, by veterinary pathologists blinded to group and sample number. (c) Quantification of hepatic triglycerides from whole-liver lysates. Pair-fed mice exhibited normal parenchymal morphology without fatty-changes. Alcohol and TuD-treated WT mice exhibited equivalent levels of steatotic changes, consistent with a chronic alcohol consumption. This was only slightly increased in the combination of TuD and alcohol. HIF1hepKO, similar to pair-fed mice exhibited no significant changes in lipid accumulation. *P < 0.05, **P<0.005, ***P<0.0005 by two-way ANOVA (n=6-14). Long arrows = glycogen-filled hepatocytes. Asterisks=immune cells. Long arrows = lipid-filled hepatocytes. Scale bars: 100 μ m. H&E liver histology from wild-type pair- and ethanol-fed mice.



Inflammation is an essential mediatory of ALD, and DAMPs released from injured hepatocytes contribute greatly to the recruitment and activation of hepatic immune cells. Given the extent of hepatic injury seen in miR-122-TuD, and in particular when the combinatorial effect with alcohol, I hypothesized there would be a cooperative increase in inflammatory markers. Further, that HIF1hepKO would be protected from this inflammation. Analysis of H&E sections and qPCR for immune cell markers revealed increased macrophage infiltration (CD68 and F4/80) and activation in anti-miR-122 TuD-treated, or alcohol-fed mice (Figure 3.5a,b, Figure 3.6a) with an even greater increase in mice treated with both TuD and alcohol together. I also found increased levels of IL-1 β , MCP-1, and TNF- α protein and mRNA (Figure 3.6b-d), in the livers of alcohol and miR-122 TuD-treated mice. HIF1hepKO mice treated with either miR-122 inhibition or chronic alcohol showed a reduction of inflammatory cell infiltration and activation compared to WT mice.

The development of fibrosis indicates progression of ALD as a result of sustained hepatocyte injury, inflammation, and stellate cell activation. However, typical 5-week murine models fail to demonstrate significant increases in early fibrotic markers, or collagen deposition seen in human disease. I found modest increases in collagen synthesis after alcohol feeding indicated by Sirius Red staining (Figure 3.7a,b) and the pro-fibrogenic markers, pro-collagen-1 α and Acta2 (Figure 3.7c,d). In miR-122 TuD mice treated with alcohol, I noted greater increases in pro-collagen-1 α and Acta2

expression, as well as in Sirius Red staining compared to pair-fed controls. The increase in fibrosis in the miR-122 TuD+Et group was abrogated in the HIF1hepKO mice.

Figure 3.5: Alcohol and miR-122 mediated hepatic inflammation is HIF-1 α dependent

qPCR analysis macrophage markers (a) F/480 and (b) CD68, total liver RNA. *P < 0.05, **P < 0.005, ***P < 0.0005 by Student's t test or two-way ANOVA (n=6-14). Scale bars: 100 μ m. H&E liver histology from wild-type pair- and ethanol-fed mice.

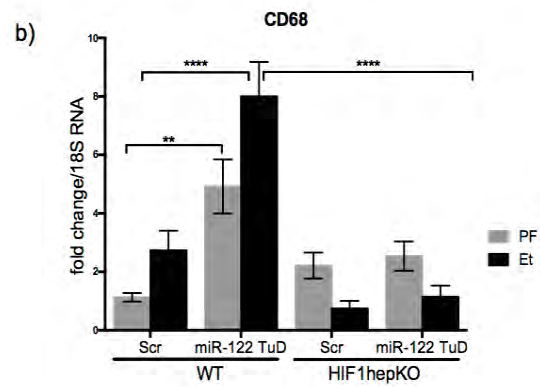
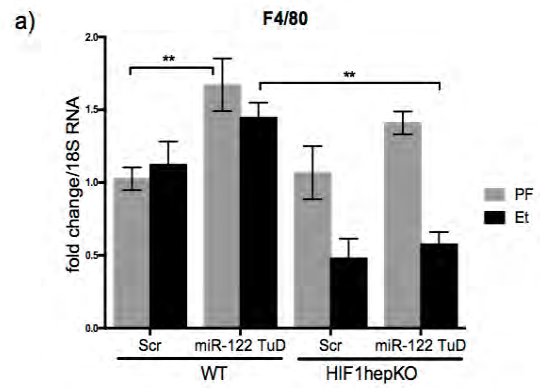


Figure 3.6: Alcohol and miR-122 mediated hepatic inflammation is HIF-1 α dependent

(a) H&E stained histological sections were scored for inflammatory cell infiltration, by veterinary pathologists blinded to group and sample number. (b-d) ELISA and qPCR analysis of pro-inflammatory cytokines MCP-1, IL-1 β , and TNF- α , from total liver lysates and total liver RNA respectively. Alcohol and TuD-treated WT mice exhibited equivalent levels of pro-inflammatory cytokines. The combination of TuD and alcohol exhibited an additive effect on hepatic inflammation. HIF1hepKO mice treated with either, alcohol, miR-122 TuD, or their combination exhibited no significant changes in expression of pro-inflammatory cytokines. *P < 0.05, **P<0.005, ***P<0.0005 by Student's t test or two-way ANOVA (n=6-14). Scale bars: 100 μ m. H&E liver histology from wild-type pair- and ethanol-fed mice.

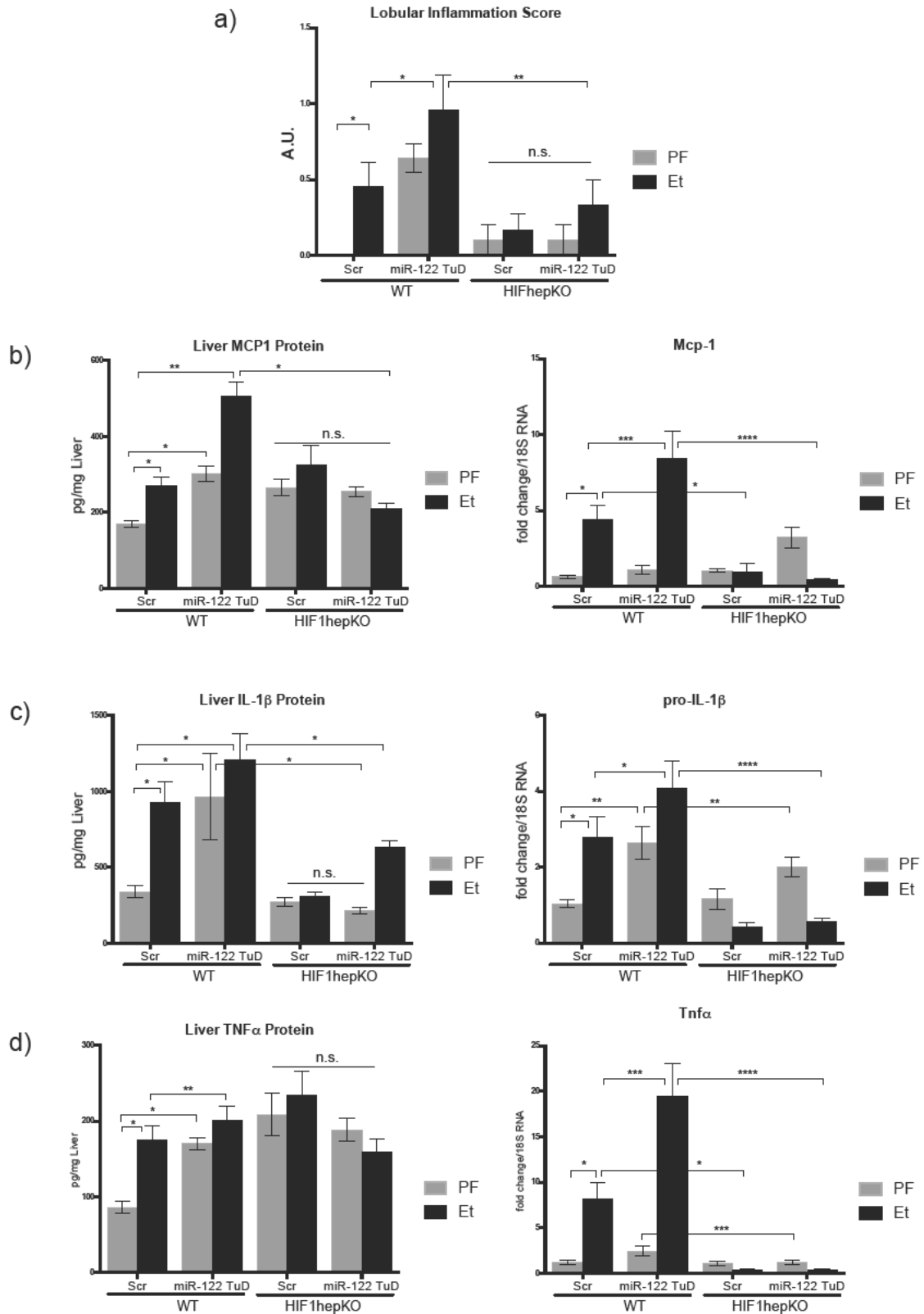


Figure 3.7: miR-122 loss mediates early fibrotic changes through HIF-1 α

Histological assessment of fibrosis was by (a) Sirius red staining of FFPE liver sections.

(b) Scoring of collagen deposition was performed by veterinary pathologists blinded to

group and sample number. qPCR analysis of stellate cell activation markers (c)

Collagen1a1 (col1a1) and (d) α -smooth muscle actin (Acta2). Treatment with either

alcohol or miR-122-TuD alone did not induced significant collagen deposition measured

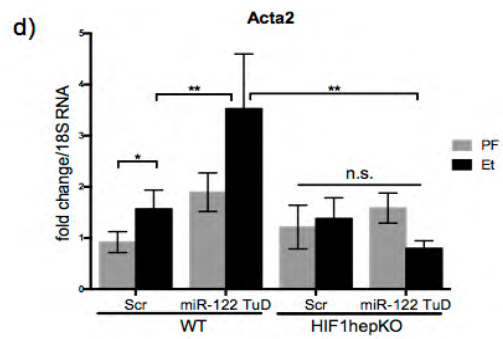
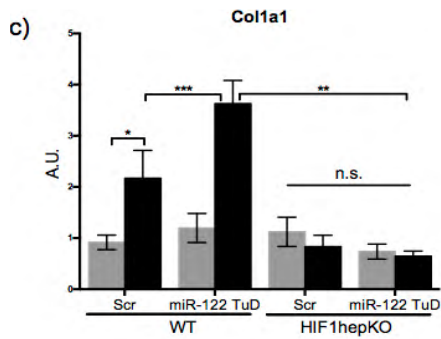
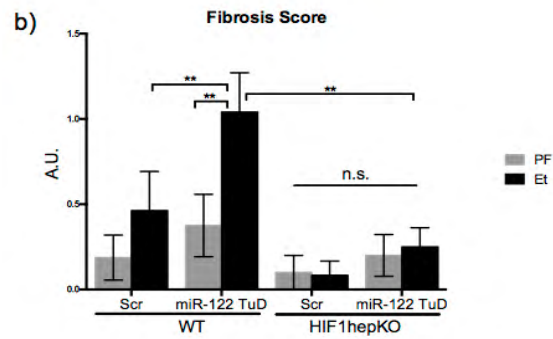
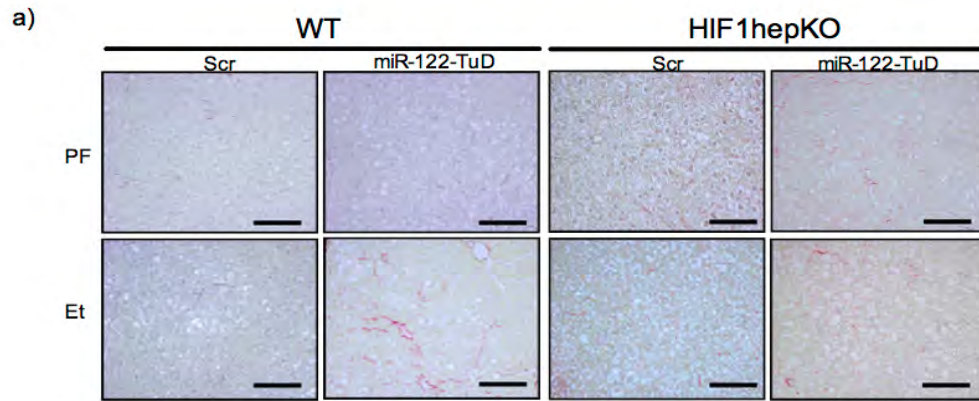
by Sirius red staining, however the combination of these two treatments resulted in

significant collagen deposition. This was associated with an increase in markers of

stellate cell activation. HIF1hepKO mice exhibited no collagen deposition or induction of

pro-fibrotic markers. *P < 0.05, **P<0.005, ***P<0.0005 by Student's t test or two-way

ANOVA (n=6-14). Scale bars: 100 μ m.



Conclusions and Discussion

In the previous chapter, I defined a direct link between miR-122 and its primary target, HIF-1 α , in vitro. Furthermore, I determined that chronic alcohol reduced miR-122 in humans and in a murine model. In this chapter I sought to explore the functional effect of miR-122 modulation on ALD pathogenesis, in vivo. Utilizing an AAV8-delivered miR-122 tough decoy resulted in sustained and efficient knockdown of miR-122 in the livers of alcohol-fed mice. As hypothesized, this inhibition was associated with a proportional increase in HIF-1 α mRNA and DNA binding activity.

A common pattern emerged throughout the data. Alcohol and miR-122 knockdown independently showed equivalent changes in direct indices of liver injury such as serum ALT, steatosis, inflammatory cytokines, and fibrotic markers while HIF1hepKO mice were protected from these effects. Furthermore, the reduction of miR-122 in the liver with alcohol (miR-122-TuD+et), resulted in dramatic increases in hepatic injury, greater than treatment with either alone.

This is identical to the phenotype our lab has previously observed using an *in vivo* degradation-resistant form of HIF-1 α in murine hepatocytes (HIF1dPA). HIF1dPA mice, which had a higher HIF-1 α expression in hepatocytes, developed steatosis and liver injury without the presence of alcohol. When given alcohol, HIF1dPA mice exhibited a synergistic phenotype similar to that seen in miR-122-TuD+Et, having greater liver injury than either treatment alone, and further increasing HIF-1 α mRNA expression and activity.

There are many potential reasons for this phenomenon. First, is that the further reduction in miR-122 seen in TuD+Et mice when compared to TuD+PF mice, allowed for a dose-responsive increase in HIF-1 α mRNA. However, Scr+Et and TuD+Et mice exhibited 50% and 85% reductions in miR-122 respectively. Therefore, if the increase is exclusively miR-122 dependent, I would have expected there to be greater HIF-1 α mRNA in TuD+Et mice when compared to Scr+Et mice. Second, is that the influence of miR-122 on HIF-1 α is limited to the availability of the transcript, and that alcohol also influences HIF-1 α transcription and activity. As described above, in the presence of hypoxia HIFs are post-transcriptionally stabilized, allowing for their accumulation and increased transcriptional activity. It is well established that chronic alcohol increases oxygen demand in the liver, and specifically, in zone 3 of the hepatic lobule. Furthermore, endotoxin or LPS in portal circulation is a common feature of human and murine models of ALD. It is therefore likely that there is a threshold by which miR-122 increases HIF-1 α mRNA and the hypoxic microenvironment within the hepatic further contributes to this via increased transcription and post-translational stabilization.

However, these explanations do not account for the slight, but significant increase in liver injury seen in HIF1hepKO mice treated with TuD+alcohol. While, HIF1hepKO TuD+Et mice exhibited dramatically reduced serum ALT and steatosis with no change in markers of inflammation, and fibrosis when compared to WT mice or other HIF1hepKO-treated mice, increases in ALT were noted. These findings could be due to hypoxic activation of HIF-2 α . Similar to HIF-1 α , degradation resistant HIF-2 α (HIF2dPA) has also been shown to induce hepatic lipid accumulation. Additionally, unpublished data

from Barath Nath, a former MD/PhD student in the lab, showed that alcohol increased both HIF-1 α and HIF-2 α . The relative role of HIF-1 α vs HIF-2 α in hepatic steatosis is not completely understood. Previous studies have suggested that HIF2dPA mice exhibit more steatosis and liver injury when compared to HIF1dPA. It is likely that the dramatic increases in liver injury seen in WT mice treated with TuD+Et, could be due to the simultaneous activation of HIF-1 α and HIF-2 α , and therefore not completely negated in HIF1hepKO mice. However, given the extent of protection from alcohol, miR-122 knockdown, and their combination afforded by removal of the HIF-1 α allele, it appears that in this model of alcoholic liver disease, the influence of other factors, such as HIF-2 α , are minimal when compared to HIF-1 α .

Finally, miR-122 has been shown to directly and indirectly regulate a complex network of genes involved in hepatic lipid homeostasis, hepatocyte differentiation, and survival pathways. It could be that in TuD+Et mice, which resulted in 90% loss of miR-122, in addition to the pleiotropic effects of alcohol, the loss of miR-122 could still drive pathogenesis through pathways outside the miR-122-HIF-1 α axis.

Amidst this pattern of data, another striking finding was apparent. The deletion of HIF-1 α in hepatocytes was sufficient to reduce the steatosis, inflammation and fibrosis due to alcohol, miR-122 inhibition or together. Together, these data suggest that the increased pro-inflammatory and pro-fibrotic state are at least partially dependent upon HIF-1 α -mediated hepatocyte injury due to the reduction of miR-122, and that restoration of miR-122 may provide therapeutic benefit.

CHAPTER 4: THERAPEUTIC RESTORATION OF MIR-122 REVERSES ALCOHOL-INDUCED LIVER INJURY VIA HIF-1ALPHA *IN VIVO*

Summary

Using AAV8 anti-miR-122 TuD based knockdown system in a murine model of alcoholic liver disease I demonstrated that the reduction of miR-122 due to chronic alcohol acts through HIF-1 α upregulation. Furthermore, hepatocyte-specific HIF-1 α -null mice were protected from this effect. In this chapter, I sought to determine whether therapeutic restoration of miR-122 in alcohol-fed mice could reverse hepatic injury. Using a similar AAV8-delivery system, I overexpressed miR-122 the livers of alcohol-fed mice. Therapeutic restoration resulted in a significant improvement in serum ALT, and inflammation suggesting a protective role for miR-122 in ALD.

Acknowledgements

I particularly would like to acknowledge the work of Sitara Rao for her technical assistance and dedication to this work in performing and analyzing data in figures 4.4-4.5. I would also like to thank Shashi Bala, Aditya Ambade, Benedek Gyongyosi, Arvin Iracheta-Vellve and Patrick Lowe, and other members of Szabo lab for their stimulating intellectual discussions and scientific input throughout all the experiments outlined here. I thank Dr. David Garlick of Cancer Biology Department at UMASS and Dr. Jin-Kyu Park DVM, PhD, a former lab member, for histopathological examination of liver tissue sections. The authors are grateful to services provided by Mass Histology for tissue sectioning and staining, My collaborators at the UMass Vector Core and Gao lab (AAV production) and CFAR (Primer Synthesis) core facilities at UMASS Medical School.

Introduction

Alcohol-triggered hepatocyte steatosis and cell death results in the activation and infiltration of immune cells within the liver leading to advanced hepatic injury. The subsequent release of inflammatory cytokines such as TNF- α and IL-1 β causes further hepatocyte cell death resulting in a continuous feedback loop of cellular injury, driving ALD pathogenesis.^{11,14,15} While the etiology of ALD and abundance of evidence clearly indicates that abstinence is the best treatment, even with abstinence, many patients still progress to hepatic cirrhosis. Additionally, with a high rate of recidivism, undiagnosed alcohol abuse, comorbidities and an ever-increasing mortality rate, necessitates the development of additional medical interventions.^{276 10,11}

Lifestyle changes are the cornerstone of ALD treatment.²⁷⁶ Due to the significant calorie consumption from alcohol and diminished intestinal absorptive capabilities, nutritional deficiencies of macro and micronutrients are a common issue among chronic alcoholics.²⁷⁷⁻²⁷⁹ Patients have been found to have deficiencies in protein consumption as well as vitamins A, D, thiamine, folate, zinc.^{10,11,280,281} Gross calorie replenishment, and specifically, the promotion of a positive nitrogen balance has shown some efficacy in improving liver function and reversing metabolic syndrome, a significant comorbidity and contribute to disease progression.^{282,283} Complimentary to nutritional deficiencies, is the depletion of antioxidants leading to a reduced capacity of hepatocytes to safeguard against reactive oxygen species. Three well studied treatments involve supplementation with Vitamin E, silymarin (milk thistle), and N-acetyl cysteine (NAC). Silymarin and NAC both function by increasing glutathione (GSH) in the liver, an essential antioxidant.

Together, all three have been shown to protect against lipid peroxidation and oxidative damage induced by free radicals in animal models of chronic alcohol.^{31,284-286 287}

However, their efficacy in humans has been minimal, particularly in cases of severe alcoholic hepatitis.²⁸⁸⁻²⁹² The failure of these may be the persistence of oxidant stress within the liver along with other comorbidities.

Pharmacologically, there are two classes of therapeutics that have been explored; immunomodulatory and metabolic, to inhibit hepatic inflammation and reverse steatosis respectively. Immunosuppressive therapies first emerged 40 years ago with the use of corticosteroids.²⁹³ Since these initial studies, they remain the standard of care in spite of lackluster efficacy.²⁹⁴ Subsequently, several agents have been studied to inhibit inflammatory pathways targeting cytokines, specifically TNF- α . One such agent tested to inhibit TNF- α was a phosphodiesterase (PDE) inhibitor, pentoxifylline (PTX).²⁹⁵ This orally bioavailable PDE inhibitor was shown to reduce the production of many pro-inflammatory cytokines, including TNF- α . While initial studies demonstrated reduced mortality at three months, subsequent studies have failed to recapitulate these robust findings. The use of PTX is approved for patients with severe alcoholic hepatitis.²⁹⁶ Additionally, specific anti-TNF- α therapies using monoclonal antibodies against (infliximab) as well as TNF- α receptor antagonists (etanercept) have also been explored.^{297,298} However, given the essential role TNF- α has in liver regeneration and in pathogen defense, raised questions about its safety.^{299 10} While mortality was moderately decreased when compared to control groups, studies were halted due to complications due to opportunistic infections.^{10,12,300,301}

Currently, emerging therapeutics include the use of nuclear receptor (RXR/FXR) agonists to reverse hepatic steatosis, IL-1 β receptor antagonists to inhibit cytokine-induced cellular damage, as well as S-adenosylmethionine supplementation to buffer against ROS. As with previous therapies, all have shown efficacy in animal models, and clinical trials are ongoing.^{274,302}

Amidst scores of studies and years of potential therapies, a common theme that multi-targeted approaches are necessary, and further, that immunosuppressive monotherapy, without correction of parenchymal cell function, is insufficient to reverse ALD pathogenesis.

In the previous chapters I found that hepatic miR-122 levels are 2-fold lower in hepatocytes of alcohol-fed mice and human alcoholic cirrhosis patients compared to controls. Using AAV-delivered anti-miR-122 TuDs, I have demonstrated a causal link between the alcohol-induced reduction of miR-122, and ALD pathogenesis via HIF-1 α . These studies showed that the loss of miR-122 directly correlated with increasing steatosis, inflammation, and fibrosis. Given these findings, I hypothesized that therapeutically restoring miR-122 in alcohol-fed mice could reverse chronic alcohol-induced liver injury.

Many mechanisms have been developed for modulation of miRNAs, and specifically miR-122, in the liver. ASOs, LNAs, and miRNA sponges have all been extensively studied and modified to enhance specificity, potency, and stability. However, contrary to ASOs, delivery of small single-stranded or duplex miRNA mimics has proven difficult. These naked RNA molecules lack specificity and stability and while chemical

modifications can improve these parameters, the issue of TLR activation has not been overcome (Figure 1.5).

Currently, two strategies for delivery have been developed; cationic lipid (liposomes) carriers and viral-vector based delivery systems (AAVs). These liposomes consist of cationic lipid bilayers complex with the anionic nucleic acid cargo, the result is a positively charged bilayer able to bind the anionic surface of target cells.^{256,257} Further, the addition of surface modifications can facilitate cell or organ specific delivery or subcellular release in either the nucleus, cytoplasm, or endosome.²⁵⁸⁻²⁶⁰ While these modifications can increase functional efficiency of the liposomes, their utility has not matched that of AAVs.²³⁸

Many AAV serotypes have been used to deliver transgenes to the liver, including AAVs 2, 8, and 9. However, AAV8 has shown to have the most selective tropism and least immunological memory among the population. Given this, the use of AAV8 to deliver Factor IX to Hemophilia B patients has successfully completed clinical trials and is approved for use in patients.^{264,265,269} It is important to mention that the over expression of short hairpin RNA in rats has been shown to cause hepatotoxicity, organ failure and death.¹⁵⁹ This toxicity been associated caused by the saturation of exportin-5. However, it has been suggested that if the delivered transgene produces pri-miRNA constructs more similar to that of endogenous transcripts, this toxicity can be reduced or mitigated.^{159,270-272}

Taking these into consideration, through my collaboration with the Gao lab, we modified the anti-miR-122-TuD system described in chapter 3 by replacing the TuD with

a pri-miR-122 insert under the control of a U6 promoter (miR-122-OX). Using an AAV8, mice were treated with the overexpression construct while on chronic alcohol. The restoration of miR-122 effectively reduced the steatosis, inflammation and hepatic injury associated with chronic alcohol.

Methods

Animal Studies

All animals received care in compliance with protocols approved by the Institutional Animal Use and Care Committee (IACUC) of the University of Massachusetts Medical School. Wild-type (WT) mice (C57/B16), Alb-Cre, and HIF-1 α ^{flox/flox} mice were purchased from Jackson Laboratories (Bar Harbor, ME) and backcrossed onto a C57/B16 background. 6-8 week old mice were gradually acclimated to a Lieber-DeCarli liquid diet with 5% ethanol (vol/vol) over a period of 1 week, then maintained on the 5% diet for 4 weeks (total of 5 weeks). Consumption was recorded daily and isocaloric amounts of a control diet (in which dextran-maltose replaced calories from ethanol) were dispensed to pair-fed (PF) animals. Weights were recorded weekly. At the conclusion of the 5-week feeding, mice were weighed, blood collected, and euthanized. Livers were dissected, weighed and divided into lipid nitrogen for protein and biochemical assays, fixed in 10% phosphate-buffered formalin for histological analysis, preserved in OCT frozen section preparation solution, or soaked in RNALater (Qiagen, Hilden, Germany, Hilden, Germany). Blood was allowed to clot and serum obtained using gel-based serum separator tubes.

Isolation of primary mouse hepatocytes and LMNCs

Anesthetized animals were perfused by way of portal vein with saline solution, followed by enzymatic digestion, as previously described.⁷⁵ The hepatocytes were separated by centrifugation. In vitro experiments. Primary hepatocytes were cultured in

low-glucose DMEM supplemented with 10% fetal bovine serum, 1% Anti-Anti, 1% gentamycin, 1% insulin, transferrin, selenium solution. Primary hepatocytes were seeded in 6-well collagen-coated plates (Biocoat, Becton Dickinson). Before starting stimulation experiments, hepatocytes were rested for 4 hours.

RNA extraction and real-time PCR

Total RNA was extracted using the Quiagen miRNeasy kit (Quiagen, Hilden, Germany, Hilden, Germany) according to the manufacturer's instructions. Briefly, tissue samples were lysed in QIAzol Lysis reagent (Quiagen, Hilden, Germany), homogenized with stainless steel beads in TissueLyser II (Quiagen, Hilden, Germany) followed by miRNA isolation following manufacturer's instructions and DNase 1 Digest. RNA was quantified using Nanodrop 2000 (Thermo Scientific, Waltham, MA). Complementary DNA (cDNA) synthesis was performed by reverse transcription of 1 ug total RNA using the iScript Reverse Transcription Supermix (Bio-rad, Hercules, CA). Real-time quantitative PCR was performed using Bio-Rad iTaq Universal SYBR Green Supermix and a CFX96 real-time detection system (Bio-Rad Laboratories). Primers were synthesized by IDT, Inc. **The** primer sequences are listed in Table 2.1. Relative gene expression was calculated by the comparative cycle threshold (Ct) method. The expression level of target genes was normalized to the house-keeping gene, 18S rRNA, in each sample and the fold-change in the target gene expression between experimental groups was expressed as a ratio. Melt-curve analysis was used to confirm the authenticity of the PCR products.

miRNA Analysis

Reverse transcription (30 min - 16°C; 30 min - 42°C; 5 min - 85°C) was performed in Eppendorf Mastercycler (Eppendorf, New York, USA) using 10 ng RNA, TaqMan primers and miRNA Reverse Transcription Kit (Applied Biosystems, Foster City, CA) followed by quantitative RT- in CFX96 (Bio-rad, Hercules, CA) using TaqMan Universal Probes Master Mix (Bio-rad, Hercules, CA). All samples were normalized to snoRNA202, or U6 expression based on Normfinder (<http://moma.dk/normfinder-software>) analysis of loading control stability. hsa-miR-122-FAM, U6-FAM, and sno202-FAM primer sets were purchased from Applied Biosystems.

Construction of miR-122 antagonist and overexpression plasmids

The scAAV-anti-miR-122 TuD and scAAV-anti-SCR TuD constructed were made as previously described Xie et al., 2012.²²¹ The BamHI fragment carrying anti-miR-122 TuD was replaced with the pri-miR-122 sequence amplified from C57/b6 mouse genome DNA to generate scAAV-pri-miR-122 construct using primers: GCGGGATCCGACTGCAGTTTCAGCGTTTGG, and CGCGGATCCAAAAAAGACTCTAGGGCCCGACTTTACA.²²¹ Mice were treated by tail vein injection with AAV vectors at 6×10^{11} genome copies/mouse or approximately 3×10^{13} genome copies/kg.²²¹

Biochemical Assays

Serum alanine aminotransferase (ALT) levels were determined using a commercially available reagent (Advanced Diagnostics Inc) as described. Serum alanine aminotransferase (ALT) was determined using a commercially available reagent (Advanced Diagnostics Inc, Plainfield, NJ). 15ul of serum was mixed 1:10 with assay reagent diluted according to the instructions of the manufacturer, and UV absorbance at 37 degrees C was measured over three minutes. The average change in absorbance per minute interval is then multiplied by a conversion factor to yield ALT levels.

Liver triglycerides were extracted using a 5% NP-40 lysis solution buffer. Triglycerides were quantified using a commercially available kit (Wako Chemicals) followed normalization to protein amount.

Protein concentration was determined by by BCA protein assay (ThermoFisher Scientific) by using 10 uL of 1:10 or serially diluted lysate and incubating in assay reagent for 30 minutes at 37 degrees C. Absorbance was measured at 562nm on a 96 well plate using a plate reader. Concentrations were interpolated using 4-PL regression derived from a standard curve generated using bovine serum albumin standard (Pierce).

Nuclear Extraction

50mg of snap-frozen liver tissue was washed in 10-fold excess volume TKM-0.32 buffer (0.32M sucrose, 50mM Tris-HCl, 25mM KCl, 5mM MgCl, 5mM PMSF), with protease inhibitor tablets 1 per 10 mL, (Roche) and homogenized using a hand-held homogenizer. Homogenates were transferred to microcentrifuge tubes and centrifuged (1000rpm for 10 minutes at 4 degrees C). Pelleted material was resuspended in TKM-2.0

buffer (2M sucrose, 50mM Tris- HCl, 25mM KCl, protease inhibitor cocktail) and homogenized again by handheld homogenizer. Pellets were collected by centrifugation (14000rpm for 30 minutes at 4 degrees C) and resuspended in 500ul Buffer A (10mM Hepes/KOH, pH 7.9, 2mM MgCl, 1mM EDTA, 10mM KCl, 1mM DTT, 5mM PMSF, 1 protease inhibitor tablet). Pellets were again collected by centrifugation (14000rpm for 30 minutes at 4 degrees C) and resuspended in 50ul Buffer B (10mM Hepes/KOH pH 7.9, 2mM MgCl, 1mM EDTA, 50mM KCl, 300mM NaCl, 2mM DTT, and 5mM PMSF with protease inhibitor tablets 1 per 10 mL, (Roche), 10% glycerol. Pellet was resuspended was sonicated at 40% duty cycle 1 second on/off cycle, frozen at -80 degrees overnight, and thawed with gentle agitation at 4 degrees Celsius. Supernatant containing nuclear extract was collected after centrifugation (14000rpm for 30 minutes at 4 degrees C) and assayed for protein concentration.

Electrophoretic Mobility Shift Assay

The DNA binding activity of HIF-1 α was assessed by electrophoretic mobility shift assay as described previously (Nath B., *Hepatology*. 2011 May;53(5):1526-3).⁷⁵ A consensus double-stranded Hypoxia Response Element (HRE) (Santa Cruz Biotech, CA) oligonucleotide was used for EMSA. End-labeling was accomplished by treatment with T4 kinase in the presence of [P32]ATP. Labeled oligonucleotides were purified on a polyacrylamide copolymer column (Bio-rad, Hercules, CA). Five micrograms of liver or hepatocyte nuclear protein was added to a binding reaction mixture containing 50 mM Tris-HCl, pH 7.5, 5 mM MgCl₂, 2.5 mM EDTA, 2.5 mM DTT, 250 mM NaCl, 20%

glycerol, 20 &g/ml BSA, 2 & poly(dI–dC) and 50,000 cpm $\gamma^{32}\text{P}$ -labeled HIF-1 α consensus oligonucleotide. Cold competition was done by adding a 20-fold excess of specific unlabeled double-stranded probe to the reaction mixture. Samples were incubated at room temperature for 30 min. Reactions were run on a 4% polyacrylamide gel and the dried gel was exposed to an X-ray film at -80°C overnight. Band density was quantified using ImageJ64 image analysis.

Whole Cell Lysate

Approximately 50 mg of liver tissue was washed in ice cold PBS and homogenized in lysis buffer (9.5ml RIPA buffer, 1mM NaF, 2mM Na₃VO₄, 1 protease inhibitor tablet, 5mM PMSF) with stainless steel beads in TissueLyser II (Qiagen, Hilden, Germany, Hilden, Germany). After 10 minutes of incubation on ice, homogenates were centrifuged at 14,000xg for 10 minutes at 4 degrees C. The supernatant (clarified whole cell lysate) was collected and stored in aliquots at -80 degrees C.

ELISA

Cytokine levels were monitored in 25 mg of liver whole cell lysates diluted in assay diluent following manufacturer instructions. MCP-1 and TNF α were measured by use of specific anti-mouse ELISA from BioLegend. IL-1 β was measured by use of specific anti-mouse ELISA (R&D Systems) that recognizes both pro- and cleaved- IL-1 β .

Histopathological analysis

Sections of formalin-fixed, paraffin-embedded livers were stained with hematoxylin and eosin (H&E), or Sirius Red and assessed for histological features of steatosis, inflammatory cell invasion, and fibrosis.

Statistical Analysis

Statistical significance between two groups was determined using two-tailed t-test. Two-way ANOVA and Dunnett's multiple comparison post-test were used to compare the means of multiple groups. Outliers were determined using ROUT method with a q of 1%. Data are shown as mean \pm SEM and were considered statistically significant at $P < 0.05$. GraphPad Prism 6.02 (GraphPad Software Inc.) was used for analysis.

Results

To assess the therapeutic potential of miR-122 restoration on the pathogenesis of alcoholic liver disease, I developed an rAAV8 vector expressing miR-122 (miR-122-OX) or a scrambled (scr). In a preliminary experiment, I established that wild-type alcohol-fed mice develop significant liver injury by week 2 of the 5-week alcohol model (Figure 4.1a) and that the rAAV8 miR-122-OX construct requires 3 weeks for full expression in the liver (Figure 4.1b). Therefore, I treated pair-fed and alcohol-fed mice with 6×10^{11} viral particles containing Scr or miR-122-OX construct by tail-vein injection on week two of a five-week alcohol feeding model (Figure 4.1c).

qPCR analysis demonstrated treatment with rAAV8-miR-122-OX effectively increased mature miR-122 levels in the livers of pair-fed and alcohol-treated mice

(

Figure 4.2a). However, I found that in isolated hepatocytes, it appeared that the vector did not increase miR-122 in isolated hepatocytes in miR-122-OX+PF mice (

Figure 4.2b). To confirm this finding, I performed a northern blot from total RNA isolates from hepatocytes which showed a similar patterns of expression (

Figure 4.2c).

In spite of these findings, consistent with the *in vitro* data presented in chapter 2 (Figure 2.6a), *in vivo* overexpression of miR-122 prevented the alcohol-induced increase in HIF-1 α mRNA and DNA binding activity (Figure 4.3a,b). Overexpression of miR-122 in hepatocytes resulted in dramatic reductions in serum ALT (Figure 4.4a), and steatosis on histology and in liver triglycerides induced by alcohol (Figure 4.4b,c). Furthermore, miR-122-OX treatment prevented induction of inflammatory cytokines in ALD including TNF- α , MCP1, and IL-1 β (Figure 4.5a-c).

Conclusions and Discussion

Herein, I hypothesized that correction of the alcohol-induced inhibition of miR-122 via ectopic expression could reverse liver injury in a murine model of alcoholic liver disease. Using an AAV8 miR-122-OX vector system developed by my collaborators in the Gao lab, I was able to restore miR-122 in the livers of alcohol fed mice. Furthermore, this restoration was associated with the reduction in multiple indices alcohol-induced liver injury including steatosis, serum ALT, and inflammatory markers. Taken together,

these data suggest that restoration of miR-122 in the liver may be a viable therapeutic option.

Figure 4.1: Design of miR-122 treatment model.

(a) Serum ALT from week 2, of a Liber DeCarli chronic alcohol feeding model. (b) Secreted Gaussia Luciferase (Gluc) activity measured weekly from (n=3-5) alcohol-fed mice given 6×10^{11} viral particles by tail vein injection. Vector expression increased steadily week by week reaching a peak at 3 weeks post injection. (c) Schematic representation of rAAV8-miR-122-OX treatment model. *P < 0.05, **P < 0.005, ***P < 0.0005 by Student's t test or two-way ANOVA.

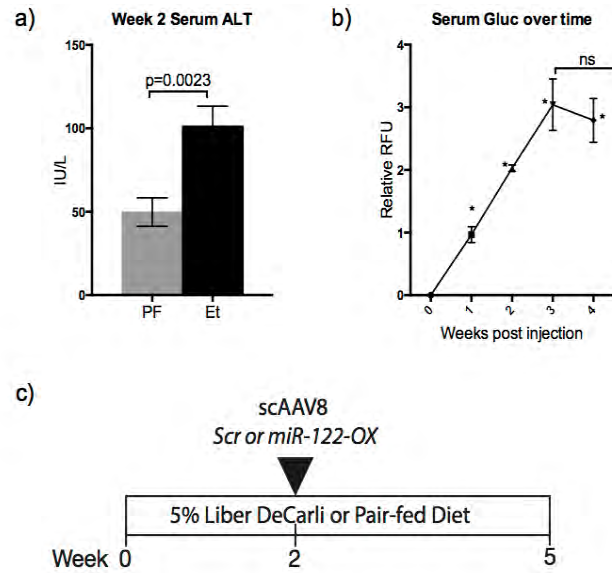


Figure 4.2: miR-122 expression in AAV8-miR-122-OX treated mice. qPCR analysis of expression from (a) total liver and (b) hepatocyte RNA. (c) Northern blot for hepatocyte miR-122. U6 was used as a loading control. Data is represented as fold change relative to WT-PF mice. Treatment of PF and Et-fed WT mice with rAAV8 –pri-miR-122 (miR-122-OX) increased miR-122 expression in total livers when compared to respective PF-fed controls. qPCR and northern blot from hepatocyte RNA extracts revealed a reduced, but not statistically significant, level of miR-122 in PF+miR-122-OX mice. Alcohol-fed mice treated with miR-122-OX demonstrated significant increases in miR-122 in both total liver and hepatocytes. *P < 0.05, **P<0.005, ***P<0.0005 by two-way ANOVA. (n=5)

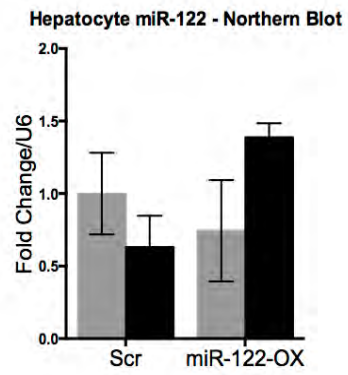
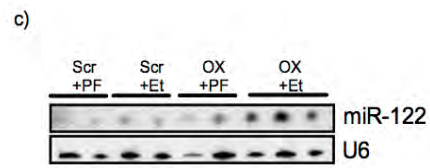
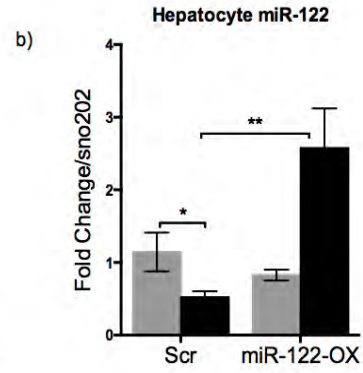
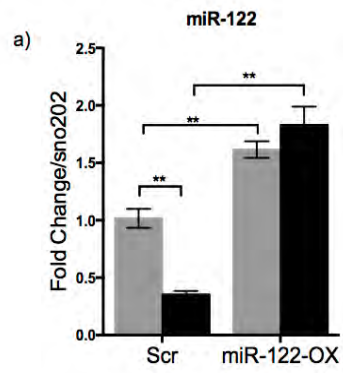


Figure 4.3: Restoration of miR-122 inhibits alcohol-induced increases of HIF-1 α

HIF- α (a) mRNA and (b) DNA binding activity in hepatocytes measured by qPCR and EMSA respectively. EMSA analysis was performed from hepatocyte nuclear extracts from PF and ET-fed mice treated with either AAV8 Scr or miR-122-OX. Ectopic expression of miR-122 inhibits the alcohol-induced increase of HIF-1 α mRNA and DNA binding activity in hepatocytes. *P < 0.05, **P<0.005, ***P<0.0005 by two-way ANOVA. (n=5)

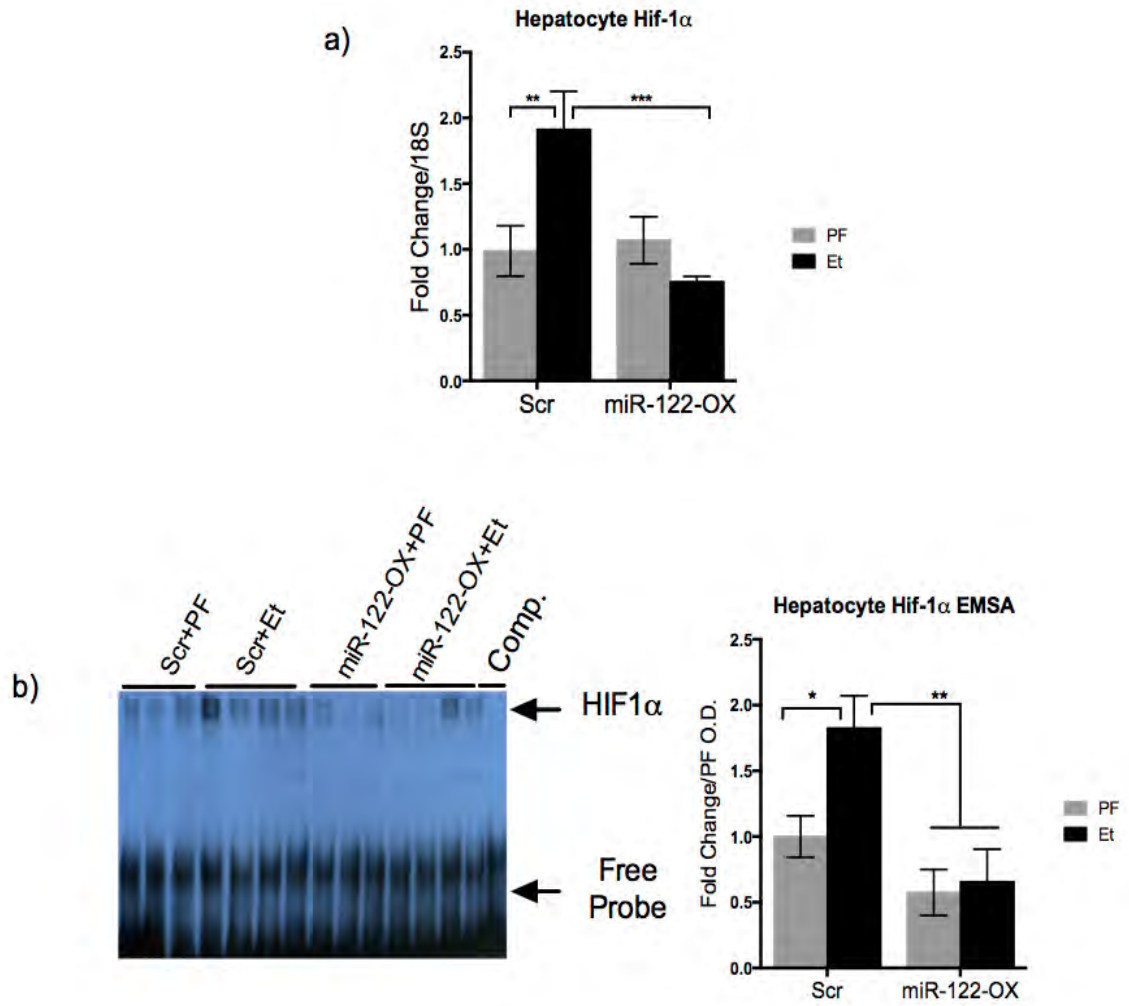


Figure 4.4: Treatment with rAAV8-miR-122-OX reverses alcohol-induced liver injury and steatosis

(a) Serum ALT, (b) H&E histology and (c) hepatic triglycerides from livers of either PF- or Et-fed WT mice treated with rAAV8-Scr or rAAV8-miR-122-OX vectors. Restoration of miR-122 reduced liver injury and hepatic steatosis in alcohol-fed mice. Alcohol-fed mice exhibited extensive steatosis and glycogen depletion. miR-122-OX-treated PF and Et-fed mice exhibited no evidence of steatosis or parenchymal changes. (n=8-12) Long arrows = glycogen-filled hepatocytes. Asterisks=immune cells. Long arrows = lipid-filled hepatocytes. Scale bars; 100 μ m. *P < 0.05, **P<0.005, ***P<0.0005 by two-way ANOVA.

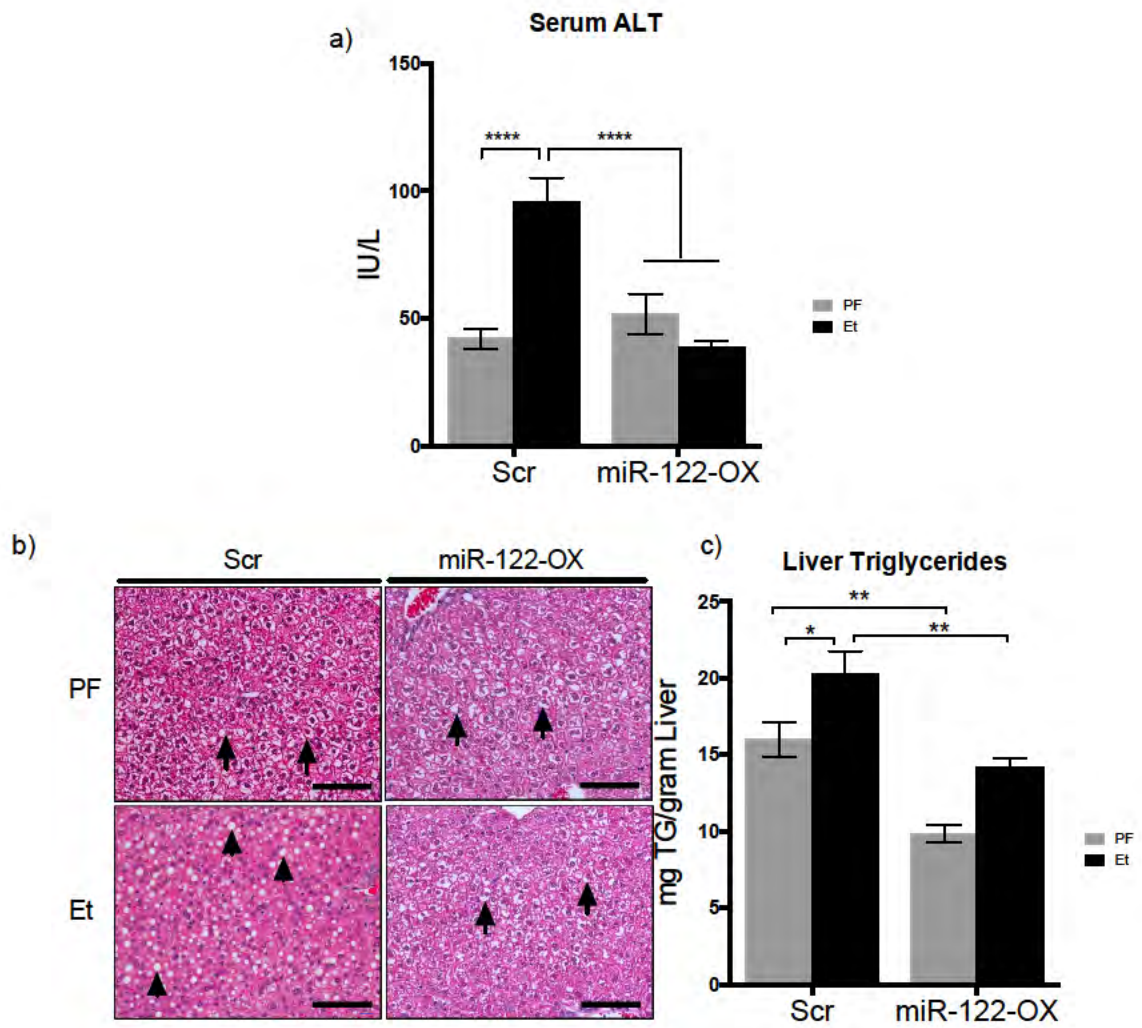
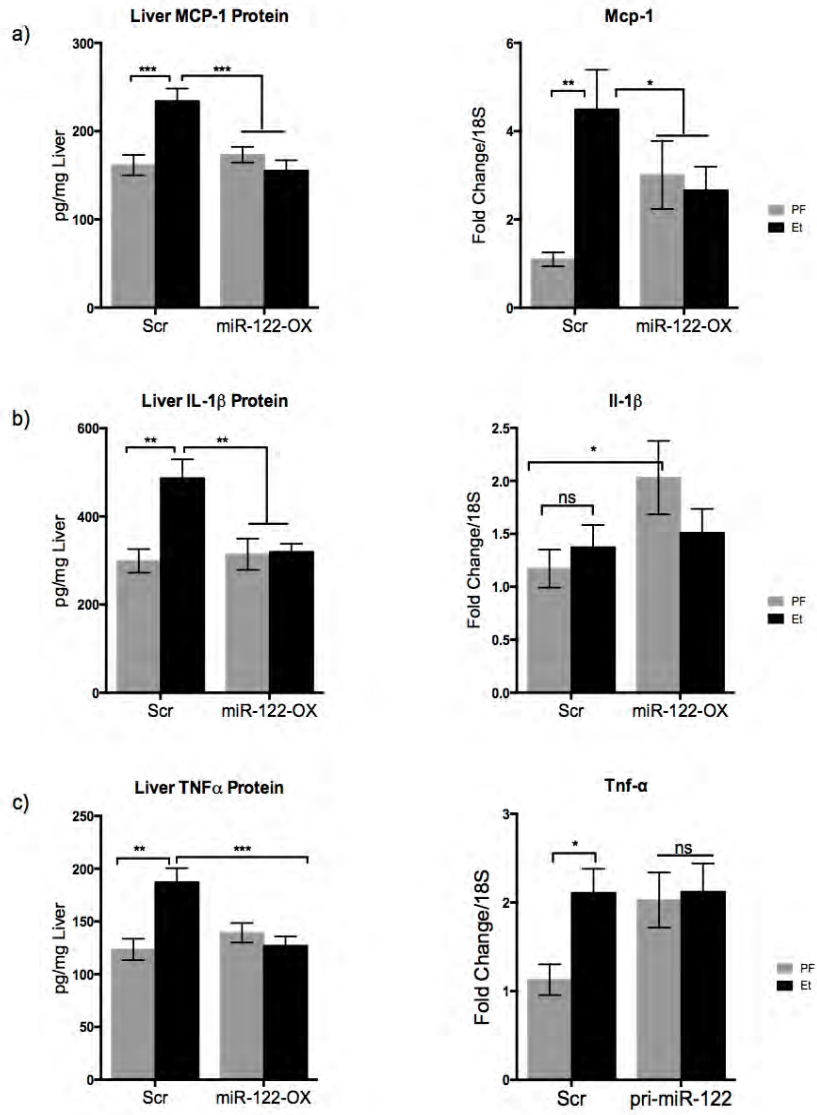


Figure 4.5: Treatment with rAAV8-miR-122-OX reverses alcohol-induced inflammation

(a-c) ELISA and qPCR analysis of pro-inflammatory cytokines MCP-1, IL-1 β , and TNF- α , from total liver lysates and total liver RNA respectively. Et-fed mice treated with rAAV8-miR-122-OX vectors demonstrated reduced pro-inflammatory cytokines when compared to scramble treated controls. (n=8-12) Scale bars; 100 μ m. *P < 0.05, **P<0.005, ***P<0.0005 by two-way ANOVA.



Amidst the data, it was surprising to find that in hepatocytes isolated from pair-fed mice treated with the AAV8 miR-122 overexpression construct did not appear to have increased miR-122 when assessed by qPCR and northern blot. In contrast, ethanol-fed-mice treated with the overexpression vector did indeed exhibit increased miR-122 expression in total liver extracts and isolated hepatocytes by qPCR and northern blot analysis.

As described before, saturation of exportin 5 (XPO5) during overexpression of shRNAs has been described. This is unlikely given that studies demonstrating saturation of miRNA biogenesis pathways used shRNA expression vectors on non-endogenous products and only noted toxicity at high vector doses (1×10^{12}) while I used 1/2 this dose (6×10^{11}).^{159,303} While I did not observe any mortality or increase in serum ALT in either pair-fed or alcohol-fed mice, this effect may have been evident given an extended time period.^{159,303} Alternatively, it may be that pair-fed mice, when treated with the AAV8 exhibited transient hepatotoxicity due to XPO5 saturation in the three weeks between injection of the vector and the completion of our study. Given that liver regeneration studies have shown a doubling in liver mass within 48 hours after 2/3 partial hepatectomy studies, a transient toxicity would greatly reduce the number of hepatocytes expressing the miR-122 transgene but exhibit no observable defects at the time of necropsy. It has also been shown that kupffer cells in the liver may be capable of expressing AAV8 delivered transgenes. While AAV8 does transduce 90-95% hepatocytes depending on dose, it has been shown that macrophages may in fact be either directly infected or in their capacity as phagocytic cells, internalize the viral particles.^{238,304-306} Therefore, KCs may

function as a reservoir for miR-122 transgene expression while it is lost in hepatocytes. Alternatively, given that no ALT or mortality was noted, a yet, undefined feedback mechanism for mature miR-122 levels may exist.

Finally, one other disparity regarding this data remains unanswered; why did both the hepatocyte and total liver qPCR and northern blot from alcohol-fed mice treated with the miR-122-OX construct, appropriately reflect the increase in miR-122 when PF mice did not? As described before, this may be an extension of the toxicity due to XPO5 saturation. As will be explored in the following chapter, the decrease in miR-122 observed with alcohol is due a decrease in pri-miR-122 transcription, thereby decreasing the amount of pre-miR-122 requiring nuclear export via XPO5. Therefore, the introduction of a transgene encoding the pre-miR-122 in alcohol-fed mice would be below the toxic threshold allowing sustained expression in hepatocytes.

Overall, these data demonstrate that restoration of miR-122 in hepatocytes can suppress the pathogenic features of ALD via inhibition of HIF-1 α *in vivo* and indicates that hepatocyte-specific miR-122 delivery could be a therapeutic consideration in ALD.

CHAPTER 5: ALCOHOL REGULATES MIR-122 THROUGH ALTERNATIVE SPLICING OF GRAINYHEAD PROTEINS

Summary

The data presented in previous chapters clearly demonstrates that essential role of miR-122 in maintaining hepatic normalcy and that sustained inhibition can cause an ALD-like phenotype. However, the question still remained as to the mechanism by which alcohol inhibits miR-122. The high level of miR-122 in the liver is maintained by host of hepatocyte specific transcription factors. Recently, it has been shown that grainyhead-like 2 (GRHL2), a transcription factor not typically expressed in mature hepatocytes, could be a potential inhibitor of miR-122 expression. In this chapter I will provide evidence to suggest that not only does alcohol regulate miR-122 through upregulation of GRHL2 in hepatocytes, but that alcohol regulates alternative splicing events within the grainyhead family of proteins.

Acknowledgements

I would like to acknowledge the work of Sitara Rao whose technical assistance was very much appreciated. I would also like to thank Ying-Chao Hsueh for his help with generation of the miR-122 promoter assays. I am thankful to Arvin Iracheta-Vellve for his assistance in confocal microscopy staining and acquisition of the images. The hGRHL2-FL and hGRHL2-S plasmids were a kind gift by Dr. Volker Assmann of the Institute of Tumor Biology at University Medical Center Hamburg-Eppendorf. I thank Dr. David Garlick of Cancer Biology Department at UMASS for histopathological examination of liver tissue sections. I am grateful to services provided by DERC morphology (Immunohistochemistry), our collaborators at the Vector core(AAV production) and CFAR (Primer Synthesis) core facilities at UMASS Medical School. Lastly, the authors thank Dr. Jeffrey Nickerson, Dr. Jean Underwood, and the Cell & Development Biology Confocal Core at UMass Medical School for their training and support in the use of the Leica TCS SP5 II Laser Scanning Confocal Microscope.

Introduction

The question remained as to the mechanism by which miR-122 expression is reduced. As shown in chapter 2, while AAV8-miR-122-TuD achieved a robust knockdown of miR-122 in pair-fed mice, I consistently observed a further ~50% reduction in miR-122 in alcohol-fed mice. Furthermore, while I have demonstrated that restoration of the mature form of miR-122, and HIF-1 α -null mice are protected from the phenotype of ALD, the inhibitory effect of alcohol on miR-122 expression appeared to still be present. Additionally, in chapter 3, both PF and Et mice treated with the U6-driven AAV8-miR-122-OX achieved similar mature miR-122 expression levels from total liver RNA. Given that the transgene encoded a large segment of the pri-miR-122 genomic region requiring processing via endogenous miRNA biogenesis pathways, and suggesting that the change in promoter was able to negate this inhibitory effect therefore, I hypothesized that alcohol was not effecting the processing of of miR-122, rather its transcription.

Many transcription factors have been shown to regulate miR-122 transcription, including hepatocyte nuclear factors (HNFs) 1, 3, 4, and 6.^{135,185,187,241} Recent studies have pointed to grainyhead like-2 (GRHL2), a homolog of the drosophila grainyhead (GRH) transcriptional regulator, as a potential repressor of miR-122 expression in hepatic progenitor cells during hepatobilliary differentiation.³⁰⁷

GRHL2, a homolog of the *Drosophila* protein Grainyhead (GRH), is one of the three mammalian proteins within the Grainyhead-like (GRHL) family of transcription factors.

The three GRHL proteins are numbered 1-3, however they have gone by other names as well; GRHL1 (mammalian grainyhead, MGR, LBP-32), GRHL2 (brother of mammalian grainyhead, BOM), and GRHL3 (sister of mammalian grainyhead, SOM). Within the mammalian GRHL family, each of the three grainyhead proteins have been found to have tissue and developmentally distinct expression patterns.^{308 309} They are found primarily in epithelial tissues, in organs such as epidermis, oral and olfactory epithelium, kidneys and urogenital tract, stomach and the digestive tract, heart and lung.
308,310,309

Structurally, all grainyhead proteins are remarkably similar, containing an evolutionarily conserved CP2 DNA binding domain flanked by an N-terminal transactivation domain and a C-terminal DNA binding domain.^{311, 312 313 314 309} In fact, amino acid sequence comparison revealed that the human homologue of murine GRHL1 to be 94% identical at the amino acid level.³¹⁵ Further, GRHL1 and GRHL2 share 90% sequence homology at the amino acid level, with much of the differences being within the N-terminal transactivation domain, linker regions, and the C-terminal dimerization domains. Wilanowski et al. found that while GRHLs 1 and 2 (and theoretically 3) function as homodimers, their activity is enhanced as heterodimers. Together, these data suggest that the GRHL family of proteins were derived from gene duplication events during evolution.³⁰⁹

The first studies in *Drosophila* demonstrated the essential role for GRH in development and specifically dorsal/ventral patterning and CNS development.³¹⁶⁻³¹⁸ In mammalian systems, it appears that in mammals the pleotropic functions of GRH in

drosophila have been delegated amongst the three grainyhead-like proteins, though still central to functions within cells of epithelial origin. GRHL1 and GRHL2 have been shown to be essential regulators of cell-cell junctions. GRHL1 null mice exhibit palmoplantar keratoderma, desmosomal abnormalities, skin barrier defects, and improper differentiation of keratinocytes.^{319,320} Homozygous deletion of GRHL2 is embryonically lethal due to failure of neural tube closures.^{321,322}³²¹ However, autosomal recessive knockouts have also shown its importance in regulation of barrier function and keratinocyte differentiation.^{319,323} While not embryonically lethal, GRHL3-null mice die at birth with defects in neural tube closure. Using adult specific GRHL3 knockout mice groups have shown the loss of GRHL3 severely impairs wound healing and skin barrier functions.³²²^{324,325}

Aside from knockout-based developmental studies, the majority of recent work into the function of the GRHL proteins has centered on their roles in cancer with complex and often conflicting results. Briefly, GRHL1 expression in neuroblastomas is associated with a favorable prognosis, reduced cellular proliferation, and increased xenograft growth in mice.³²⁶ However, given its role in skin differentiation, GRHL1-null mice rapidly develop squamous cell carcinoma (SSC), through this is likely due to the lack of terminal differentiation at birth.³²⁷

Many more studies have explored the role of GRHL2 and particularly in breast cancer. Studies first characterized GRHL2 as a suppressor of EMT, where breast and colon cancer cells with increased expression exhibited reduced xenograft growth and expression of stem cell markers as well as increased chemosensitivity.³²⁸⁻³³⁰

Mechanistically, it was found that GRHL2 directly enhances E-cadherin expression while inhibiting ZEB1, a prominent driver of EMT.^{320,331,332} However, it was also found that ZEB1, in response to β -catenin/TGF- β stimulation can directly repress GRHL2 indicating a reciprocal feedback loop.³²⁸⁻³³¹ While seemingly at odds, they are in line with the paradoxical effect of TGF- β in cancer progression. In the early stages TGF- β functions as a tumor suppressor, while in later stages it promotes growth, metastasis, and EMT.³²⁸⁻³³⁰ While these results are far from conclusive, it could be that GRHL2 expression and its effect on cancer is dependent on the stage of cellular differentiation.

In addition to simple increases or decreases in expression, it has also been shown that GRHL undergoes alternative splicing events, dramatically changing their functional activity. First described in neuroblast cells in *Drosophila*, selective mutation of this isoform resulted in lethality and movement disorders, demonstrating its functional significance. Mechanistically, previous studies in *drosophila* revealed that the mutant protein preferentially forms heteromeric complexes with the full-length grainyhead, blocking the formation of grainyhead homodimers. These heteromeric complexes fail to activate gene expression despite the presence of one functional activation domain.³³³ This suggests that the ability of spliced GRHL1 to homodimerise or heterodimerise with grainyhead family proteins may have similar functional consequences. In a seminal paper, Wilanowski et al discovered the presence of homologous alternatively spliced isoforms of mammalian GRHL proteins as well. In their study, alignment of these proteins and mapping of the genomic locus revealed that the longer (p70 or full-length,

FL) isoform and the shorter (p49 or spliced, S) isoform contained similar core DNA-binding and C-terminal dimerization domains but varied significantly at their N-termini (

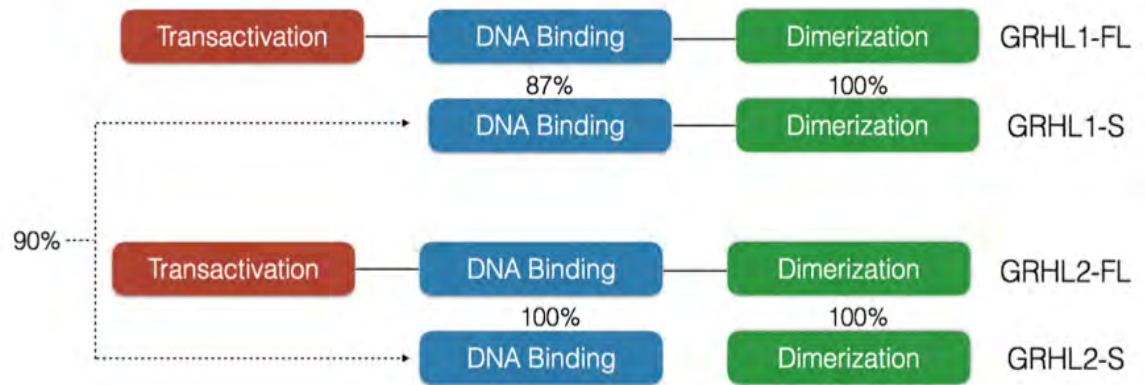
Figure 5.1) Upon mapping the corresponding cDNAs to their genomic loci, they found that the first three coding exons corresponding to the conserved transactivation domain are exclusive to the FL isoform of GRHL1. Given that this region contained the conserved transactivation domain (TAD), they hypothesized that the spliced isoform may function in dominant-negative fashion similar to those found in drosophila. Indeed, ectopic expression of either the full-length and TAD alone in GRHL-naïve cells activated GRHL-responsive reporters while introduction of the spliced isoform nullified transcriptional activity. Further, in situ hybridization in mice and cDNA mapping of human tissue revealed that these GRHL1 isoforms exist in a variety of tissues exhibiting independent expression.³⁰⁹

Since their discovery, there have been no reported studies characterizing the role of GRHL1 splicing in mammalian systems. Recently however, Werner et al has demonstrated the presence and functional consequence of grainyhead-like 2 splicing in breast cancer. Similar to GRHL1, GRHL2 also undergoes splicing within its coding exon producing a N-terminal truncated protein. Interestingly, the cDNA revealed that splicing retained a large portion of the TAD. Due to the proximity of the start codon to the 5' end of the transcript, an alternative, downstream translation start site is favored, creating the 49 kDa spliced isoform. In their study, they found that ectopic expression of the spliced GRHL2 isoforms in breast cancer cell lines exerted a dominant negative effect on the tumor-suppressive function of endogenous GRHL2. However, as noted above, this effect is highly dependent on the breast cancer subtype tested. While the nuances of their work

Figure 5.1: Schematic representation of GRHL 1 &2 full length and spliced proteins

Structurally, all grainyhead proteins are remarkably similar, containing an evolutionarily conserved CP2 DNA binding domain flanked by an N-terminal transactivation domain and a C-terminal DNA binding domain. The splice variants result in a truncated protein packing the N-terminal transactivation domain (TAD) found largely remain intact.

Percentages indicate similarity between indicated domains between the spliced and the full length variants.



are beyond the scope of this report, suffice to say that the functional role of GRHL2 is nuanced and cell specific.³²⁹

In the liver, proteomic and immunohistochemistry screens of hepatic tissue have demonstrated that GRHL2 is restricted to the biliary epithelium, while GRHL1 is specific for hepatocytes in the normal liver. Furthermore, RNAseq data suggests that GRHL1 expression is decreased 1.8-fold in a study of HCC tumor samples when compared to normal tissue. This decrease in GRHL1 is analogous to the 2-fold decrease in miR-122 previously described in HCC tumor samples as well. Tanaka et al. found an association between a genome copy number gain of GRHL2 in tumor tissues of patients with recurrent HCC.³³⁴ However, it is key to note that these findings denoted increases of the GRHL2 genomic locus on chromosome 8, a frequent occurrence in HCC, and that increased copy number of GRHL2 has been shown not to translate into increased protein or mRNA. Furthermore, their work demonstrating that siRNA knockdown of GRHL2 inhibits HCC tumor growth was performed in Huh-6 cells lines which lack GRHL2 mRNA while harboring copy number gains of chromosome 8.^{334,335} While they went on to demonstrate that siRNA knockdown of GRHL2 inhibited HUH-6 (human HCC cell line) proliferation. However, more recent studies have shown that the HUH-6 cells used in this study, while having a copy number gain at the genomic locus for GRHL2, do not have any detectable GRHL2 transcript. The first study to define GRHL2's function in the liver was done by Tanimizu, et al. They determined that GRHL2 downregulation was required for the development of mature hepatoblasts from neonatal cholangiocytes.

However, the significance of these findings or any insight into the role the grainyhead proteins in hepatic pathophysiology have never been described.

Together, these studies led me to hypothesize that the loss of GRHL1, the predominant homolog in hepatocytes, is involved in maintaining miR-122 expression and its loss associated with an increase in GRHL2, due to alcohol, may epigenetically regulate miR-122 and ALD pathogenesis.

Methods

Procurement of Human Specimens

Paraffin embedded blocks and flash frozen human liver tissue was obtained from healthy controls, alcoholic cirrhosis, and HCV cirrhosis, were obtained through the Liver Tissue Cell Distribution System, Minneapolis, Minnesota, which was funded by NIH Contract # N01-DK-7-0004/HHSN26700700004C.

Animal Studies

All animals received care in compliance with protocols approved by the Institutional Animal Use and Care Committee (IACUC) of the University of Massachusetts Medical School. Wild-type (WT) mice (C57/B16), Alb-Cre, and HIF-1 α ^{flox/flox} mice were purchased from Jackson Laboratories (Bar Harbor, ME) and backcrossed onto a C57/B16 background. 6-8 week old mice were gradually acclimated to a Lieber-DeCarli liquid diet with 5% ethanol (vol/vol) over a period of 1 week, then maintained on the 5% diet for 4 weeks (total of 5 weeks). Consumption was recorded daily and isocaloric amounts of a control diet (in which dextran-maltose replaced calories from ethanol) were dispensed to pair-fed (PF) animals. Weights were recorded weekly.

At the conclusion of the 5-week feeding, mice were weighed, blood collected, and euthanized. Livers were dissected, weighed and divided into lipid nitrogen for protein and biochemical assays, fixed in 10% phosphate-buffered formalin for histological analysis, preserved in OCT frozen section preparation solution, or soaked in RNALater (Qiagen, Hilden, Germany, Hilden, Germany). Blood was allowed to clot and serum obtained using gel-based serum separator tubes.

Isolation of primary mouse hepatocytes and LMNCs

Anesthetized animals were perfused by way of portal vein with saline solution, followed by enzymatic digestion, as previously described.⁷⁵ The hepatocytes were separated by centrifugation, Primary hepatocytes were cultured in low-glucose DMEM supplemented with 10% fetal bovine serum, 1% Anti-Anti, 1% gentamycin, 1% insulin, transferrin, selenium solution. Primary hepatocytes were seeded in 6-well collagen-coated plates (Biocoat, Becton Dickinson). Before starting stimulation experiments, hepatocytes were rested for 4 hours.

RNA extraction and real-time PCR

Total RNA was extracted using the Quiagen miRNeasy kit (Qiagen, Hilden, Germany, Hilden, Germany) according to the manufacturer's instructions. Briefly, tissue samples were lysed in QIAzol Lysis reagent (Qiagen, Hilden, Germany), homogenized with stainless steel beads in TissueLyser II (Qiagen, Hilden, Germany) followed by miRNA isolation following manufacturer's instructions and DNase 1 Digest. RNA was

quantified using Nanodrop 2000 (Thermo Scientific, Waltham, MA). Complementary DNA (cDNA) synthesis was performed by reverse transcription of 1 ug total RNA using the iScript Reverse Transcription Supermix (Bio-rad, Hercules, CA). Real-time quantitative PCR was performed using Bio-Rad iTaq Universal SYBR Green Supermix and a CFX96 real-time detection system (Bio-Rad Laboratories). Primers were synthesized by IDT, Inc. The primer sequences are listed in chapter 1. Relative gene expression was calculated by the comparative cycle threshold (Ct) method. The expression level of target genes was normalized to the house-keeping gene, 18S rRNA, in each sample and the fold-change in the target gene expression between experimental groups was expressed as a ratio. Melt-curve analysis was used to confirm the authenticity of the PCR products.

Pri-miRNA Analysis

Reverse transcription was performed from total RNA as described above and diluted 5-fold. TaqMan primers and miRNA Reverse Transcription Kit (Applied Biosystems, Foster City, CA) followed by quantitative RT- in CFX96 (Bio-rad, Hercules, CA) using TaqMan Universal Probes Master Mix (Bio-rad, Hercules, CA). All samples were normalized to snoRNA202, or U6 expression based on Normfinder (<http://moma.dk/normfinder-software>) analysis of loading control stability. hsa-miR-122-FAM, GAPDH-FAM, and mmu-miR-122-FAM primer sets were purchased from Applied Biosystems.

Whole Cell Lysate

Approximately 50 mg of liver tissue was washed in ice cold PBS and homogenized in lysis buffer (9.5ml RIPA buffer, 1mM NaF, 2mM Na₃VO₄, 1 protease inhibitor tablet, 5mM PMSF) with stainless steel beads in TissueLyser II (Qiagen, Hilden, Germany, Hilden, Germany). After 10 minutes of incubation on ice, homogenates were centrifuged at 14,000xg for 10 minutes at 4 degrees C. The supernatant (clarified whole cell lysate) was collected and stored in aliquots at -80 degrees C.

Western Blotting

Approximately 10-20 ug of total liver lysate was resolved on 10% polyacrylamide gels and transferred overnight to nitrocellulose support. Membranes were blocked overnight with blocking buffer (5% bovine serum albumin in Tris-Borate-SDS with 0.01% Tween 20) with refrigeration, and subsequently probed overnight with GRHL2 (Atlas antibodies, HPA004898) and GRHL2 (Atlas antibodies, HPA004820) rabbit polyclonal antibodies. Detection was performed using an anti-rabbit horseradish-peroxidase conjugated secondary antibody and chemiluminescent substrates. Band density was quantified using ImageJ64.

Confocal microscopy – Immunofluorescence.

Confocal images were processed as previously described. Primary hepatocytes were fixed, permeablized and stained O/N with either anti-GRHL2 (Atlas antibodies, HPA004820), or normal Rabbit IgG sc-2027 (Santa Cruz Biotechnology, Dallas, Texas). Actin was stained using ActinGreen 488 anti-ReadyProbes Reagent #R37110 (Molecular Probes, Eugene, OR). Secondary antibody used was anti-rabbit Alexa Fluor 594 #A-

21207 (Molecular Probes, Eugene, OR). Images were acquired using Leica TCS SP5 II Laser Scanning Confocal Microscope.

Immunohistochemistry

Immunohistochemistry staining for GRHL2 (Atlas antibodies, HPA004898) and GRHL2 (Atlas antibodies, HPA004820) were performed on formalin-fixed, paraffin-embedded livers according to the manufacturer's instructions. ImageJ (NIH) was used for image analysis.

Results

Utilizing taqman probes specific for the miR-122 primary transcript (pri-miR-122), I found that alcohol reduces pri-miR-122 expression approximately 2-fold in human alcoholic cirrhosis patients (Figure 5.2a) while there was no change in patients with HCV cirrhosis. Livers of alcohol-fed mice and specifically hepatocytes also showed a significant reduction in pri-miR-122 expression (Figure 5.2b) similar to the reduction of mature miR-122 (Figure 2.4). Furthermore, while I have demonstrated that restoration of the mature form of miR-122, and HIF-1 α -null mice are protected from the phenotype of ALD, the inhibitory effect of alcohol on pri-miR-122 expression was still present (Figure 5.2c,d). These findings led me to hypothesize that chronic alcohol specifically regulates miR-122 at the transcriptional level.

The high baseline level of miR-122 in hepatocytes is maintained by many transcription factors including HNF4, and HNF6.^{185,187,236} However, none of these transcription factors showed changes in the livers of alcohol-fed mice compared to control mice that would result in reduced miR-122-transcription (

Figure 5.3a,b). Recent studies have identified grainyhead like-2 (GRHL2), a homolog of the drosophila grainyhead transcriptional regulator, as a potential repressor of miR-122

expression in progenitor cells during hepatic differentiation.³⁰⁷ However, the role the grainyhead proteins in hepatic pathophysiology is yet to be described.

In silico analysis revealed a conserved grainyhead dimer binding site approximately 300 bps upstream of the miR-122 transcription start site (TSS), (Figure 5.4a). First, I performed chromatin immunoprecipitation-qPCR (ChIP-qPCR) in HUH-7 cells that confirmed the putative GRHL binding site in the miR-122 promoter (Figure 5.4b).

Immunohistochemistry (IHC) revealed that while GRHL1 staining is confined to hepatocytes, no clear change in staining was apparent (

Figure 5.5a). GRHL2 staining revealed its expression is restricted to the biliary epithelium in healthy controls and pair-fed mice, however, alcoholic cirrhosis patients and alcohol-fed mice had notably increased staining within hepatocytes (

Figure 5.5b). IHC for GRHL2 of FFPE and immunofluorescence also showed that alcohol-fed mice had increased GRHL2 staining within hepatocytes (

Figure 5.5, Figure 5.6a,b). Next, I sought to characterize the mRNA expression of GRHL1 and GRHL2 in alcoholic cirrhosis patients, and found a decrease in the full-length GRHL1 (Figure 5.7a) and a significant increase in total GRHL2 (Figure 5.7b) mRNA when compared to healthy controls and HCV cirrhosis. Furthermore, this 18-fold increase in GRHL2 mRNA demonstrated a significant inverse correlation with miR-122 expression in alcoholic human livers (Figure 5.7b, $r^2=0.6803$, $P<0.0001$). Alcohol-fed mice showed a modest but statistically not significant increase in full length GRHL2 expression (Figure 5.7c) and no change in either total or full length GRHL1 expression (Figure 5.7d). However, using primers specific for the spliced form, there appeared to be a trend towards an increase.

Western blot from total liver lysates revealed that that while GRHL1-FL was decreased in alcoholic patients (Figure 5.8a), the expression of the GRHL2-FL was unchanged in either murine or human livers (Figure 5.8c). However, expression of the spliced variants of both of GRHL1 and 2, previously described in the literature as dominant-negative isoforms, were significantly increased in both alcohol-fed murine and human alcoholic cirrhosis livers (Figure 5.8a-d). These isoforms, are the result of alternative splicing events in exon 1 characteristic of the Grainyhead-family proteins which result in proteins containing the conserved C-terminal DNA binding and dimerization domains, but lacking N-terminal transactivation domain, thereby inhibiting transcriptional activity at its targeted binding sites (

Figure 5.1). Taken together, this led me to hypothesize that alcohol increases the spliced or “dominant-negative”, variants of GRHL1 and 2 in hepatocytes, allowing them to hetero-dimerize, and repress miR-122 expression.

Figure 5.2: Chronic alcohol inhibits pri-miR-122. Pri-miR-122 expression in (a) human livers (n=10-12), alcohol-fed WT murine (b) livers (n=8-14) and hepatocytes (n=5). (c) Pri-miR-122 expression in HIF1hepKO hepatocytes from pair-fed and alcohol-fed treated with either Scr or miR-122-TuD.(d) Pri-miR-122 expression in WT, PF or Et-fed hepatocytes treated with either Scr or or miR-122-OX. *P < 0.05, **P<0.005, ***P<0.0005 by Student's t test (n=8-12).

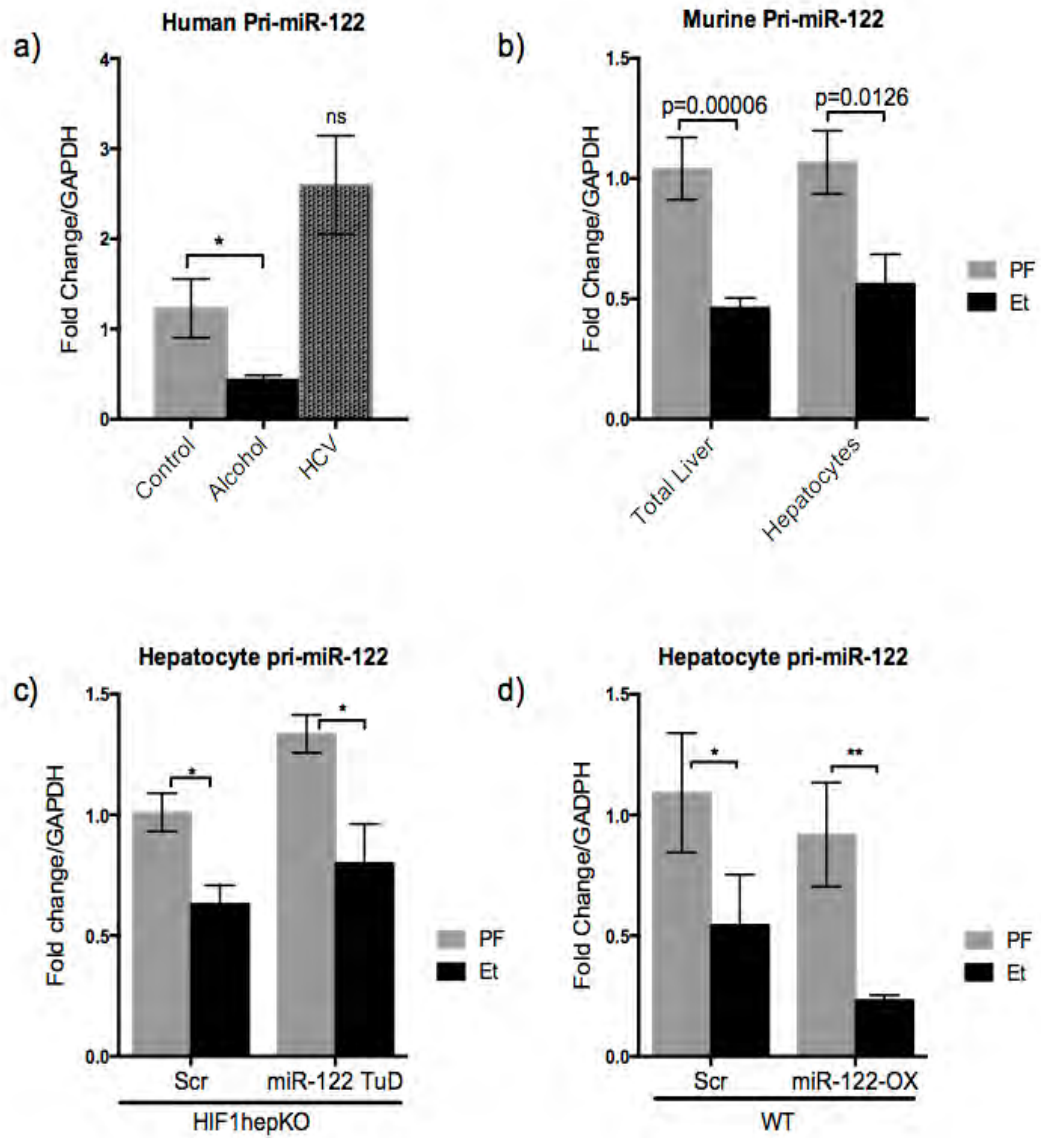
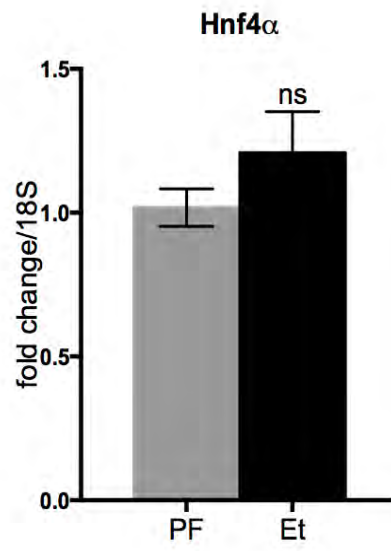


Figure 5.3: Expression of HNF-4 α and HNF6 β in murine livers.

Expression of (a) HNF4 α , and (b) HNF6 in the livers of PF and Et-fed mice. *P < 0.05,

P<0.005, *P<0.0005 by Student's t test (n=8-14).

a)



b)

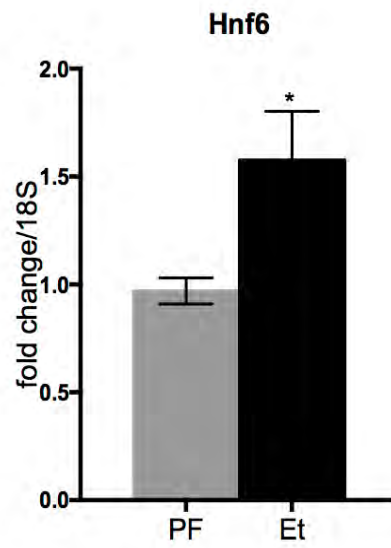


Figure 5.4: miR-122 promoter contains a conserved grainyhead binding site.

Schematic representation of the GRHL1/2 binding site ~300 bp upstream of the TSS. (b)

% input GRHL1 chromatin immunoprecipitation from HUH-7 cells.

a)



b)

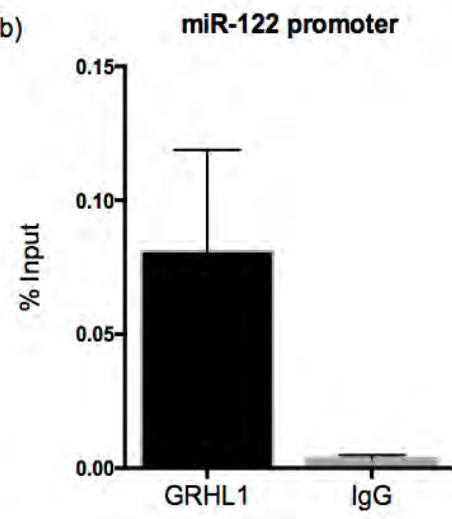


Figure 5.5: Grainyhead-like 1 and 2 immunohistochemistry.

Immunostaining for (a) GRHL1 and (b) GRHL2 in FFPE liver sections from healthy controls and alcoholic cirrhosis patients. GRHL2 histology in (a) murine and (b) human livers. (c) Immunostaining of FFPE liver sections from PF- and Et-fed mice. Scale bars; full-size=100 μm , inset=50 μm .

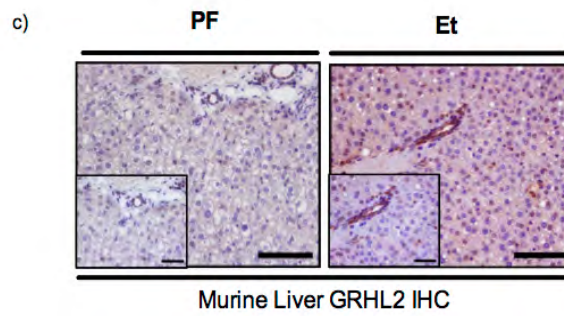
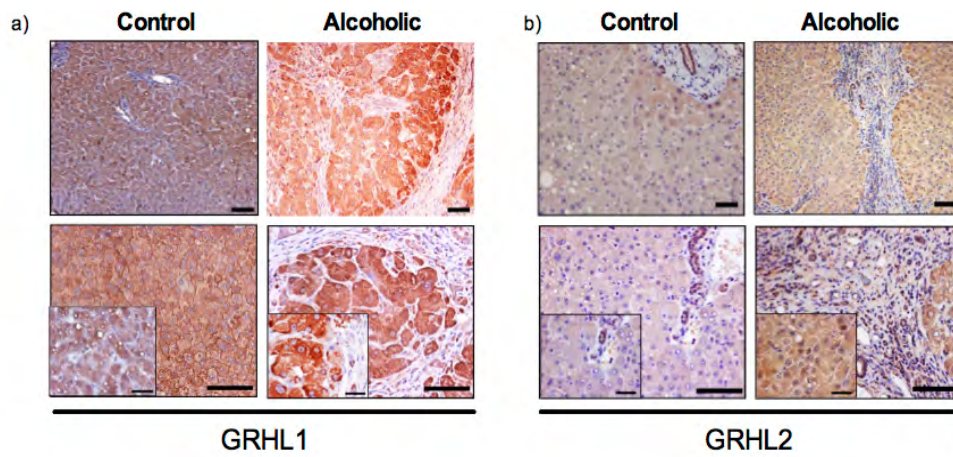


Figure 5.6: Chronic alcohol increases GRHL2 expression in murine hepatocytes.

Immunofluorescence staining using anti-GRHL2 or normal rabbit IgG control antibody in primary murine hepatocytes isolated from alcohol and pair-fed mice. Scale bars; (a)7.5 μm , (b)PF=25 μm , PF=10 μm , Et+IgG=25 μm . DAPI – Blue, GRHL2 – Red, Actin – Green.

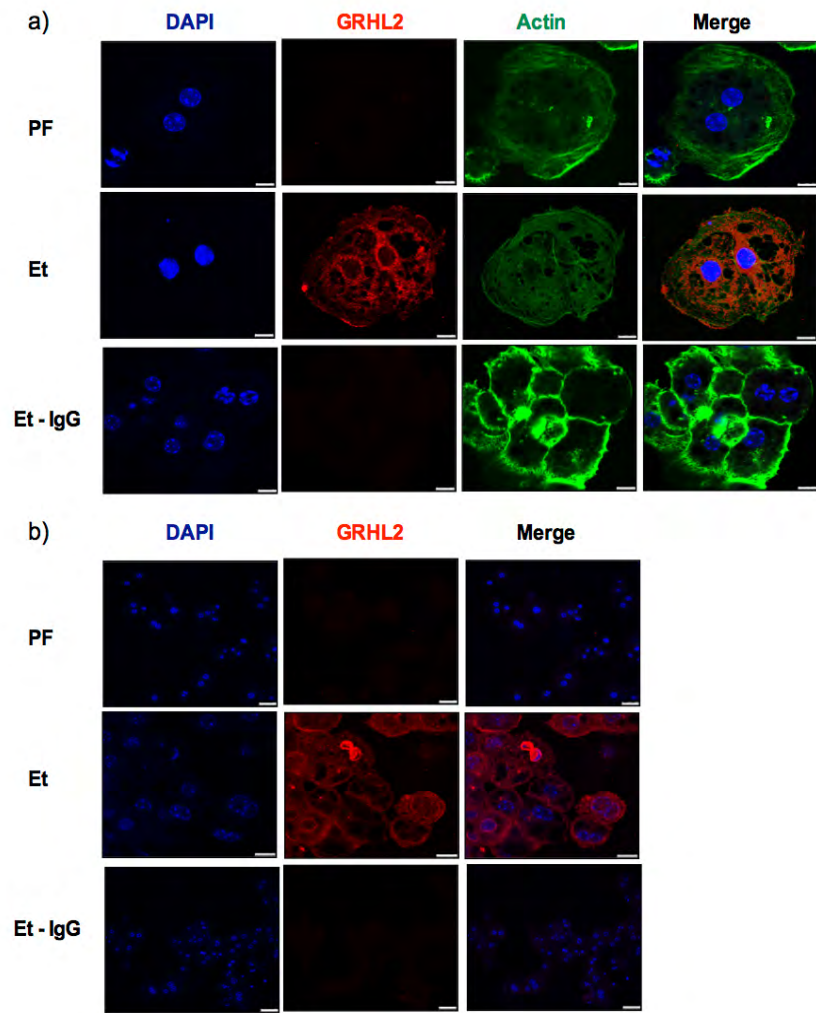
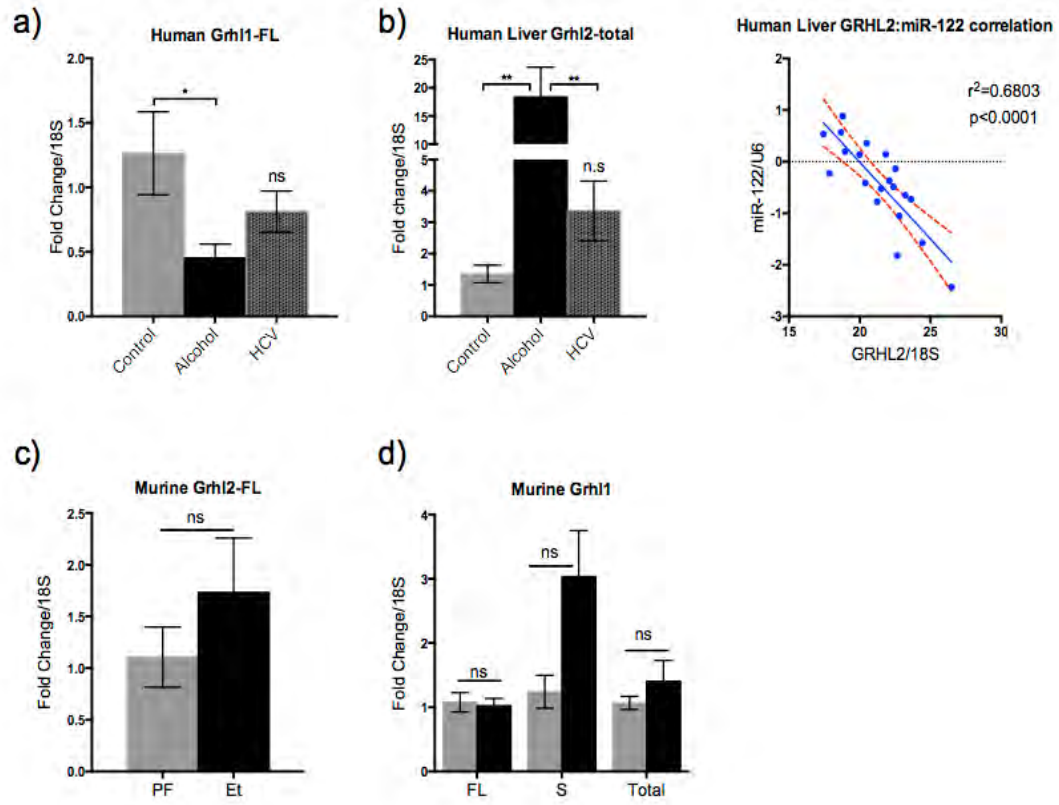


Figure 5.7: Expression of grainyhead-like proteins in murine and human livers.

mRNA expression of (a) GRHL1-FL and (b) Grhl2-total in the livers of patients with alcoholic cirrhosis, HCV cirrhosis, and healthy controls. (c) Pearson correlation between miR-122 expression and GRHL2 mRNA. (n=10-12) mRNA expression of murine (d) GRHL1-FL and spliced (S) isoforms and (e) Grhl-FL in the livers alcohol and pair-fed mice (n=6-14).. *P < 0.05, **P<0.005, ***P<0.0005 by Student's t test.



To examine the inhibitory effect of the spliced isoforms on miR-122, I cloned the promoter region of the human miR-122 gene into an empty PGL4 luciferase plasmid devoid of an enhancer or promoter. Furthermore, I mutated the putative GRHL binding site (Figure 5.4) and created a truncated promoter which contains the essential HNF binding sites but is 50 bp downstream of the GRHL site. I co-transfected each promoter construct with either GRHL1-FL, GRHL2-FL, or the GRHL2-S alone and in combination into HUH-7 cells which has the highest miR-122 expression of any hepatocyte cell line.¹⁸² Surprisingly, GRHL1, 2, and 2-S alone or in combination all inhibit miR-122 promoter activity equally (Figure 5.9a). Furthermore, both the truncated and the reporter with the of mutated putative GRHL binding site not only enhanced baseline promoter activity and only blocked the inhibitory effect of GRHL1-FL, and not of either GRHL2 isoforms ((Figure 5.9a). HUH-7 cells, while having high miR-122 expression, their levels are nearly 10-fold lower than primary human hepatocytes. Therefore, to confirm the abovementioned findings, I transfected either the GRHL1-FL, 2-FL or 2-S isoforms independently or in combination into primary human hepatocytes. 48-hours later, total RNA was collected and assayed for pri-miR-122 expression. Oddly, neither GRHL1, GRHL2-FL, or the GRHL2-S inhibited pri-miR-122, while the combination of GRHL1 and GRHL2/GRHL2-S both enhanced expression (Figure 5.9b). Taken together these data suggests that alcohol regulates miR-122 expression by selectively increasing the spliced form of GRHL1 and 2 in hepatocytes.

Conclusions and Discussion

These data indicate that the grainyhead family of transcription factors are essential in the regulation of miR-122 expression. I hypothesized that chronic alcohol increases GRHL2 expression within hepatocytes, inhibiting miR-122 transcription. As expected, GRHL2 expression was induced by chronic alcohol in humans and mice and inhibited miR-122 promoter activity *in vitro*. Surprisingly, I found that chronic alcohol induces alternative splicing of GRHL2 and GRHL1. Previous reports have shown that GRHL1 is constitutively expressed in hepatocytes while GRHL2 is predominantly in biliary cells.³³⁵ I too find that GRHL2 expression is restricted to the biliary epithelium in normal livers, while GRHL2 is expressed in hepatocytes in ALD in humans and mice upon exposure to chronic alcohol. However, in murine hepatocytes, IHC and immunofluorescence staining for GRHL2 revealed that while all hepatocytes exhibited significantly increased staining, this was largely localized perinuclear/cytoplasmic staining distribution, with only a few cells showing strong nuclear staining. This is puzzling given that the grainyhead proteins typically exhibit constitutive nuclear localization and no regulators of their nuclear translocation are known.

Figure 5.8: Chronic alcohol induces alternative splicing of GRHL1 and GRHL2.

Representative immunoblot for GRHL1 from (a) human (n=5) and (b) murine (n=5) from total liver lysate. Representative immunoblot for GRHL2 from (c) human (n=5) and (e) murine (n=5) from total liver lysate. β -actin was used as a loading control.

* $P < 0.05$, ** $P < 0.005$, *** $P < 0.0005$ by Student's t test.

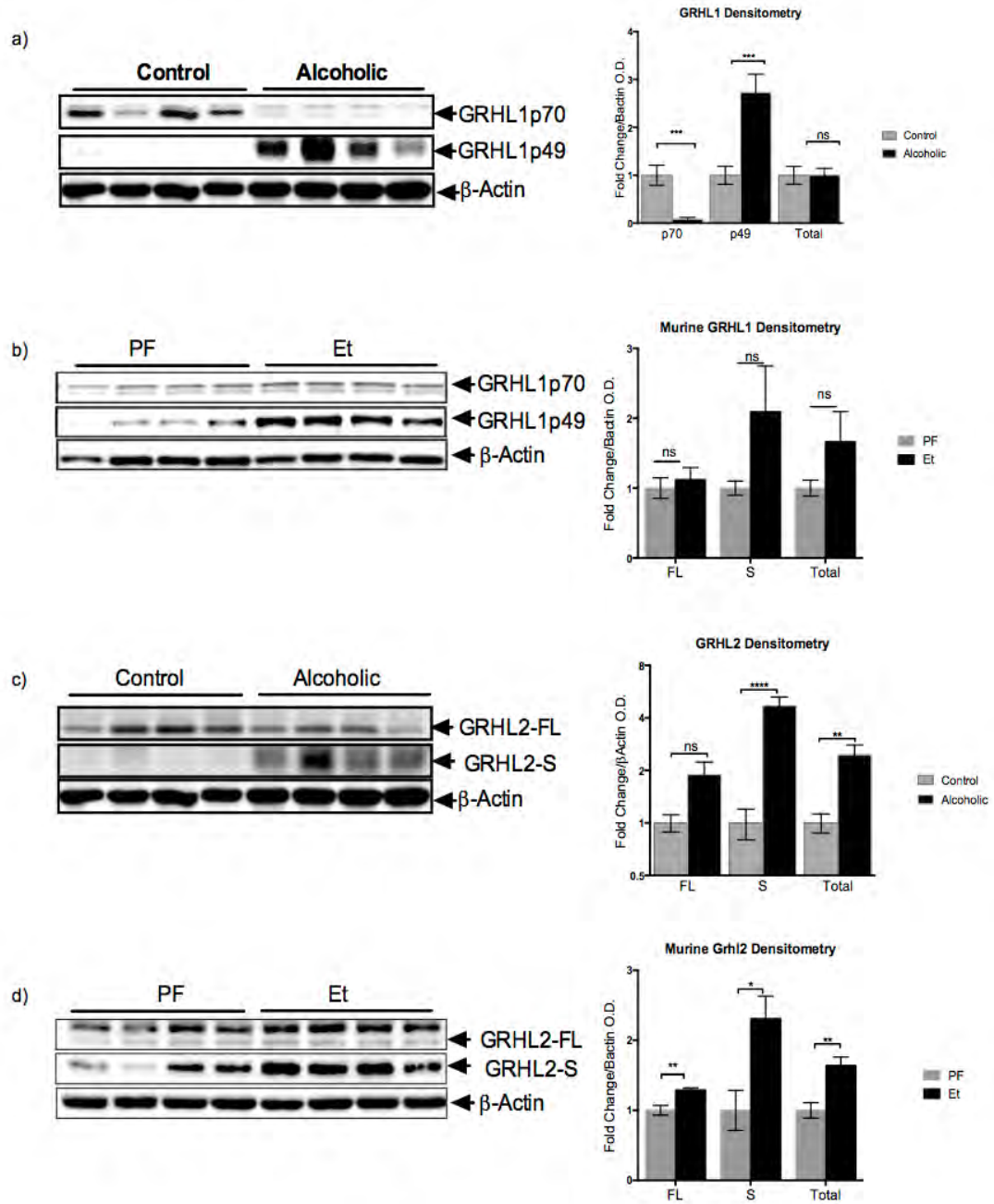
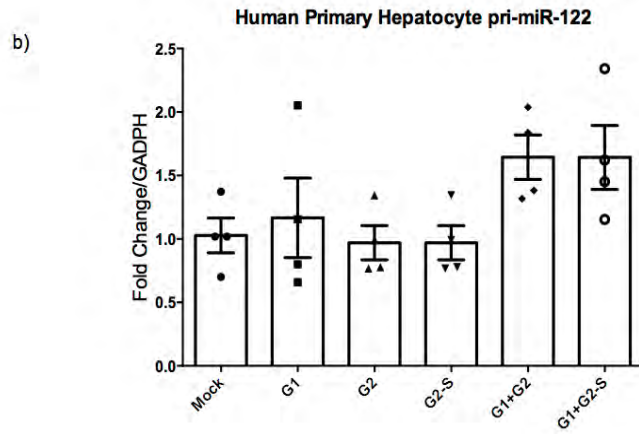
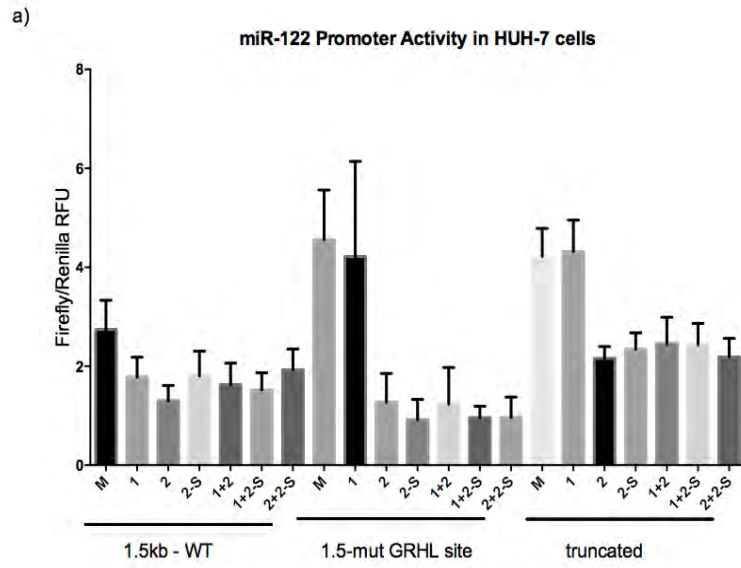


Figure 5.9: Role of grainyhead isoforms on miR-122 expression.

(a) Firefly luciferase activity driven by either a WT, Mut (mutated GRHL site, or truncated human miR-122 promoter in HUH7 cells. Each promoter was co-transfected with human cDNA clones of either the GRHL1-FL, GRHL2-FL, or GRHL2-S alone, or in combination. (b) expression of pri-miR-122 in primary human hepatocytes containing ectopically expressed either GRHL proteins as described above. Cells were incubated for 48 hours, then harvested for luciferase assay (a) or total RNA extracted for qPCR analysis(b). M= Mock, G1= GRHL1-FL, G2=GRHL2-FL, G2-S=GRHL2-Spliced.



Interestingly, immunoblot from murine and human livers revealed that the increase in GRHL2 and GRHL1 corresponded to increases in their respective splice variants. In advanced alcoholic cirrhosis, there is switch in GRHL1 from its full-length to its spliced form. This appeared to support my initial hypothesis that GRHL1 activates miR-122 expression and that with alcohol, either the decrease in GRHL1 or the loss of its TAD would cause a decrease in miR-122. Consistent with previous reports and my hypothesis, GRHL2 significantly inhibited miR-122 promoter activity in vitro. Though it is key to mention that Tanimizu et al performed these miR-122 promoter assays in human 293T cells using murine miR-122 promoter construct which in my hands exhibited little to no miR-122 promoter activity at baseline.³⁰⁷ Surprisingly, while hepatocytes have been shown to express GRHL1, the ectopic expression of GRHL1 in hepatocytes inhibited miR-122 promoter activity. Furthermore, removal of the putative consensus GRHL binding site within the miR-122 promoter enhanced baseline expression and removed the inhibitory effect of GRHL1 on miR-122 promoter activity. However, this had no effect on mitigating the inhibition due to either GRHL2 isoform. Furthermore, in primary human hepatocytes, it appears that neither GRHL1, nor either GRHL2 isoform independently effect pri-miR-122, but in combination with GRHL1, enhance pri-miR-122 expression.

While I have included the data from the primary hepatocytes here, though experimental conditions may not have been optimal. Primary hepatocytes are known to rapidly de-differentiate *ex vivo*. I received these cells two days after their harvesting and the experiment was subsequently performed over the course of 60 hours, potentially

confounding these results. However, if the primary hepatocyte data are indeed representative of the effects of GRHL1 and GRHL2 on miR-122 in vivo, the disparity in the findings could be due to epigenetic factors such as methylation of the genomic locus which are frequently changed in many cancers as well as in alcohol which could affect GRHL2 binding. In general, alcohol leads to a hypomethylated state. This would be better represented in the in vitro experimental conditions using the cloned miR-122 promoter, which by virtue of being an exogenous construct would escape methylation. Indeed, in these conditions I did observe a downregulation of miR-122 promoter activity by both GRHL1 and GRHL2. As confirmation, repeating this experiment in primary cells following the use of a chemical methylation inhibitor would be a prudent course of action. Additionally, in the case of the primary cells, I directly measured pri-miR-122 levels while in the HUH-7 cells a luciferase reporter was used. Given that the pri-miR-122 transcript is short-lived, and exhibits circadian oscillation, even in vitro, there may be diurnal variations in transcript that do not accurately reflect overall promoter activity.

The data from HUH-7 suggests that mutation or removal of the conserved GRHL binding site only mitigates the effect of GRHL1 suggesting that the constitutive expression of GRHL1, which is naturally found in hepatocytes, exerts an inhibitory effect on miR-122 at baseline. Further, that mutation and truncation did not affect the role of GRHL2. This suggests there may be additional binding sites more specific for GRHL2 within the miR-122 promoter. Given that ectopic expression of GRHL2 alone and in combination with GRHL1 was able to inhibit promoter activity in the mutated and truncated promoters, it is reasonable to hypothesize that this second site is either GRHL1

independent, or at the very least, requires GRHL2 for binding. Indeed, *in silico* analysis determined an additional predicted heterodimer binding site ~50 bp downstream of the GRHL1 site within the miR-122 promoter. While this site is less favorable, in this synthetic system where ectopic protein expression is far greater than physiological levels, this site may still be activated. Further studies titrating the GRHL concentrations and mutation of this second site is warranted.

It is also possible that the introduction of one or multiple versions of the GRHL proteins have an indirect effect on miR-122. For example, Tanimizu et al showed that overexpression of GRHL2 drove hepatic progenitor cells to a cholangiocyte phenotype which is associated with a loss of many hepatocyte nuclear factors essential for driving miR-122 expression.³⁰⁷ Though the exact effect of GRHL proteins on the HNF network is not known, the loss of these HNFs could also result in diminished promoter activity.

Finally, a recent study in drosophila keratinocytes has shown that GRH activity is regulated by ERK-dependent phosphorylation, but only in response to wound healing. In fact, its role during differentiation is independent of ERK and terminally differentiated keratinocytes exhibit “dormant” GRH constitutively present but inactive. Upon injury, ERK-mediated phosphorylation activates grainyhead – a required process for wound healing.³³⁶ Homologous phosphorylation site have been predicted on the mammalian grainyheads proteins as well. In alcohol, the role of LPS-induced inflammation via TLR4, and MAPK/ERKs 1/2 in hepatocytes and immune cells is well characterized.^{94,337} Therefore, one would hypothesize that alcohol may upregulate GRHL2 expression,

and/or splicing but in an inactive, or minimally active form. Upon ERK activation, GRHL activity is increased, inhibiting miR-122 expression. While the *in vitro* system used in this study do not seem to require these modifications, as they inhibited miR-122 promoter activity, forced overexpression of the grainyhead proteins may bypass these regulatory steps. Given the essential role of LPS/TLR4/MAPK in ALD, repeating these studies inflammatory mediators such as LPS or selective MAPK/ERK inhibitors would aid in elucidating their role.

Overall, these results establish the role of GRHL1 and 2 is regulating miR-122 expression in chronic alcohol. While many questions remain, further studies as outlined above, would aid in the understanding the role of the grainyhead proteins on hepatic biology and pathophysiology.

CHAPTER 6: FINAL SUMMARY, DISCUSSION, & FUTURE DIRECTIONS

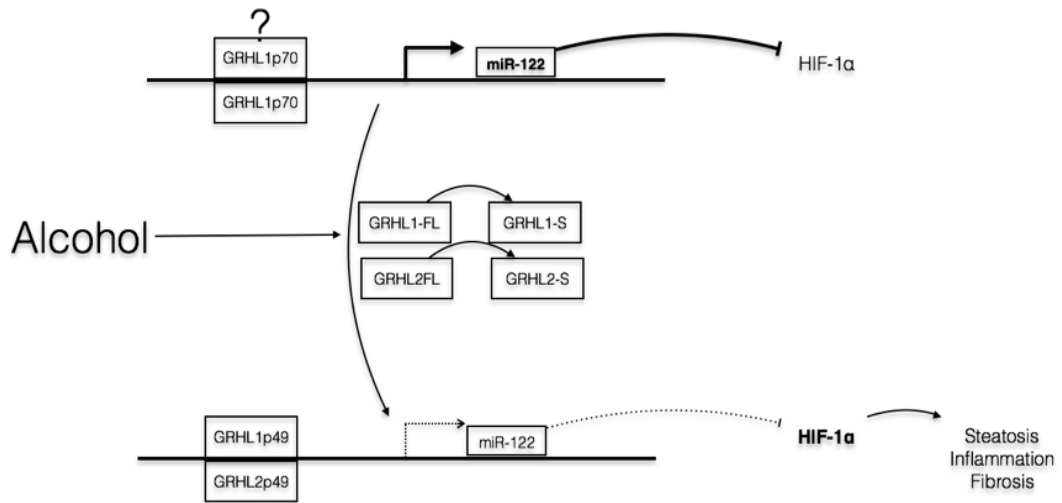
My work presented here demonstrates a role for miR-122 in the pathogenesis of alcoholic liver disease. The evidence to support this claim can be summarized as four particular areas. I first described that chronic alcohol inhibits miR-122 expression. Second, that this reduction of miR-122 directly increases its downstream target, HIF-1 α , inducing steatosis, and augmenting alcohol-induced liver injury. Third, that restoration of miR-122 expression can reverse alcohol-associated pathologies in the liver. Finally, I supply evidence to suggest alcohol-induced dysregulation of grainyhead-like proteins mediates the inhibition of miR-122 (Figure 6.1).

Alcohol, miR-122, and HIF-1 α

I found that hepatic miR-122 levels are 2-fold lower in hepatocytes of alcohol-fed mice and human alcoholic cirrhosis patients compared to controls and that this loss of miR-122 inversely correlates with its primary target, HIF-1 α . Using an AAV8-anti-miR-TuD system I show that *in vivo* inhibition of miR-122 increases HIF-1 α , recapitulating the phenotype of ALD. Although the relationship between alcohol and HIF-1 α has previously been described, I define a specific mechanism and pathophysiological role for its dysregulation via miR-122 in ALD.⁷⁵ The results presented here show that miR-122 expression is an essential factor in maintaining hepatocyte homeostasis in alcohol by targeting HIF-1 α . Through this mechanism, AAV8-mediated restoration of miR-122 reduced hepatic injury via inhibiting HIF-1 α after alcoholic stress indicating a role for its ability to reduce alcohol-associated steatosis, inflammation, and fibrosis.

Figure 6.1: Proposed model of findings

The high level of miR-122 in hepatocytes constitutively inhibits HIF-1 α . Exposure to chronic alcohol induces increased levels of the grainyhead-like 1 and 2 spliced isoforms. These then in turn, hetero, or homodimerize, and bind the miR-122 promoter, inhibiting miR-122 transcription. The loss of miR-122 relieves the inhibitory effect on HIF-1 α which then accumulates within the hypoxic hepatocyte, driving ALD pathogenesis. The data in Chapter IV, suggests the presence of a GRHL1 site at -300 bp from the miR-122 TSS that, in HUH7 cells, exert a persistent inhibitory role on miR-122 promoter activity.



The reduction of miR-122 in the liver with alcohol (miR-122-TuD+et), resulted in dramatic increases in hepatic injury, greater than treatment with either alone. As stated above, the inhibition of miR-122 resulted in a baseline increase in HIF-1 α , steatosis, and hepatocyte injury. This is identical to the phenotype we previously observed using an *in vivo* degradation resistant form of HIF-1 α in murine hepatocytes (HIF1dPA). These mice, which had a higher HIF-1 α expression, (albeit due to protein, not mRNA, stabilization) in hepatocytes, developed steatosis and liver injury without the presence of alcohol. When given alcohol, HIF1dPA mice exhibited a synergistic phenotype similar to that seen in miR-122-TuD+Et, having greater liver injury than either treatment alone. This phenomenon may be due to the further reduction in miR-122 seen in TuD+Et mice when compared to TuD+PF mice.

However, while the combination of TuD treatment alone reduced miR-122 levels approximately 85%, greater than the 50% due to alcohol, yet resulted in an approximately equivalent increases in HIF-1 α expression. Furthermore, TuD+Et reduced miR-122 an additional 50% when compared to TuD-treatment alone. This was associated with only a minimal increase in HIF-1 α expression and activity relative to the large loss of miR-122. Together, this suggests that that other mechanisms may be important in regulating HIF-1 α . Previous studies have found other miRNAs, specifically, miR-155, miR-424, and miR-107, which directly regulate HIF-1 α .^{338,339} Specifically in regards to ALD, the role miR-155 in HIF-1 α regulation is intriguing. Our lab and others have shown that miR-155 is increased in hepatic immune cells, and hepatocytes in response to alcohol, driving TNF- α expression.³⁴⁰⁻³⁴² It stands to reason that miR-155, and other miRNAs, may also

contribute to the regulation of HIF-1 α as well. As my current analysis stands, I have not assessed expression changes and the relative contribution of these or other miRNAs, and therefore cannot exclude them as contributing to the regulation of HIF-1 α in my model. To this effect, it would be pertinent to perform whole a transcriptome analyses, such as small RNAseq experiments, from hepatocytes of PF and Et-fed mice to explore other miRNAs which may be contributing to HIF-1 α regulation

How does HIF- α cause steatosis?

One question that has been left unanswered the mechanism by which HIF-1 α drives steatosis and liver injury. The association between hypoxia inducible factors and lipid accumulation has been described in a variety of tissues with conflicting results.

By simultaneously knocking out VHL with either HIF- α or HIF-2 α , Rankin et al have described dramatically more steatosis in mice with only HIF-2 α (HIF1/VHL-null) when compared to HIF-1 α mice (HIF2/VHL-null) suggesting that in fact, it is HIF-2 which drives steatosis.⁷³ However, Kim et al, using selective HIF-1dPA and HIF-2dPA mice, found that HIF-2 plays a minor role in hepatic lipid accumulation, rather, they reported increased angiogenesis in HIF2dPA mice.⁶⁷ These reports are reconcilable when we examine the system used by Rankin et al. Their system relied on removal of VHL, which blocks degradation of all hypoxia inducible factors. While they selectively deleted HIF-1 and HIF-2, they failed to account for HIF-3 α . If, as Kim et al described, HIF-2dPA mice drive angiogenesis rather than steatosis, then that would suggest that the profound steatosis noted by Rankin et al. in their combination HIF-1/VHL knockouts was due to HIF-3 α .^{67,73} Interestingly, it has been shown that HIF-3 α is inducible by HIF-1 α .³⁴³ If

we extrapolate these findings to the studies presented in this dissertation; where the combination of miR-122 knockdown and alcohol synergistically increased HIF-1 α , the disproportionate increase in overall liver injury could be due to the involvement of HIF-3 α .

It is also key to mention work by Nishiyama et al, which stands in stark contrast to the findings in our lab. Using a similar Liber DeCarli chronic alcohol model and hepatocyte-specific knockout mice, they show that the up regulation of HIF-1 α is protective in ALD. Specifically, they show that the loss of HIF-1 α results in triglyceridemia and an up regulation of SREBP1c, a key regulator in alcohol-induced steatosis. Mechanistically, they claim that in WT mice, the up regulation of HIF-1 α due to alcohol induces the hypoxia-responsive gene DEC1, which in turn, reduces SREBP1c expression. Therefore, in HIFhepKO mice DEC1 is not induced causing worsening liver injury.⁷⁶ However, while not in the liver, a study in cardiomyocytes expressing the HIF1dPA allele were shown to have increased lipid accumulation and suppressed PPAR α , and enhancing PPAR γ .⁷⁰ While a direct link has not been established for PPAR α and hypoxia inducible factors, Krishnan et al has shown that that the PPAR γ promoter contains a conserved hypoxia responsive element ~1Kb upstream of the TSS, within its promoter region and furthermore, mice homozygous for HIF1dPA allele exhibited enhanced PPAR γ expression and FA uptake.⁷¹ Finally, in NAFLD, PPAR- γ has been shown to directly enhance SREBP-1c transcription via binding to a PPRE within the SREBP-1c promoter.⁴⁸ This would suggest that the loss of miR-122 allows for

an accumulation HIF-1 α which then directly increases PPAR γ transcription, which in turn drives SREBP1c and hepatic steatosis.

miR-122 in the liver

While this is the first report to show alcohol-induced reduction in miR-122, many previous studies that have explored the metabolic effect of miR-122 inhibition with contradictory results. The first study published by Esau et al. who utilized anti-miR-122 anti-sense-oligonucleotide (ASO) to knockdown miR-122 in the liver in a high fat diet (HFD) model.³⁴⁴ In their report, Esau et al. found that inhibition of miR-122 in the liver reduced steatosis in HFD-fed mice. These findings, are in sharp contrast to work by Hsu, et al. whose liver-specific knockouts of miR-122^{-/-} (122^{-/-LKO}) developed spontaneous steatosis, fibrosis, and increased susceptibility to myc-induced HCC.²³⁸ While the work I have presented in this dissertation supports their findings that the loss of miR-122 itself induces liver injury however, the use of knockouts confounds their results. miR-122, via CUTL1, is required for terminal hepatocyte differentiation as well as for coordination through positive feedback loops with many essential HNF transcription factors.^{185,345,346} Therefore, it is difficult to extrapolate their findings to adult onset or acquired disease states.

Therapeutic inhibition of miR-122 using Miravirsen or SPC3649, a Locked Nucleic Acid (LNA) anti-miR-122 oligo, was developed to treat HCV infection.^{123,124,233} It has been shown that miR-122 is an essential host factor for HCV replication and represents a therapeutic target in HCV infection.^{124,199,223,347} Recently completed phase 2a trials using Miravirsen to treat HCV infection yielded reduced HCV viral load at low

therapeutic concentrations, with no adverse events.^{223,233} Additionally, these groups and others have demonstrated a cardio-protective role for miR-122 inhibition, via reduction of cholesterol and serum triglycerides. AAV-, ASO-, and LNA-mediated inhibition of miR-122 have all demonstrated a decrease in serum cholesterol and triglycerides without hepatotoxicity.^{221,223,233} While this is not in line with the findings I have presented here where the knockdown of miR-122 alone induced liver injury, a significant difference between my work and that of the above-mentioned studies are the difference in diets. In order to achieve a robust phenotype in our murine models of alcoholic liver disease, both control and alcohol-treated mice a calorie dense diet rich in fats and simple sugars. This added caloric stimulus may be the tipping point between anti-miR-122 therapy being cardioprotective or hepatotoxic. Additionally, caution is warranted as miravirsen, an anti-HCV therapy enters phase 3 trials, as sustained inhibition of miR-122 may result in progressive liver injury, and a potential complication of chronic miR-122 inhibitor therapies.^{222,233}

miR-122 therapy in ALD

In chapter IV, I utilized a rAAV8 vector to overexpress miR-122 in the livers of alcohol-fed mice. Through inhibition of HIF-1 α , I was able to reverse steatosis, inflammation, and overall liver injury due to alcohol these results show that of miR-122 expression is a key component in HIF-1 α regulation and hepatocyte homeostasis.

When first introduced, the use of viral vector gene therapy was fraught with skepticism and questions of safety. However, recent clinical trials in the UK using rAAV8 vectors to treat Hemophilia B deficiency has demonstrated that a single

peripheral-vein dose can safely and effectively achieve sustained transgene expression for 16 months after treatment.²⁶⁴ This single dose approach provides an added benefit in treating patients with ALD who are frequently lost to follow-up compared to other miRNA therapies that require monthly dosing.¹¹¹ Of note, in mice treated with rAAV8 miR-122-OX, the degree to which we restored miR-122 was greater than anticipated; however, there was minimal hepatotoxicity as a result. Given that 130,000 copies of miR-122 are in each hepatocyte, treatments that over-express miR-122 may have a large therapeutic window.¹⁸² However, long term studies at varying concentrations would be prudent in elucidating potential toxicities and off-target effects of sustained expression.

The use of AAV systems once would preclude that patient from receiving additional doses due to seropositivity to the vector should the need an additional dose. Furthermore, in my data I noted that pair-fed hepatocytes did not achieve robust overexpression of miR-122 while alcohol-fed hepatocytes did. Though unlikely, this may be due to the observation by some of exportin 5 saturation when using U6-pol III based promoters causing cellular toxicity, and loss of the transgene. The use of less active and more selective promoters may mitigate the unwanted toxicity while retaining effectiveness. It is clear that further studies in mice as well as larger mammals must be conducted to ensure the low level of toxicity holds true.

In these studies, I utilized scrambled sequences as controls for the TuD or miRNA overexpression constructs. These sequences were screened *in silico* against the mouse transcriptome to ensure that it did not target any known transcript. While unlikely, this does not preclude the possibility of an off-target effect by the AAV8 vector or the

scrambled construct via interference with an unanticipated transcript in these studies or future work. Therefore, it would be prudent to perform RNAseq analysis of livers from AAV8-scrambled, AAV8-empty vector, and PBS treated animals to be monitored for changes in RNA expression patterns due to the control constructs.

While delivery of miRNA mimics is burdened with difficulty, recent advances in liposomal delivery systems may provide an effective delivery strategy to the liver. Alternatively, recent development of GalNac-conjugated ASOs which achieve surprising potency and specificity to the liver following sub cutaneous administration, may represent an alternative strategy which allows for titration of dose and ease of delivery. It is important to note though that studies using GalNac-conjugated nucleic acid molecules have only been shown with using siRNAs, not longer miRNAs.²⁵⁵ While this technology holds much promise it remains to be seen if it can be used for miRNA therapeutics.

Grainyhead proteins

In Chapter V, by measuring pri-miR-122 expression, I demonstrated that chronic alcohol inhibits miR-122 at the transcriptional level, in patients with alcoholic cirrhosis and alcohol-fed mice. This suggested that miR-122 was transcriptionally repressed. Furthermore, this decrease in miR-122 was associated with an increased mRNA expression of grainyhead-like 2, a recently described transcription factor shown to inhibit the miR-122 promoter. IHC studies corroborated the increase in GRHL2 staining within hepatocytes. Additionally, western blots demonstrated that the increase associated with chronic alcohol of GRHL2 was that of its spliced form which does not contain a transactivation domain. Indeed, examination of GRHL1 which is traditionally found

within hepatocytes, by the same measures, revealed similar patterns of alternative splicing. However, *in vitro* studies into the role of these full length and spliced forms yielded conflicting results. As I have extensively discussed the results of these work in the discussion section of chapter V, I will focus here on the potential implications of grainyhead on hepatic pathophysiology.

The exact role of GRHL2 in cancer is far from clear. However, if we accept its role in inhibition of miR-122, an interesting association arises. Tanimizu et al, noted that the gain of GRHL2 represented differentiation of hepatic progenitor cells to a cholangiocyte phenotype.³⁰⁷ Furthermore, studies that revealed that HNF6 was a positive regulator of miR-122, found that overexpression of HNF6 resulted in irregular biliary cell morphology and hepatic tissue architecture.¹⁸⁹ The first studies to report increased tumor burden in miR-122 knockout mice using a DEN model, also noted increased biliary cyst formation, a precursor lesion to HCC. Our lab and others have also shown this process is accelerated by alcohol.³⁴¹ Furthermore, many studies have demonstrated the inverse correlation between miR-122 and HCC initiation, metastasis, and mortality. Therefore, if we consider the totality of these findings, this could suggest that the interplay between alcohol, GRHL2, and miR-122 regulate hepatocyte plasticity and possibly hepatic tumorigenesis. Little is known about the full-length or spliced isoforms of GRHL2, and their biological significance in hepatic pathology. Given that alcohol is the single greatest risk factor for HCC development, our data suggests that the alcohol-induced increase in GRHL2 in mature hepatocytes not only inhibits miR-122 and drives ALD pathogenesis, but it may represent an early epigenetic alteration promoting neoplastic changes in the

liver.

In these studies, we utilized scrambled oligos as controls for the TuD or miRNA overexpression constructs. These sequences were screened *in silico* against the mouse transcriptome to ensure that it did not target any known transcript. While unlikely, this does not preclude the possibility of an off-target effect by the AAV8 vector or the scrambled construct via interference with an unanticipated transcript. Therefore, it would be prudent to perform RNAseq analysis of livers from AAV8-scrambled, AAV8-empty vector, and PBS treated mice to be analyzed for changes in RNA expression patterns due to the control constructs.

Concluding remarks

The treatment of alcoholic liver disease is a complex process involving reversal of parenchymal cell injury and suppression of inflammation. After 40 years of clinical trials, steroids remain the controversial standard of care, with no FDA-approved treatment available.¹⁰ Recent clinical trials studying phosphodiesterase inhibitor (pentoxifylline) and anti-TNF agent (infliximab) treatments to target key inflammatory mediators in ALD have proven ineffective compared to placebo or failed due to the need for repeated dosing and constant monitoring for increased susceptibility to opportunistic infections. This is of particular concern in the ALD patient population which is often lost to follow-up.

^{10,12,274,296} Furthermore, these trials have demonstrated that a reduction in inflammation without correction of parenchymal cell dysfunction is not sufficient in abating ALD pathogenesis in humans.

Based on our results, I speculate that GRHL2 may serve as a prognostic marker of hepatocyte differentiation or disease progression and that *in vivo* therapeutic correction of GRHL2 splicing or expression changes in ALD may be beneficial to correct miR-122 dysregulation. However, until the role GRHL2 in liver disease is explored further, I propose, that downstream intervention with miR-122 restoration to treat alcoholic liver disease may constitute a safer, simpler, and more effective approach.

miR-122 restoration has been considered as an HCC therapy, where its loss has been reported.^{16,216,244,275} However, treatment at such a late stage of the ALD is difficult and gene therapy is often precluded due to tumor size.²³⁸ Our data supports a potential novel treatment indication for miR-122 restoration, through regulation of HIF-1 α , as a therapy in early alcoholic liver disease to prevent and reverse hepatic injury that warrants further exploration in the clinical setting.

BIBLIOGRAPHY

1. Lívoro, F. A. & Acco, A. Molecular basis of alcoholic fatty liver disease: From incidence to treatment. *Hepatol Res* **46**, 111–123 (2016).
2. Welte, J., Barnes, G., Wieczorek, W., Tidwell, M. C. & Parker, J. Alcohol and gambling pathology among U.S. adults: prevalence, demographic patterns and comorbidity. *J. Stud. Alcohol* **62**, 706–712 (2001).
3. Propst, A. *et al.* Prognosis and life expectancy in chronic liver disease. *Dig. Dis. Sci.* **40**, 1805–1815 (1995).
4. Shoreibah, M. *et al.* Alcoholic liver disease presents at advanced stage and progresses faster compared to non-alcoholic fatty liver diseases. *Ann Hepatol* **15**, 183–189 (2016).
5. World Health Organization. *Global Status Report on Alcohol and Health*. (2011).
6. Lefkowitz, J. H. Morphology of alcoholic liver disease. *Clin Liver Dis* **9**, 37–53 (2005).
7. Menon, K. V., Gores, G. J. & Shah, V. H. Pathogenesis, diagnosis, and treatment of alcoholic liver disease. *Mayo Clin. Proc.* **76**, 1021–1029 (2001).
8. Theise, N. D. Histopathology of alcoholic liver disease. *Clinical Liver Disease* **2**, 64–67 (2013).
9. Espinoza, P. *et al.* Interobserver agreement in the physical diagnosis of alcoholic liver disease. *Dig. Dis. Sci.* **32**, 244–247 (1987).
10. Frazier, T. H., Stocker, A. M., Kershner, N. A., Marsano, L. S. & McClain, C. J. Treatment of alcoholic liver disease. *Therap Adv Gastroenterol* **4**, 63–81 (2011).
11. O'Shea, R. S., Dasarathy, S., McCullough, A. J. Practice Guideline Committee of the American Association for the Study of Liver Diseases and the Practice Parameters Committee of the American College of Gastroenterology. Alcoholic liver disease. *Hepatology* **51**, 307–328 (2009).
12. Sanyal, A. J., Gao, B. & Szabo, G. Gaps in Knowledge and Research Priorities for Alcoholic Hepatitis. **149**, 4–9 (2015).
13. Lucey, M. R. & Weinrieb, R. M. Alcohol and Substance Abuse. *Semin. Liver Dis.* **29**, 066–073 (2009).
14. Morgan, T. R., Mandayam, S. & Jamal, M. M. Alcohol and hepatocellular carcinoma. **127**, S87–S96 (2004).
15. Sidharthan, S. & Kottlil, S. Mechanisms of alcohol-induced hepatocellular carcinoma. *Hepatol Int* **8**, 452–457 (2014).
16. Coulouarn, C., Factor, V. M., Andersen, J. B., Durkin, M. E. & Thorgeirsson, S. S. Loss of miR-122 expression in liver cancer correlates with suppression of the hepatic phenotype and gain of metastatic properties. *Oncogene* **28**, 3526–3536 (2009).
17. Punzalan, C. S., Bukong, T. N. & Szabo, G. Alcoholic hepatitis and HCV interactions in the modulation of liver disease. *J. Viral Hepat.* **22**, 769–776 (2015).
18. Hou, W., Bukong, T. N., Kodys, K. & Szabo, G. Alcohol Facilitates HCV RNA Replication Via Up-Regulation of miR-122 Expression and Inhibition of Cyclin

- G1 in Human Hepatoma Cells. *Alcohol. Clin. Exp. Res.* **37**, 599–608 (2012).
19. Bode, C., Kugler, V. & Bode, J. C. Endotoxemia in patients with alcoholic and non-alcoholic cirrhosis and in subjects with no evidence of chronic liver disease following acute alcohol excess. *J. Hepatol.* **4**, 8–14 (1987).
 20. Videla, L. A. & Valenzuela, A. Alcohol ingestion, liver glutathione and lipoperoxidation: Metabolic interrelations and pathological implications. *Life Sciences* **31**, 2395–2407 (1982).
 21. Shaw, D. S., Rubin, K. P. & Lieber, C. S. Depressed hepatic glutathione and increased diene conjugates in alcoholic liver disease. *Dig. Dis. Sci.* **28**, 585–589 (1983).
 22. Aykaç, G. *et al.* The effect of chronic ethanol ingestion on hepatic lipid peroxide, glutathione, glutathione peroxidase and glutathione transferase in rats. *Toxicology* **36**, 71–76 (1985).
 23. Jewell, S. A. *et al.* Decreased hepatic glutathione in chronic alcoholic patients. *J. Hepatol.* **3**, 1–6 (1986).
 24. Tanner, D. A. R. *et al.* Depressed selenium and vitamin E levels in an alcoholic population. *Dig. Dis. Sci.* **31**, 1307–1312 (1986).
 25. Boveris, A., Fraga, C. G., Varsavsky, A. I. & Koch, O. R. Increased chemiluminescence and superoxide production in the liver of chronically ethanol-treated rats. *Archives of Biochemistry and Biophysics* **227**, 534–541 (1983).
 26. Keen, C. L., Tamura, T., Lönnerdal, B., Hurley, L. S. & Halsted, C. H. Changes in hepatic superoxide dismutase activity in alcoholic monkeys. *American Journal of Clinical Nutrition* **41**, 929–932 (1985).
 27. Sun, Y., Oberley, L. W. & Li, Y. A simple method for clinical assay of superoxide dismutase. *Clin. Chem.* **34**, 497–500 (1988).
 28. McClain, C. J. *et al.* S-Adenosylmethionine, cytokines, and alcoholic liver disease. *Alcohol* **27**, 185–192 (2002).
 29. Ozaras, R., Tahan, V., Aydın, S., Uzun, H. & Kaya, S. N-acetylcysteine attenuates alcohol-induced oxidative stress in the rat. *World Journal of ...* (2003).
 30. Ronis, M. J. J. *et al.* Effects of N-acetylcysteine on ethanol-induced hepatotoxicity in rats fed via total enteral nutrition. *Free Radical Biology and Medicine* **39**, 619–630 (2005).
 31. Baumgardner, J. N. *et al.* N-acetylcysteine attenuates progression of liver pathology in a rat model of nonalcoholic steatohepatitis. *J. Nutr.* **138**, 1872–1879 (2008).
 32. Manouchehr, K., Akbar, A. & Koorosh, M. N-acetylcysteine improves liver function in patients with non-alcoholic Fatty liver disease. *Hepatitis ...* (2010).
 33. Blair, A. H. & Vallee, B. L. Some Catalytic Properties of Human Liver Alcohol Dehydrogenase *. *Biochemistry* **5**, 2026–2034 (1966).
 34. Pikkarainen, P. H. & Riih , N. C. R. Development of Alcohol Dehydrogenase Activity in the Human Liver. *Pediatric Research* **1**, 165–168 (1967).
 35. Li, T. K. & Theorell, H. Human liver alcohol dehydrogenase: inhibition by pyrazole and pyrazole analogs. *Acta Chem Scand* (1969).

36. Eriksson, C. J., Marselos, M. & Koivula, T. Role of cytosolic rat liver aldehyde dehydrogenase in the oxidation of acetaldehyde during ethanol metabolism in vivo. *Biochemical Journal* **152**, 709–712 (1975).
37. French, S. W. *et al.* Effect of Ethanol on Cytochrome P450 2E1 (CYP2E1), Lipid Peroxidation, and Serum Protein Adduct Formation in Relation to Liver Pathology Pathogenesis. *Experimental and Molecular Pathology* **58**, 61–75 (1993).
38. Carpenter, S. P., Lasker, J. M. & Raucy, J. L. Expression, induction, and catalytic activity of the ethanol-inducible cytochrome P450 (CYP2E1) in human fetal liver and hepatocytes. *Mol Pharmacol* **49**, 260–268 (1996).
39. French, S. W. *et al.* Lipid peroxidation, CYP2E1 and arachidonic acid metabolism in alcoholic liver disease in rats. *J. Nutr.* **127**, 907S–911S (1997).
40. Ingelman-Sundberg, M., Johansson, I., Penttilä, K. E., Glaumann, H. & Lindros, K. O. Centrilobular expression of ethanol-inducible cytochrome P-450 (IIE1) in rat liver. *BIOCHEMICAL AND BIOPHYSICAL RESEARCH COMMUNICATIONS* **157**, 55–60 (1988).
41. Wan, Y.-J. Y., Morimoto, M., Thurman, R. G., Bojes, H. K. & French, S. W. Expression of the peroxisome proliferator-activated receptor gene is decreased in experimental alcoholic liver disease. *Life Sciences* **56**, 307–317 (1994).
42. Everett, L., Galli, A. & Crabb, D. The role of hepatic peroxisome proliferator activated receptors (PPARs) in health and disease. *Liver* **20**, 191–199 (2000).
43. You, M., Fischer, M., Deeg, M. A. & Crabb, D. W. Ethanol Induces Fatty Acid Synthesis Pathways by Activation of Sterol Regulatory Element-binding Protein (SREBP). *Journal of Biological Chemistry* **277**, 29342–29347 (2002).
44. Ji, C. & Kaplowitz, N. Betaine decreases hyperhomocysteinemia, endoplasmic reticulum stress, and liver injury in alcohol-fed mice. *Gastroenterology* **124**, 1488–1499 (2003).
45. Nanji, A. A., Dannenberg, A. J., Jokelainen, K. & Bass, N. M. Alcoholic liver injury in the rat is associated with reduced expression of peroxisome proliferator-alpha (PPARalpha)-regulated genes and is ameliorated by PPARalpha activation. *J Pharmacol Exp Ther* **310**, 417–424 (2004).
46. Fraulob, J. C., Souza-Mello, V., Aguila, M. B. & Mandarim-de-Lacerda, C. A. Beneficial effects of rosuvastatin on insulin resistance, adiposity, inflammatory markers and non-alcoholic fatty liver disease in mice fed on a high-fat diet. *Clin. Sci.* **123**, 259–270 (2012).
47. Hardwick, J. P., Osei-Hyiaman, D., Wiland, H., Abdelmegeed, M. A. & Song, B.-J. PPAR/RXR Regulation of Fatty Acid Metabolism and Fatty Acid omega-Hydroxylase (CYP4) Isozymes: Implications for Prevention of Lipotoxicity in Fatty Liver Disease. *PPAR Res* **2009**, 952734–20 (2009).
48. Souza-Mello, V. *et al.* Comparative effects of telmisartan, sitagliptin and metformin alone or in combination on obesity, insulin resistance, and liver and pancreas remodelling in C57BL/6 mice fed on a very high-fat diet. *Clin. Sci.* **119**, 239–250 (2010).
49. Tenenbaum, A., Motro, M. & Fisman, E. Z. Dual and pan-peroxisome

- proliferator-activated receptors (PPAR) co-agonism: the bezafibrate lessons. *Cardiovasc Diabetol* **4**, 14 (2005).
50. Brady, P. S., Marine, K. A., Brady, L. J. & Ramsay, R. R. Co-ordinate induction of hepatic mitochondrial and peroxisomal carnitine acyltransferase synthesis by diet and drugs. *Biochemical Journal* **260**, 93–100 (1989).
 51. Tomita, K. *et al.* AICAR, an AMPK Activator, Has Protective Effects on Alcohol Induced Fatty Liver in Rats. *Alcohol. Clin. Exp. Res.* **29**, 240S–245S (2005).
 52. Ji, C., Chan, C. & Kaplowitz, N. Predominant role of sterol response element binding proteins (SREBP) lipogenic pathways in hepatic steatosis in the murine intragastric ethanol feeding model. *J. Hepatol.* **45**, 717–724 (2006).
 53. Fischer, M., You, M., Matsumoto, M. & Crabb, D. W. Peroxisome proliferator-activated receptor alpha (PPARalpha) agonist treatment reverses PPARalpha dysfunction and abnormalities in hepatic lipid metabolism in ethanol-fed mice. *Journal of Biological Chemistry* **278**, 27997–28004 (2003).
 54. Pettinelli, P. & Videla, L. A. Up-regulation of PPAR-gamma mRNA expression in the liver of obese patients: an additional reinforcing lipogenic mechanism to SREBP-1c induction. *J. Clin. Endocrinol. Metab.* **96**, 1424–1430 (2011).
 55. Souza-Mello, V. Peroxisome proliferator-activated receptors as targets to treat non-alcoholic fatty liver disease. *WJH* **7**, 1012 (2015).
 56. Pettinelli, P. *et al.* Enhancement in liver SREBP-1c/PPAR-alpha ratio and steatosis in obese patients: correlations with insulin resistance and n-3 long-chain polyunsaturated fatty acid depletion. *Biochim. Biophys. Acta* **1792**, 1080–1086 (2009).
 57. Naveau, S. *et al.* Excess weight risk factor for alcoholic liver disease. *Hepatology* **25**, 108–111 (1997).
 58. Louvet, A. & Mathurin, P. Alcoholic liver disease: mechanisms of injury and targeted treatment. *Nat Rev Gastroenterol Hepatol* **12**, 231–242 (2015).
 59. Guebre Xabier, M. *et al.* Altered hepatic lymphocyte subpopulations in obesity related murine fatty livers: Potential mechanism for sensitization to liver damage. *Hepatology* **31**, 633–640 (2000).
 60. Jungermann, K. & Kietzmann, T. Zonation of parenchymal and nonparenchymal metabolism in liver. *Annu. Rev. Nutr.* **16**, 179–203 (1996).
 61. Jungermann, K. & Thurman, R. G. Hepatocyte heterogeneity in the metabolism of carbohydrates. *Enzyme* **46**, 33–58 (1992).
 62. Jungermann, K. & Kietzmann, T. Oxygen: Modulator of metabolic zonation and disease of the liver. *Hepatology* **31**, 255–260 (2000).
 63. Kronen, A., Kietzmann, T. & Jungermann, K. Perivenous localization of insulin receptor protein in rat liver, and regulation of its expression by glucose and oxygen in hepatocyte cultures. *Biochemical Journal* **348 Pt 2**, 433–438 (2000).
 64. Lindros, K. O. Zonation of cytochrome P450 expression, drug metabolism and toxicity in liver. *General Pharmacology: The Vascular System* **28**, 191–196 (1997).
 65. Broughan, T. A. *et al.* Effects of hepatic zonal oxygen levels on hepatocyte stress

- responses. *J. Surg. Res.* **145**, 150–160 (2008).
66. Jaakkola, P. *et al.* Targeting of HIF- α to the von Hippel-Lindau Ubiquitylation Complex by O₂-Regulated Prolyl Hydroxylation. *Science* **292**, 468–472 (2001).
 67. Kim, W. Y. *et al.* Failure to prolyl hydroxylate hypoxia inducible factor α phenocopies VHL inactivation in vivo. *EMBO J* **25**, 4650–4662 (2006).
 68. Belaiba, R. S. *et al.* Hypoxia up-regulates hypoxia-inducible factor-1 α transcription by involving phosphatidylinositol 3-kinase and nuclear factor kappaB in pulmonary artery smooth muscle cells. *Mol. Biol. Cell* **18**, 4691–4697 (2007).
 69. Chamboredon, S. *et al.* Hypoxia-inducible factor-1 α mRNA: a new target for destabilization by tristetraprolin in endothelial cells. *Mol. Biol. Cell* **22**, 3366–3378 (2011).
 70. Belanger, A. J. *et al.* Hypoxia-inducible factor 1 mediates hypoxia-induced cardiomyocyte lipid accumulation by reducing the DNA binding activity of peroxisome proliferator-activated receptor alpha/retinoid X receptor. *BIOCHEMICAL AND BIOPHYSICAL RESEARCH COMMUNICATIONS* **364**, 567–572 (2007).
 71. Krishnan, J. *et al.* Activation of a HIF1 α -PPAR γ axis underlies the integration of glycolytic and lipid anabolic pathways in pathologic cardiac hypertrophy. *Cell Metabolism* **9**, 512–524 (2009).
 72. Park, S.-K., Haase, V. H. & Johnson, R. S. von Hippel Lindau tumor suppressor regulates hepatic glucose metabolism by controlling expression of glucose transporter 2 and glucose 6-phosphatase. *Int. J. Oncol.* **30**, 341–348 (2007).
 73. Rankin, E. B. *et al.* Hypoxia-inducible factor 2 regulates hepatic lipid metabolism. *Mol. Cell. Biol.* **29**, 4527–4538 (2009).
 74. Scortegagna, M. *et al.* Multiple organ pathology, metabolic abnormalities and impaired homeostasis of reactive oxygen species in Epas1^{-/-} mice. *Nat Genet* **35**, 331–340 (2003).
 75. Nath, B. *et al.* Hepatocyte-specific hypoxia-inducible factor-1 α is a determinant of lipid accumulation and liver injury in alcohol-induced steatosis in mice. *Hepatology* **53**, 1526–1537 (2011).
 76. Nishiyama, Y. *et al.* HIF-1 α induction suppresses excessive lipid accumulation in alcoholic fatty liver in mice. *J. Hepatol.* **56**, 441–447 (2012).
 77. Kim, J. B. & Spiegelman, B. M. ADD1/SREBP1 promotes adipocyte differentiation and gene expression linked to fatty acid metabolism. *Genes & Development* **10**, 1096–1107 (1996).
 78. Enomoto, N. *et al.* Alcohol causes both tolerance and sensitization of rat Kupffer cells via mechanisms dependent on endotoxin. *Gastroenterology* **115**, 443–451 (1998).
 79. Rao, R. Endotoxemia and gut barrier dysfunction in alcoholic liver disease. *Hepatology* **50**, 638–644 (2009).
 80. Yang, S. Q., Lin, H. Z., Lane, M. D., Clemens, M. & Diehl, A. M. Obesity increases sensitivity to endotoxin liver injury: implications for the pathogenesis of steatohepatitis. *PNAS* **94**, 2557–2562 (1997).

81. Parlesak, A., Schäfer, C., Schütz, T., Bode, J. C. & Bode, C. Increased intestinal permeability to macromolecules and endotoxemia in patients with chronic alcohol abuse in different stages of alcohol-induced liver disease. *J. Hepatol.* **32**, 742–747 (2000).
82. Wheeler, M. D. Endotoxin and Kupffer cell activation in alcoholic liver disease. *Alcohol research and Health* (2003).
83. Choda, Y., Morimoto, Y. & Miyaso, H. Failure of the gut barrier system enhances liver injury in rats: protection of hepatocytes by gut-derived hepatocyte growth factor. *European journal of ...* (2004).
84. Petrasek, J. *et al.* Metabolic danger signals, uric acid and ATP, mediate inflammatory cross-talk between hepatocytes and immune cells in alcoholic liver disease. *J. Leukoc. Biol.* **98**, 249–256 (2015).
85. Paik, Y.-H. *et al.* Toll-like receptor 4 mediates inflammatory signaling by bacterial lipopolysaccharide in human hepatic stellate cells. *Hepatology* **37**, 1043–1055 (2003).
86. Nanji, A. A. *et al.* Increased severity of alcoholic liver injury in female rats: role of oxidative stress, endotoxin, and chemokines. *Am. J. Physiol. Gastrointest. Liver Physiol.* **281**, G1348–56 (2001).
87. Bautista, A. P. Chronic alcohol intoxication primes Kupffer cells and endothelial cells for enhanced CC-chemokine production and concomitantly suppresses phagocytosis and chemotaxis. *Front. Biosci.* **7**, a117–25 (2002).
88. Jaruga, B. *et al.* Chronic alcohol consumption accelerates liver injury in T cell-mediated hepatitis: alcohol dysregulation of NF-kappaB and STAT3 signaling pathways. *Am. J. Physiol. Gastrointest. Liver Physiol.* **287**, G471–9 (2004).
89. Machida, K. *et al.* Toll-like receptor 4 mediates synergism between alcohol and HCV in hepatic oncogenesis involving stem cell marker Nanog. **106**, 1548–1553 (2009).
90. Yin, M. *et al.* Reduced early alcohol-induced liver injury in CD14-deficient mice. *The Journal of Immunology* **166**, 4737–4742 (2001).
91. Uesugi, T. *et al.* Role of lipopolysaccharide-binding protein in early alcohol-induced liver injury in mice. *The Journal of Immunology* **168**, 2963–2969 (2002).
92. Hritz, I. *et al.* The critical role of toll-like receptor (TLR) 4 in alcoholic liver disease is independent of the common TLR adapter MyD88. *Hepatology* **48**, 1224–1231 (2008).
93. Kawanaka, H. *et al.* Defective mitogen-activated protein kinase (ERK2) signaling in gastric mucosa of portal hypertensive rats: potential therapeutic implications. *Hepatology* **34**, 990–999 (2001).
94. Aroor, A. R., Jackson, D. E. & Shukla, S. D. Elevated activation of ERK1 and ERK2 accompany enhanced liver injury following alcohol binge in chronically ethanol-fed rats. *Alcohol. Clin. Exp. Res.* **35**, 2128–2138 (2011).
95. Ribeiro, P. S. *et al.* Hepatocyte apoptosis, expression of death receptors, and activation of NF-kappaB in the liver of nonalcoholic and alcoholic steatohepatitis patients. *The American Journal of Gastroenterology* **99**, 1708–1717 (2004).
96. Song, Z. *et al.* Alcohol-induced S-adenosylhomocysteine accumulation in the

- liver sensitizes to TNF hepatotoxicity: possible involvement of mitochondrial S-adenosylmethionine transport. *Biochem. Pharmacol.* **74**, 521–531 (2007).
97. Song, Z. *et al.* S-adenosylhomocysteine sensitizes to TNF- α hepatotoxicity in mice and liver cells: a possible etiological factor in alcoholic liver disease. *Hepatology* **40**, 989–997 (2004).
 98. Pastorino, J. G. & Hoek, J. B. Ethanol potentiates tumor necrosis factor α cytotoxicity in hepatoma cells and primary rat hepatocytes by promoting induction of the mitochondrial permeability transition. *Hepatology* **31**, 1141–1152 (2000).
 99. García-Ruiz, C. *et al.* Effect of chronic ethanol feeding on glutathione and functional integrity of mitochondria in periportal and perivenous rat hepatocytes. *J. Clin. Invest.* **94**, 193–201 (1994).
 100. Fernández-Checa, J., Hirano, T., Tsukamoto, H. & Kaplowitz, N. Mitochondrial glutathione depletion in alcoholic liver disease. *Alcohol* **10**, 469–475 (1993).
 101. Cahill, A., Stabley, G. J., Wang, X. & Hoek, J. B. Chronic ethanol consumption causes alterations in the structural integrity of mitochondrial DNA in aged rats. *Hepatology* **30**, 881–888 (1999).
 102. Colell, A. *et al.* Selective glutathione depletion of mitochondria by ethanol sensitizes hepatocytes to tumor necrosis factor. *Gastroenterology* **115**, 1541–1551 (1998).
 103. Kubes, P. & Mehal, W. Z. Sterile inflammation in the liver. *Gastroenterology* **143**, 1158–1172 (2012).
 104. McDonald, B. & Kubes, P. Neutrophils and intravascular immunity in the liver during infection and sterile inflammation. *Toxicol Pathol* **40**, 157–165 (2012).
 105. Szabo, G. & Petrasek, J. Inflammasome activation and function in liver disease. *Nat Rev Gastroenterol Hepatol* **12**, 387–400 (2015).
 106. Ogura, Y., Sutterwala, F. S. & Flavell, R. A. The Inflammasome: First Line of the Immune Response to Cell Stress. *Cell* **126**, 659–662 (2006).
 107. Iracheta-Vellve, A. *et al.* Inhibition of sterile danger signals, uric acid and ATP, prevents inflammasome activation and protects from alcoholic steatohepatitis in mice. *J. Hepatol.* **63**, 1147–1155 (2015).
 108. Lee, R. C., Feinbaum, R. L. & Ambros, V. The *C. elegans* heterochronic gene *lin-4* encodes small RNAs with antisense complementarity to *lin-14*. *Cell* **75**, 843–854 (1993).
 109. Marí-Alexandre, J. *et al.* miRNAs Regulation and Its Role as Biomarkers in Endometriosis. *Int J Mol Sci* **17**, 93 (2016).
 110. Finnegan, E. F. & Pasquinelli, A. E. MicroRNA biogenesis: regulating the regulators. *Critical Reviews in Biochemistry and Molecular Biology* **48**, 51–68 (2013).
 111. Broderick, J. A. & Zamore, P. D. MicroRNA therapeutics. *Gene Therapy* **18**, 1104–1110 (2011).
 112. Landgraf, P. *et al.* A mammalian microRNA expression atlas based on small RNA library sequencing. *Cell* **129**, 1401–1414 (2007).
 113. Pasquinelli, A. E. MicroRNAs and their targets: recognition, regulation and an

- emerging reciprocal relationship. *Nature Reviews Genetics* **13**, 271–282 (2012).
114. Bartel, D. P. MicroRNAs: Target Recognition and Regulatory Functions. *Cell* **136**, 215–233 (2009).
 115. Reinhart, B. J. *et al.* The 21-nucleotide let-7 RNA regulates developmental timing in *Caenorhabditis elegans*. *Nature* **403**, 901–906 (2000).
 116. Lee, Y. S. & Dutta, A. The tumor suppressor microRNA let-7 represses the HMGA2 oncogene. *Genes & Development* **21**, 1025–1030 (2007).
 117. Büsling, I., Slack, F. J. & Grosshans, H. let-7 microRNAs in development, stem cells and cancer. *Trends Mol Med* **14**, 400–409 (2008).
 118. Lippai, D., Bala, S., Csak, T., Kurt-Jones, E. A. & Szabo, G. Chronic alcohol-induced microRNA-155 contributes to neuroinflammation in a TLR4-dependent manner in mice. *PLoS ONE* **8**, e70945 (2013).
 119. Bala, S. *et al.* Up-regulation of microRNA-155 in macrophages contributes to increased tumor necrosis factor {alpha} (TNF{alpha}) production via increased mRNA half-life in alcoholic liver disease. *J. Biol. Chem.* **286**, 1436–1444 (2011).
 120. Bruneau, J. C., Kodys, K. & Szabo, G. Alcohol-induced miR-27a regulates differentiation and M2 macrophage polarization of normal human monocytes. *The Journal of ...* (2015).
 121. Liu, G. & Abraham, E. MicroRNAs in immune response and macrophage polarization. **33**, 170–177 (2013).
 122. Jopling, C. Liver-specific microRNA-122: Biogenesis and function. *RNA Biol* **9**, 137–142 (2012).
 123. Jopling, C. L., Schütz, S. & Sarnow, P. Position-Dependent Function for a Tandem MicroRNA miR-122-Binding Site Located in the Hepatitis C Virus RNA Genome. **4**, 77–85 (2008).
 124. Sedano, C. D. & Sarnow, P. Hepatitis C Virus Subverts Liver-Specific miR-122 to Protect the Viral Genome from Exoribonuclease Xrn2. **16**, 257–264 (2014).
 125. Rodriguez, A., Griffiths-Jones, S. & Ashurst, J. L. Identification of mammalian microRNA host genes and transcription units. *Genome ...* (2004).
 126. Baskerville, S. & Bartel, D. P. Microarray profiling of microRNAs reveals frequent coexpression with neighboring miRNAs and host genes. *RNA* (2005).
 127. Lee, Y., Jeon, K., Lee, J.-T., Kim, S. & Kim, V. N. MicroRNA maturation: stepwise processing and subcellular localization. *EMBO J* **21**, 4663–4670 (2002).
 128. Bracht, J., Hunter, S., Eachus, R., Weeks, P. & Pasquinelli, A. E. Trans-splicing and polyadenylation of let-7 microRNA primary transcripts. *RNA* (2004).
 129. CAI, X. Human microRNAs are processed from capped, polyadenylated transcripts that can also function as mRNAs. *RNA* **10**, 1957–1966 (2004).
 130. Lee, J.-S. & Thorgeirsson, S. S. Genome-scale profiling of gene expression in hepatocellular carcinoma: Classification, survival prediction, and identification of therapeutic targets. **127**, S51–S55 (2004).
 131. Morlando, M. *et al.* Primary microRNA transcripts are processed co-transcriptionally. *Nat. Struct. Mol. Biol.* **15**, 902–909 (2008).
 132. Ballarino, M., Pagano, F. & Girardi, E. Coupled RNA processing and transcription of intergenic primary microRNAs. ... *and cellular biology* (2009).

133. Pawlicki, J. M. & Steitz, J. A. Subnuclear compartmentalization of transiently expressed polyadenylated pri-microRNAs: Processing at transcription sites or accumulation in SC35 foci. *Cell Cycle* **8**, 345–356 (2009).
134. Martinez, N. J., Ow, M. C. & Barrasa, M. I. A *C. elegans* genome-scale microRNA network contains composite feedback motifs with high flux capacity. (2008).
135. Wu, Q. *et al.* Decreased expression of hepatocyte nuclear factor 4 α (Hnf4 α)/microRNA-122 (miR-122) axis in hepatitis B virus-associated hepatocellular carcinoma enhances potential oncogenic GALNT10 protein activity. *J. Biol. Chem.* **290**, 1170–1185 (2015).
136. Denli, A. M., Tops, B. B. J., Plasterk, R. H. A., Ketting, R. F. & Hannon, G. J. Processing of primary microRNAs by the Microprocessor complex. *Nature* **432**, 231–235 (2004).
137. Gregory, R. I. *et al.* The Microprocessor complex mediates the genesis of microRNAs. *Nature* **432**, 235–240 (2004).
138. Yeom, K.-H., Lee, Y., Han, J., Suh, M. R. & Kim, V. N. Characterization of DGCR8/Pasha, the essential cofactor for Drosha in primary miRNA processing. *Nucleic Acids Research* **34**, 4622–4629 (2006).
139. Han, J. *et al.* Posttranscriptional crossregulation between Drosha and DGCR8. *Cell* **136**, 75–84 (2009).
140. Han, J. *et al.* The Drosha-DGCR8 complex in primary microRNA processing. *Genes & Development* **18**, 3016–3027 (2004).
141. Filippov, V., Solovyev, V., Filippova, M. & Gill, S. S. A novel type of RNase III family proteins in eukaryotes. *Gene* **245**, 213–221 (2000).
142. Fukuda, T. *et al.* DEAD-box RNA helicase subunits of the Drosha complex are required for processing of rRNA and a subset of microRNAs. *Nat Cell Biol* **9**, 604–611 (2007).
143. Suzuki, H. I. *et al.* Modulation of microRNA processing by p53. *Nature* **460**, 529–533 (2009).
144. Davis, B. N., Hilyard, A. C., Nguyen, P. H., Lagna, G. & Hata, A. Smad proteins bind a conserved RNA sequence to promote microRNA maturation by Drosha. *Molecular Cell* **39**, 373–384 (2010).
145. Davis, B. N., Hilyard, A. C., Lagna, G. & Hata, A. SMAD proteins control DROSHA-mediated microRNA maturation. *Nature* **454**, 56–61 (2008).
146. Chang, T.-C. *et al.* Transactivation of miR-34a by p53 Broadly Influences Gene Expression and Promotes Apoptosis. *Molecular Cell* **26**, 745–752 (2007).
147. Corney, D. C., Flesken-Nikitin, A., Godwin, A. K., Wang, W. & Nikitin, A. Y. MicroRNA-34b and MicroRNA-34c are targets of p53 and cooperate in control of cell proliferation and adhesion-independent growth. *Cancer Research* **67**, 8433–8438 (2007).
148. Tarasov, V. *et al.* Differential regulation of microRNAs by p53 revealed by massively parallel sequencing: miR-34a is a p53 target that induces apoptosis and G1-arrest. *Cell Cycle* **6**, 1586–1593 (2007).
149. Massagué, J., Seoane, J. & Wotton, D. Smad transcription factors. *Genes &*

- Development* **19**, 2783–2810 (2005).
150. Warner, D. R. *et al.* Functional interaction between Smad, CREB binding protein, and p68 RNA helicase. *BIOCHEMICAL AND BIOPHYSICAL RESEARCH COMMUNICATIONS* **324**, 70–76 (2004).
 151. Lei, E. P. & Silver, P. A. Protein and RNA Export from the Nucleus. *Developmental Cell* **2**, 261–272 (2002).
 152. Brownawell, A. M. & Macara, I. G. Exportin-5, a novel karyopherin, mediates nuclear export of double-stranded RNA binding proteins. *J Cell Biol* **156**, 53–64 (2002).
 153. Yi, R., Qin, Y., Macara, I. G. & Cullen, B. R. Exportin-5 mediates the nuclear export of pre-microRNAs and short hairpin RNAs. *Genes & Development* **17**, 3011–3016 (2003).
 154. Bohnsack, M. T., Czaplinski, K. & Gorlich, D. Exportin 5 is a RanGTP-dependent dsRNA-binding protein that mediates nuclear export of pre-miRNAs. *RNA* **10**, 185–191 (2004).
 155. Lund, E., Güttinger, S., Calado, A., Dahlberg, J. E. & Kutay, U. Nuclear export of microRNA precursors. *Science* **303**, 95–98 (2004).
 156. Zeng, Y., Yi, R. & Cullen, B. R. Recognition and cleavage of primary microRNA precursors by the nuclear processing enzyme Drosha. *EMBO J* **24**, 138–148 (2005).
 157. Gwizdek, C. *et al.* Exportin-5 mediates nuclear export of minihelix-containing RNAs. *Journal of Biological Chemistry* **278**, 5505–5508 (2003).
 158. Zeng, Y. & Cullen, B. R. Structural requirements for pre-microRNA binding and nuclear export by Exportin 5. *Nucleic Acids Research* **32**, 4776–4785 (2004).
 159. Grimm, D. *et al.* Fatality in mice due to oversaturation of cellular microRNA/short hairpin RNA pathways. *Nature* **441**, 537–541 (2006).
 160. Ketting, R. F. *et al.* Dicer functions in RNA interference and in synthesis of small RNA involved in developmental timing in *C. elegans*. *Genes & Development* **15**, 2654–2659 (2001).
 161. Hutvagner, G. A Cellular Function for the RNA-Interference Enzyme Dicer in the Maturation of the let-7 Small Temporal RNA. *Science* **293**, 834–838 (2001).
 162. Knight, S. W. & Bass, B. L. A role for the RNase III enzyme DCR-1 in RNA interference and germ line development in *Caenorhabditis elegans*. *Science* **293**, 2269–2271 (2001).
 163. MacRae, I. J., Zhou, K. & Doudna, J. A. Structural determinants of RNA recognition and cleavage by Dicer. *Nat. Struct. Mol. Biol.* **14**, 934–940 (2007).
 164. Park, J.-E. *et al.* Dicer recognizes the 5[prime] end of RNA for efficient and accurate processing. *Nature* **475**, 201–205 (2011).
 165. Lee, E. J. *et al.* Systematic evaluation of microRNA processing patterns in tissues, cell lines, and tumors. *RNA* **14**, 35–42 (2008).
 166. Forman, J. J., Legesse-Miller, A. & Collier, H. A. A search for conserved sequences in coding regions reveals that the let-7 microRNA targets Dicer within its coding sequence. *Proc. Natl. Acad. Sci. U.S.A.* **105**, 14879–14884 (2008).
 167. Ma, E., MacRae, I. J., Kirsch, J. F. & Doudna, J. A. Autoinhibition of Human

- Dicer by Its Internal Helicase Domain. *Journal of Molecular Biology* **380**, 237–243 (2008).
168. Suzuki, H. I. *et al.* MCPIP1 ribonuclease antagonizes dicer and terminates microRNA biogenesis through precursor microRNA degradation. *Molecular Cell* **44**, 424–436 (2011).
 169. Gregory, R. I., Chendrimada, T. P., Cooch, N. & Shiekhattar, R. Human RISC Couples MicroRNA Biogenesis and Posttranscriptional Gene Silencing. *Cell* **123**, 631–640 (2005).
 170. Tolia, N. H. & Joshua-Tor, L. Slicer and the argonautes. *Nat. Chem. Biol.* **3**, 36–43 (2007).
 171. Höck, J. & Meister, G. The Argonaute protein family. *Genome Biol.* (2008).
 172. Okamura, K. *et al.* The regulatory activity of microRNA species has substantial influence on microRNA and 3' UTR evolution. *Nat. Struct. Mol. Biol.* **15**, 354–363 (2008).
 173. Shin, C. Cleavage of the star strand facilitates assembly of some microRNAs into Ago2-containing silencing complexes in mammals. *Molecules and cells* (2008).
 174. Guo, H., Ingolia, N. T., Weissman, J. S. & Bartel, D. P. Mammalian microRNAs predominantly act to decrease target mRNA levels. *Nature* **466**, 835–840 (2010).
 175. Huntzinger, E. & Izaurralde, E. Gene silencing by microRNAs: contributions of translational repression and mRNA decay. *Nature Reviews Genetics* **12**, 99–110 (2011).
 176. Baek, D. *et al.* The impact of microRNAs on protein output. *Nature* **455**, 64–71 (2008).
 177. Chatterjee, S. & Grosshans, H. Active turnover modulates mature microRNA activity in *Caenorhabditis elegans*. *Nature* **461**, 546–549 (2009).
 178. Katoh, T. *et al.* Selective stabilization of mammalian microRNAs by 3' adenylation mediated by the cytoplasmic poly(A) polymerase GLD-2. *Genes & Development* **23**, 433–438 (2009).
 179. Möröy, T. *et al.* Rearrangement and enhanced expression of c-myc in hepatocellular carcinoma of hepatitis virus infected woodchucks. *Nature* **324**, 276–279 (1986).
 180. Etiemble, J., Möröy, T., Jacquemin, E. & Tiollais, P. Fused transcripts of c-myc and a new cellular locus, hcr in a primary liver tumor. *Oncogene* (1989).
 181. Möröy, T., Etiemble, J., Bougueleret, L. & Hadchouel, M. Structure and expression of hcr, a locus rearranged with c-myc in a woodchuck hepatocellular carcinoma. *Oncogene* (1989).
 182. Chang, J. *et al.* miR-122, a mammalian liver-specific microRNA, is processed from hcr mRNA and may downregulate the high affinity cationic amino acid transporter CAT-1. *RNA Biol* **1**, 106–113 (2004).
 183. Wienholds, E. *et al.* MicroRNA Expression in Zebrafish Embryonic Development. *Science* **309**, 310–311 (2005).
 184. Xu, H. *et al.* Liver enriched transcription factors regulate MicroRNA 122 that targets CUTL1 during liver development. *Hepatology* **52**, 1431–1442 (2010).
 185. Laudadio, I. *et al.* A Feedback Loop Between the Liver-Enriched Transcription

- Factor Network and Mir-122 Controls Hepatocyte Differentiation. *Gastroenterology* **142**, 119–129 (2012).
186. Yamasaki, H. *et al.* Suppression of C/EBP α expression in periportal hepatoblasts may stimulate biliary cell differentiation through increased Hnf6 and Hnf1b expression. *Development* **133**, 4233–4243 (2006).
 187. Li, Z.-Y. *et al.* Positive regulation of hepatic miR-122 expression by HNF4 α . *J. Hepatol.* **55**, 602–611 (2011).
 188. Beaudry, J. B. *et al.* Threshold Levels of Hepatocyte Nuclear Factor 6 (HNF-6) Acting in Synergy with HNF-4 and PGC-1 Are Required for Time-Specific Gene Expression during Liver Development. **26**, 6037–6046 (2006).
 189. Wang, K. & Holterman, A.-X. Pathophysiologic role of hepatocyte nuclear factor 6. *Cellular Signalling* **24**, 9–16 (2012).
 190. Gatfield, D. *et al.* Integration of microRNA miR-122 in hepatic circadian gene expression. *Genes & Development* **23**, 1313–1326 (2009).
 191. D'Ambrogio, A., Gu, W., Udagawa, T., Mello, C. C. & Richter, J. D. Specific miRNA Stabilization by Gld2-Catalyzed Monoadenylation. *Cell Reports* **2**, 1537–1545 (2012).
 192. Kojima, S., Gatfield, D., Esau, C. C. & Green, C. B. MicroRNA-122 Modulates the Rhythmic Expression Profile of the Circadian Deadenylation Nocturnin in Mouse Liver. *PLoS ONE* **5**, e11264 (2010).
 193. Cermelli, S., Ruggieri, A., Marrero, J. A., Ioannou, G. N. & Beretta, L. Circulating microRNAs in patients with chronic hepatitis C and non-alcoholic fatty liver disease. *PLoS ONE* **6**, e23937 (2011).
 194. Chen, Y. *et al.* A pilot study of serum microRNA signatures as a novel biomarker for occult hepatitis B virus infection. *Med. Microbiol. Immunol.* **201**, 389–395 (2012).
 195. Tomimaru, Y. *et al.* Circulating microRNA-21 as a novel biomarker for hepatocellular carcinoma. *J. Hepatol.* **56**, 167–175 (2012).
 196. Bala, S. *et al.* Circulating microRNAs in exosomes indicate hepatocyte injury and inflammation in alcoholic, drug-induced, and inflammatory liver diseases. *Hepatology* **56**, 1946–1957 (2012).
 197. Bala, S. *et al.* Biodistribution and function of extracellular miRNA-155 in mice. *Sci Rep* **5**, 10721 (2015).
 198. Shigehara, K. *et al.* Real-time PCR-based analysis of the human bile microRNAome identifies miR-9 as a potential diagnostic biomarker for biliary tract cancer. *PLoS ONE* **6**, e23584 (2011).
 199. Bukong, T. N., Momen-Heravi, F., Kodys, K., Bala, S. & Szabo, G. Exosomes from hepatitis C infected patients transmit HCV infection and contain replication competent viral RNA in complex with Ago2-miR122-HSP90. *PLoS Pathog.* **10**, e1004424 (2014).
 200. Ji, F. *et al.* Circulating microRNAs in hepatitis B virus-infected patients. *J. Viral Hepat.* **18**, e242–51 (2011).
 201. Xu, J. *et al.* Circulating MicroRNAs, miR-21, miR-122, and miR-223, in patients with hepatocellular carcinoma or chronic hepatitis. *Mol. Carcinog.* **50**, 136–142

- (2010).
202. Gui, J. *et al.* Serum microRNA characterization identifies miR-885-5p as a potential marker for detecting liver pathologies. *Clin. Sci.* **120**, 183–193 (2011).
 203. Momen-Heravi, F. *et al.* Increased number of circulating exosomes and their microRNA cargos are potential novel biomarkers in alcoholic hepatitis. *J Transl Med* **13**, 261 (2015).
 204. Bala, S., Petrasek, J., Mundkur, S., Catalano, D. & Levin, I. Circulating microRNAs in exosomes indicate hepatocyte injury and inflammation in alcoholic, drug induced, and inflammatory liver diseases. ... (2012).
 205. Antoine, D. J. *et al.* Mechanistic biomarkers provide early and sensitive detection of acetaminophen-induced acute liver injury at first presentation to hospital. *Hepatology* **58**, 777–787 (2013).
 206. Ward, J. *et al.* Circulating microRNA profiles in human patients with acetaminophen hepatotoxicity or ischemic hepatitis. *Proc. Natl. Acad. Sci. U.S.A.* **111**, 12169–12174 (2014).
 207. Ruoquan, Y., Wanpin, N., Qiangsheng, X., Guodong, T. & Feizhou, H. Correlation between plasma miR-122 expression and liver injury induced by hepatectomy. *Journal of International Medical Research* **42**, 77–84 (2014).
 208. Tryndyak, V. P. *et al.* Plasma microRNAs are sensitive indicators of inter-strain differences in the severity of liver injury induced in mice by a choline- and folate-deficient diet. *Toxicol. Appl. Pharmacol.* **262**, 52–59 (2012).
 209. Gibbins, D. J., Ciaudo, C., Erhardt, M. & Voinnet, O. Multivesicular bodies associate with components of miRNA effector complexes and modulate miRNA activity. *Nat Cell Biol* **11**, 1143–1149 (2009).
 210. Arroyo, J. D. *et al.* Argonaute2 complexes carry a population of circulating microRNAs independent of vesicles in human plasma. *Proc. Natl. Acad. Sci. U.S.A.* **108**, 5003–5008 (2011).
 211. Valadi, H. *et al.* Exosome-mediated transfer of mRNAs and microRNAs is a novel mechanism of genetic exchange between cells. *Nat Cell Biol* **9**, 654–659 (2007).
 212. Mittelbrunn, M. I. A. *et al.* Unidirectional transfer of microRNA-loaded exosomes from T cells to antigen-presenting cells. *Nature Communications* **2**, 282–10 (2011).
 213. Zernecke, A. *et al.* Delivery of microRNA-126 by apoptotic bodies induces CXCL12-dependent vascular protection. *Sci Signal* **2**, ra81–ra81 (2009).
 214. Lotvall, J. & Valadi, H. Cell to cell signalling via exosomes through esRNA. *Cell Adh Migr* **1**, 156–158 (2007).
 215. Momen-Heravi, F., Bala, S., Kodys, K. & Szabo, G. Exosomes derived from alcohol-treated hepatocytes horizontally transfer liver specific miRNA-122 and sensitize monocytes to LPS. *Sci Rep* **5**, 9991 (2015).
 216. Bandiera, S., Pfeffer, S., Baumert, T. F. & Zeisel, M. B. miR-122--a key factor and therapeutic target in liver disease. *J. Hepatol.* **62**, 448–457 (2015).
 217. John, K. *et al.* MicroRNAs play a role in spontaneous recovery from acute liver failure. *Hepatology* **60**, 1346–1355 (2014).

218. Castoldi, M. *et al.* The liver-specific microRNA miR-122 controls systemic iron homeostasis in mice. *J. Clin. Invest.* **121**, 1386–1396 (2011).
219. Krützfeldt, J. *et al.* Silencing of microRNAs in vivo with [antagomirs]. *Nature* **438**, 685–689 (2005).
220. Esau, C. *et al.* miR-122 regulation of lipid metabolism revealed by in vivo antisense targeting. *Cell Metabolism* **3**, 87–98 (2006).
221. Xie, J. *et al.* Long-term, efficient inhibition of microRNA function in mice using rAAV vectors. *Nat Meth* **9**, 403–409 (2012).
222. Lanford, R. E. *et al.* Therapeutic silencing of microRNA-122 in primates with chronic hepatitis C virus infection. *Science* **327**, 198–201 (2010).
223. Elmen, J. *et al.* Antagonism of microRNA-122 in mice by systemically administered LNA-antimiR leads to up-regulation of a large set of predicted target mRNAs in the liver. *Nucleic Acids Research* **36**, 1153–1162 (2007).
224. Mueller, S., Millionig, G. & Seitz, H. K. Alcoholic liver disease and hepatitis C: a frequently underestimated combination. *WJG* **15**, 3462–3471 (2009).
225. Donato, F. *et al.* Alcohol and hepatocellular carcinoma: the effect of lifetime intake and hepatitis virus infections in men and women. *American Journal of Epidemiology* **155**, 323–331 (2002).
226. Filipowicz, W. & Grosshans, H. The liver-specific microRNA miR-122: biology and therapeutic potential. *Prog Drug Res* **67**, 221–238 (2011).
227. Jopling, C. L., Yi, M., Lancaster, A. M., Lemon, S. M. & Sarnow, P. Modulation of hepatitis C virus RNA abundance by a liver-specific MicroRNA. *Science* **309**, 1577–1581 (2005).
228. Chang, J. *et al.* Liver-Specific MicroRNA miR-122 Enhances the Replication of Hepatitis C Virus in Nonhepatic Cells. **82**, 8215–8223 (2008).
229. Narbus, C. M. *et al.* HepG2 cells expressing microRNA miR-122 support the entire hepatitis C virus life cycle. *J. Virol.* **85**, 12087–12092 (2011).
230. Henke, J. I. *et al.* microRNA 122 stimulates translation of hepatitis C virus RNA. *EMBO J* **27**, 3300–3310 (2008).
231. Shimakami, T., Yamane, D. & Jangra, R. K. Stabilization of hepatitis C virus RNA by an Ago2–miR-122 complex. in (2012). doi:10.1073/pnas.1112263109/-/DCSupplemental
232. Pedersen, I. M. *et al.* Interferon modulation of cellular microRNAs as an antiviral mechanism. *Nature* **449**, 919–922 (2007).
233. Janssen, H. L. A. *et al.* Treatment of HCV infection by targeting microRNA. *N. Engl. J. Med.* **368**, 1685–1694 (2013).
234. Chen, Y. *et al.* A liver-specific microRNA binds to a highly conserved RNA sequence of hepatitis B virus and negatively regulates viral gene expression and replication. *FASEB J.* **25**, 4511–4521 (2011).
235. Wang, S. *et al.* Loss of microRNA 122 expression in patients with hepatitis B enhances hepatitis B virus replication through cyclin G1 modulated P53 activity. *Hepatology* **55**, 730–741 (2012).
236. Song, K. *et al.* Epigenetic regulation of MicroRNA-122 by peroxisome proliferator activated receptor-gamma and hepatitis b virus X protein in

- hepatocellular carcinoma cells. *Hepatology* **58**, 1681–1692 (2013).
237. Cheung, O. *et al.* Nonalcoholic steatohepatitis is associated with altered hepatic MicroRNA expression. *Hepatology* **48**, 1810–1820 (2008).
238. Hsu, S.-H. *et al.* Essential metabolic, anti-inflammatory, and anti-tumorigenic functions of miR-122 in liver. *J. Clin. Invest.* **122**, 2871–2883 (2012).
239. Tsai, W.-C. *et al.* MicroRNA-122 plays a critical role in liver homeostasis and hepatocarcinogenesis. *J. Clin. Invest.* **122**, 2884–2897 (2012).
240. Kutay, H. *et al.* Downregulation of miR-122 in the rodent and human hepatocellular carcinomas. *J. Cell. Biochem.* **99**, 671–678 (2006).
241. Deng, X. G. *et al.* Overexpression of miR 122 promotes the hepatic differentiation and maturation of mouse ESCs through a miR 122/FoxA1/HNF4a positive feedback loop. *Liver International* **34**, 281–295 (2014).
242. Wang, S.-C. *et al.* MicroRNA-122 triggers mesenchymal-epithelial transition and suppresses hepatocellular carcinoma cell motility and invasion by targeting RhoA. *PLoS ONE* **9**, e101330 (2014).
243. Fornari, F. *et al.* MiR-122/cyclin G1 interaction modulates p53 activity and affects doxorubicin sensitivity of human hepatocarcinoma cells. *Cancer Research* **69**, 5761–5767 (2009).
244. Bai, S. *et al.* MicroRNA-122 inhibits tumorigenic properties of hepatocellular carcinoma cells and sensitizes these cells to sorafenib. *J. Biol. Chem.* **284**, 32015–32027 (2009).
245. Hsu, S.-H. *et al.* Hepatic Loss of miR-122 Predisposes Mice to Hepatobiliary Cyst and Hepatocellular Carcinoma upon Diethylnitrosamine Exposure. *The American Journal of Pathology* **183**, 1719–1730 (2013).
246. Tsai, W.-C. *et al.* MicroRNA 122, a tumor suppressor microRNA that regulates intrahepatic metastasis of hepatocellular carcinoma. *Hepatology* **49**, 1571–1582 (2009).
247. Burchard, J. *et al.* microRNA-122 as a regulator of mitochondrial metabolic gene network in hepatocellular carcinoma. *Molecular Systems Biology* **6**, 1–12 (2010).
248. Gao, Y. *et al.* An insertion/deletion polymorphism at miRNA-122-binding site in the interleukin-1 3' untranslated region confers risk for hepatocellular carcinoma. *Carcinogenesis* **30**, 2064–2069 (2009).
249. Ameres, S. L. *et al.* Target RNA-directed trimming and tailing of small silencing RNAs. *Science* **328**, 1534–1539 (2010).
250. Ling, H., Fabbri, M. & Calin, G. A. MicroRNAs and other non-coding RNAs as targets for anticancer drug development. *Nature Reviews Drug Discovery* **12**, 847–865 (2013).
251. Lennox, K. A. & Behlke, M. A. Chemical modification and design of anti-miRNA oligonucleotides. *Gene Therapy* **18**, 1111–1120 (2011).
252. Orom, U. A., Kauppinen, S. & Lund, A. H. LNA-modified oligonucleotides mediate specific inhibition of microRNA function. *Gene* **372**, 137–141 (2006).
253. Elmén, J. *et al.* LNA-mediated microRNA silencing in non-human primates. *Nature* **452**, 896–899 (2008).

254. Obad, S. *et al.* Silencing of microRNA families by seed-targeting tiny LNAs. *Nat Genet* **43**, 371–378 (2011).
255. Nair, J. K. *et al.* Multivalent N-Acetylgalactosamine-Conjugated siRNA Localizes in Hepatocytes and Elicits Robust RNAi-Mediated Gene Silencing. *J. Am. Chem. Soc.* **136**, 16958–16961 (2014).
256. Vasdekis, A. E., Scott, E. A., O'Neil, C. P., Psaltis, D. & Hubbell, J. A. Precision intracellular delivery based on optofluidic polymersome rupture. *ACS Nano* **6**, 7850–7857 (2012).
257. Banerjee, S., Sen, K., Pal, T. K. & Guha, S. K. Poly(styrene-co-maleic acid)-based pH-sensitive liposomes mediate cytosolic delivery of drugs for enhanced cancer chemotherapy. *Int J Pharm* **436**, 786–797 (2012).
258. Lo, A., Lin, C.-T. & Wu, H.-C. Hepatocellular carcinoma cell-specific peptide ligand for targeted drug delivery. *Mol Cancer Ther* **7**, 579–589 (2008).
259. Soto, E. R. & Ostroff, G. R. Characterization of Multilayered Nanoparticles Encapsulated in Yeast Cell Wall Particles for DNA Delivery. *Bioconjugate Chem.* **19**, 840–848 (2008).
260. Singh, S., Narang, A. S. & Mahato, R. I. Subcellular Fate and Off-Target Effects of siRNA, shRNA, and miRNA. *Pharm Res* **28**, 2996–3015 (2011).
261. Haraguchi, T., Ozaki, Y. & Iba, H. Vectors expressing efficient RNA decoys achieve the long-term suppression of specific microRNA activity in mammalian cells. *Nucleic Acids Research* (2009).
262. Lesnik, J. K. & Antes, T. J. Knocking down microRNA function using miRZips™. *BioTechniques* (2010).
263. Hsu, S.-H. *et al.* Cationic lipid nanoparticles for therapeutic delivery of siRNA and miRNA to murine liver tumor. *Nanomedicine: Nanotechnology, Biology and Medicine* **9**, 1169–1180 (2013).
264. Nathwani, A. C. *et al.* Adenovirus-associated virus vector-mediated gene transfer in hemophilia B. *N. Engl. J. Med.* **365**, 2357–2365 (2011).
265. Nathwani, A. C. *et al.* Long-term safety and efficacy of factor IX gene therapy in hemophilia B. *N. Engl. J. Med.* **371**, 1994–2004 (2014).
266. Hebert, M. L., Grimm, D., Storm, T. A. & Kay, M. A. 489. Treatment for Hemophilia B Using Self-Complimentary AAV8 Vectors. *Mol. Ther.* **13**, S189–S190 (2006).
267. Sabatino, D. E. *et al.* Efficacy and Safety of Long-term Prophylaxis in Severe Hemophilia A Dogs Following Liver Gene Therapy Using AAV Vectors. *Mol. Ther.* **19**, 442–449 (2011).
268. Gao, G. *et al.* Biology of AAV Serotype Vectors in Liver-Directed Gene Transfer to Nonhuman Primates. *Molecular Therapy* **13**, 77–87 (2006).
269. Zhang, R., Wang, Q., Zhang, L. & Chen, S. Optimized human factor IX expression cassettes for hepatic-directed gene therapy of hemophilia B. *Front Med* **9**, 90–99 (2015).
270. Diederichs, S. & Haber, D. A. Dual Role for Argonautes in MicroRNA Processing and Posttranscriptional Regulation of MicroRNA Expression. *Cell* **131**, 1097–1108 (2007).

271. McBride, J. L., Boudreau, R. L. & Harper, S. Q. Artificial miRNAs mitigate shRNA-mediated toxicity in the brain: implications for the therapeutic development of RNAi. in (2008).
272. Beer, S., Bellovin, D. I., Lee, J. S. & Komatsubara, K. Low-level shRNA cytotoxicity can contribute to MYC-induced hepatocellular carcinoma in adult mice. *Molecular ...* (2010).
273. Altekruse, S. F., McGlynn, K. A. & Reichman, M. E. Hepatocellular Carcinoma Incidence, Mortality, and Survival Trends in the United States From 1975 to 2005. *Journal of Clinical Oncology* **27**, 1485–1491 (2009).
274. Chalasani, N. & Szabo, G. *Alcoholic and Non-Alcoholic Fatty Liver Disease*. (Springer, 2015). doi:10.1007/978-3-319-20538-0_15
275. Spaniel, C. *et al.* microRNA-122 Abundance in Hepatocellular Carcinoma and Non-Tumor Liver Tissue from Japanese Patients with Persistent HCV versus HBV Infection. *PLoS ONE* **8**, e76867 (2013).
276. Bergheim, I., McClain, C. J. & Arteel, G. E. Treatment of alcoholic liver disease. *Dig Dis* **23**, 275–284 (2005).
277. Carvalho, L. & Parise, E. R. Evaluation of nutritional status of nonhospitalized patients with liver cirrhosis. *Arq Gastroenterol* **43**, 269–274 (2006).
278. Seitz, H. K., Suter, P. M., Kotsonis, F. N. & Mackey, M. A. Ethanol toxicity and nutritional status. *Nutritional toxicology* (2002).
279. Marsano, L. & McClain, C. J. Review: Nutrition and Alcoholic Liver Disease. *JPEN J Parenter Enteral Nutr* **15**, 337–344 (1991).
280. Lieber, C. S. Pathogenesis and treatment of alcoholic liver disease: progress over the last 50 years. *Rocz Akad Med Bialymst* (2005).
281. HERBERT, V., ZALUSKY, R. & DAVIDSON, C. S. Correlation of Folate Deficiency with Alcoholism and Associated Macrocytosis, Anemia, and Liver Disease. *Ann Intern Med* **58**, 977–988 (1963).
282. Stickel, F., Hoehn, B., Schuppan, D. & Seitz, H. K. Review article: Nutritional therapy in alcoholic liver disease. *Alimentary Pharmacology & Therapeutics* **18**, 357–373 (2003).
283. Lieber, C. S. ALCOHOL: its metabolism and interaction with nutrients. *Annu. Rev. Nutr.* **20**, 395–430 (2000).
284. Soden, J. S. *et al.* Subcutaneous vitamin E ameliorates liver injury in an in vivo model of steatocholestasis. *Hepatology* **46**, 485–495 (2007).
285. Lieber, C. S., Leo, M. A., Cao, Q. & Ren, C. Silymarin retards the progression of alcohol-induced hepatic fibrosis in baboons. *Journal of clinical ...* (2003).
286. Morante, M. *et al.* Vitamin E deficiency induces liver nuclear factor- κ B DNA-binding activity and changes in related genes. *Free Radical Research* **39**, 1127–1138 (2009).
287. Gao, B. & Bataller, R. Alcoholic Liver Disease: Pathogenesis and New Therapeutic Targets. *Gastroenterology* **141**, 1572–1585 (2011).
288. Mezey, E., Potter, J. J., Rennie-Tankersley, L., Caballeria, J. & Pares, A. A randomized placebo controlled trial of vitamin E for alcoholic hepatitis. *J. Hepatol.* **40**, 40–46 (2004).

289. Parés, A. *et al.* Effects of silymarin in alcoholic patients with cirrhosis of the liver: results of a controlled, double-blind, randomized and multicenter trial. *J. Hepatol.* **28**, 615–621 (1998).
290. Bunout, D. *et al.* [Controlled study of the effect of silymarin on alcoholic liver disease]. *Rev Med Chil* **120**, 1370–1375 (1992).
291. Stewart, S., Jones, D. & Day, C. P. Alcoholic liver disease: new insights into mechanisms and preventative strategies. *Trends Mol Med* **7**, 408–413 (2001).
292. Nguyen-Khac, E. *et al.* Glucocorticoids plus N-acetylcysteine in severe alcoholic hepatitis. *N. Engl. J. Med.* **365**, 1781–1789 (2011).
293. Porter, H. P., Simon, F. R., Pope, C. E., II, Volwiler, W. & Fenster, L. F. Corticosteroid Therapy in Severe Alcoholic Hepatitis. *N. Engl. J. Med.* **284**, 1350–1355 (1971).
294. Christensen, E. & Gluud, C. Glucocorticoids are ineffective in alcoholic hepatitis: a meta-analysis adjusting for confounding variables. *Gut* **37**, 113–118 (1995).
295. Akriviadis, E. *et al.* Pentoxifylline improves short-term survival in severe acute alcoholic hepatitis: A double-blind, placebo-controlled trial. *Gastroenterology* **119**, 1637–1648 (2000).
296. DiNubile, M. J. Prednisolone or Pentoxifylline for Alcoholic Hepatitis. *N. Engl. J. Med.* **373**, 281–282 (2015).
297. Menon, K. V. N. *et al.* A Pilot Study of the Safety and Tolerability of Etanercept in Patients with Alcoholic Hepatitis. *The American Journal of Gastroenterology* **99**, 255–260 (2004).
298. Spahr, L. *et al.* Combination of steroids with infliximab or placebo in severe alcoholic hepatitis: a randomized controlled pilot study. *J. Hepatol.* **37**, 448–455 (2002).
299. Akerman, P. A. *et al.* Long term ethanol consumption alters the hepatic response to the regenerative effects of tumor necrosis factor α . *Hepatology* **17**, 1066–1073 (1993).
300. Naveau, S. *et al.* A double-blind randomized controlled trial of infliximab associated with prednisolone in acute alcoholic hepatitis. *Hepatology* **39**, 1390–1397 (2004).
301. Boetticher, N. C. *et al.* A Randomized, Double-Blinded, Placebo-Controlled Multicenter Trial of Etanercept in the Treatment of Alcoholic Hepatitis. *Gastroenterology* **135**, 1953–1960 (2008).
302. Lieber, C. S. S-adenosyl-L-methionine: its role in the treatment of liver disorders. *The American journal of clinical nutrition* (2002).
303. Grimm, D., Wang, L. & Lee, J. S. Argonaute proteins are key determinants of RNAi efficacy, toxicity, and persistence in the adult mouse liver. *The Journal of ...* (2010).
304. BARBON, C. *et al.* AAV8-Mediated Hepatic Expression of Acid Sphingomyelinase Corrects the Metabolic Defect in the Visceral Organs of a Mouse Model of Niemann–Pick Disease. *Molecular Therapy* **12**, 431–440 (2005).

305. Sands, M. S. in *Adeno-Associated Virus* **807**, 141–157 (Humana Press, 2011).
306. Nakai, H. *et al.* Unrestricted hepatocyte transduction with adeno-associated virus serotype 8 vectors in mice. *J. Virol.* **79**, 214–224 (2005).
307. Tanimizu, N., Kobayashi, S., Ichinohe, N. & Mitaka, T. Downregulation of miR122 by grainyhead-like 2 restricts the hepatocytic differentiation potential of adult liver progenitor cells. *Development* **141**, 4448–4456 (2014).
308. Ting, S. B. *et al.* The identification and characterization of human Sister-of-Mammalian Grainyhead (SOM) expands the grainyhead-like family of developmental transcription factors. *Biochemical Journal* **370**, 953–962 (2003).
309. Wilanowski, T. *et al.* A highly conserved novel family of mammalian developmental transcription factors related to *Drosophila* grainyhead. *Mech. Dev.* **114**, 37–50 (2002).
310. Auden, A. *et al.* Spatial and temporal expression of the Grainyhead-like transcription factor family during murine development. *Gene Expr. Patterns* **6**, 964–970 (2006).
311. Bray, S. J., Burke, B., Brown, N. H. & Hirsh, J. Embryonic expression pattern of a family of *Drosophila* proteins that interact with a central nervous system regulatory element. *Genes & Development* **3**, 1130–1145 (1989).
312. Dynlacht, B. D., Attardi, L. D., Admon, A., Freeman, M. & Tjian, R. Functional analysis of NTF-1, a developmentally regulated *Drosophila* transcription factor that binds neuronal cis elements. *Genes & Development* **3**, 1677–1688 (1989).
313. Nüsslein-Volhard, C., Wieschaus, E. & Kluding, H. Mutations affecting the pattern of the larval cuticle in *Drosophila melanogaster*. *Wilhelm Roux' Archiv* **193**, 267–282 (1984).
314. Kokoszyńska, K., Ostrowski, J., Rychlewski, L. & Wyrwicz, L. S. The fold recognition of CP2 transcription factors gives new insights into the function and evolution of tumor suppressor protein p53. *Cell Cycle* **7**, 2907–2915 (2008).
315. Huang, N. & Miller, W. L. Cloning of factors related to HIV-inducible LBP proteins that regulate steroidogenic factor-1-independent human placental transcription of the cholesterol side-chain cleavage enzyme, P450_{scc}. *Journal of Biological Chemistry* **275**, 2852–2858 (2000).
316. Bray, S. J. & Kafatos, F. C. Developmental function of Elf-1: an essential transcription factor during embryogenesis in *Drosophila*. *Genes & Development* **5**, 1672–1683 (1991).
317. Huang, J. D. *et al.* Binding sites for transcription factor NTF-1/Elf-1 contribute to the ventral repression of decapentaplegic. *Genes & Development* **9**, 3177–3189 (1995).
318. Liaw, G. J. *et al.* The torso response element binds GAGA and NTF-1/Elf-1, and regulates tailless by relief of repression. *Genes & Development* **9**, 3163–3176 (1995).
319. Senga, K., Mostov, K. E., Mitaka, T., Miyajima, A. & Tanimizu, N. Grainyhead-like 2 regulates epithelial morphogenesis by establishing functional tight junctions through the organization of a molecular network among claudin3, claudin4, and Rab25. *Mol. Biol. Cell* **23**, 2845–2855 (2012).

320. Pyrgaki, C., Liu, A. & Niswander, L. Grainyhead-like 2 regulates neural tube closure and adhesion molecule expression during neural fold fusion. *Developmental Biology* **353**, 38–49 (2011).
321. Rifat, Y. *et al.* Regional neural tube closure defined by the Grainy head-like transcription factors. *Developmental Biology* **345**, 237–245 (2010).
322. Ting, S. B. *et al.* A homolog of Drosophila grainy head is essential for epidermal integrity in mice. *Science* **308**, 411–413 (2005).
323. Chen, W. *et al.* Grainyhead-like 2 (GRHL2) inhibits keratinocyte differentiation through epigenetic mechanism. *Cell Death and Disease* **3**, e450–10 (2012).
324. Ting, S. B. *et al.* Inositol- and folate-resistant neural tube defects in mice lacking the epithelial-specific factor Grhl-3. *Nat. Med.* **9**, 1513–1519 (2003).
325. Yu, Z. *et al.* The Grainyhead-like epithelial transactivator Get-1/Grhl3 regulates epidermal terminal differentiation and interacts functionally with LMO4. *Developmental Biology* **299**, 122–136 (2006).
326. Fabian, J. *et al.* GRHL1 acts as tumor suppressor in neuroblastoma and is negatively regulated by MYCN and HDAC3. *Cancer Research* **74**, 2604–2616 (2014).
327. Mlacki, M., Darido, C., Jane, S. M. & Wilanowski, T. Loss of Grainy head-like 1 is associated with disruption of the epidermal barrier and squamous cell carcinoma of the skin. *PLoS ONE* **9**, e89247 (2014).
328. Xiang, X. *et al.* Correction: grhl2 determines the epithelial phenotype of breast cancers and promotes tumor progression. *PLoS ONE* **8**, (2013).
329. Werner, S. *et al.* Dual Roles of the Transcription Factor Grainyhead-like 2 (GRHL2) in Breast Cancer. *Journal of Biological Chemistry* **288**, 22993–23008 (2013).
330. Cieply, B., Ford, H. L., Farris, J. & Frisch, S. Abstract A15: A reciprocal feedback loop between grainyhead-like-2 and ZEB1 controls EMT and tumor suppression. *Cancer Research* **73**, A15–A15 (2014).
331. Yang, X., Vasudevan, P., Parekh, V., Penev, A. & Cunningham, J. M. Bridging Cancer Biology with the Clinic: Relative Expression of a GRHL2-Mediated Gene-Set Pair Predicts Breast Cancer Metastasis. *PLoS ONE* **8**, e56195–11 (2013).
332. Cieply, B., Farris, J., Denvir, J., Ford, H. L. & Frisch, S. M. Epithelial-Mesenchymal Transition and Tumor Suppression Are Controlled by a Reciprocal Feedback Loop between ZEB1 and Grainyhead-like-2. *Cancer Research* **73**, 6299–6309 (2013).
333. Attardi, L. D., Seggern, Von, D. & Tjian, R. Ectopic expression of wild-type or a dominant-negative mutant of transcription factor NTF-1 disrupts normal Drosophila development. *PNAS* **90**, 10563–10567 (1993).
334. Tanaka, Y. *et al.* Gain of GRHL2 is associated with early recurrence of hepatocellular carcinoma. *J. Hepatol.* **49**, 746–757 (2008).
335. Riethdorf, S. *et al.* Diverse expression patterns of the EMT suppressor grainyhead-like 2 (GRHL2) in normal and tumour tissues. *Int. J. Cancer* n/a–n/a (2015). doi:10.1002/ijc.29841

336. Kim, M. & McGinnis, W. Phosphorylation of Grainy head by ERK is essential for wound-dependent regeneration but not for development of an epidermal barrier. ... *of the National Academy of Sciences* (2011). doi:10.1073/pnas.1016386108/-/DCSupplemental
337. Mandrekar, P. & Szabo, G. Signalling pathways in alcohol-induced liver inflammation. *J. Hepatol.* **50**, 1258–1266 (2009).
338. Kulshreshtha, R. *et al.* A MicroRNA Signature of Hypoxia. **27**, 1859–1867 (2007).
339. Bruning, U. *et al.* MicroRNA-155 Promotes Resolution of Hypoxia-Inducible Factor 1 Activity during Prolonged Hypoxia. **31**, 4087–4096 (2011).
340. Bala, S. *et al.* Up-regulation of microRNA-155 in macrophages contributes to increased tumor necrosis factor {alpha} (TNF{alpha}) production via increased mRNA half-life in alcoholic liver disease. *J. Biol. Chem.* **286**, 1436–1444 (2011).
341. Ambade, A., Satishchandran, A. & Szabo, G. Alcoholic hepatitis accelerates early hepatobiliary cancer by increasing stemness and miR-122-mediated HIF-1 α activation. *Sci Rep* **6**, 21340 (2016).
342. Bala, S. *et al.* Increased microRNA-155 expression in the serum and peripheral monocytes in chronic HCV infection. *J Transl Med* **10**, 151 (2012).
343. Makino, Y. *et al.* Transcriptional up-regulation of inhibitory PAS domain protein gene expression by hypoxia-inducible factor 1 (HIF-1): a negative feedback regulatory circuit in HIF-1-mediated signaling in hypoxic cells. *Journal of Biological Chemistry* **282**, 14073–14082 (2007).
344. Esau, C. *et al.* miR-122 regulation of lipid metabolism revealed by in vivo antisense targeting.
345. Lehner, F., Kulik, U., Klempnauer, J. & Borlak, J. The hepatocyte nuclear factor 6 (HNF6) and FOXA2 are key regulators in colorectal liver metastases. *The FASEB Journal* **21**, 1445–1462 (2007).
346. Doddapaneni, R. *et al.* Overexpression of microRNA 122 enhances in vitro hepatic differentiation of fetal liver derived stem/progenitor cells. *J. Cell. Biochem.* **114**, 1575–1583 (2013).
347. JOPLING, C. L., NORMAN, K. L. & SARNOW, P. Positive and negative modulation of viral and cellular mRNAs by liver-specific microRNA miR-122. *Cold Spring Harb. Symp. Quant. Biol.* **71**, 369–376 (2006).